Is timing essential in cancer chronotherapy? Circadian molecular and behavioral studies on radiotherapy of hepatocellular carcinoma in mice

Inaugural-Dissertation

zur Erlangung des Doktorgrades
der Mathematisch-Naturwissenschaftlichen Fakultät
der Heinrich-Heine-Universität Düsseldorf

vorgelegt von
Soha Abdelaliem Hassan Hassan
aus Suez, Ägypten

Düsseldorf, December 2020

aus dem Institut für Anatomie II
der Heinrich-Heine Universität Düsseldorf

Gedruckt mit der Genehmigung
der Mathematisch-Naturwissenschaftlichen Fakultät der
Heinrich-Heine-Universität Düsseldorf

"Printed with the support of the German Academic Exchange Service"

Berichterstatter:

1. Prof. Dr. Charlotte von Gall
2. Prof. Dr. Horst-Werner Korf

Tag der mündlichen Prüfung: 23.02.2021

Dedicated to

Prof. Alaa El-Din Sallam

Professor of Chronobiology, Zoology Department, Faculty of Science, Suez Canal University, Egypt

"My Spiritual father, who has taught and supported me a lot and was beside me to reach for my goals in Egypt and Germany"

Rasha, Nermeen and my uncle Atef

"I know that your souls are always around me and support me"

Contents

General introduction

Hepatocellular carcinoma

Hepatocellular carcinoma (HCC) ranks fourth among cancer-related mortalities worldwide with a mortality rate of 8.2% (782 000 deaths) and with high new incidence cases (about 841 080) in 2018 (IARC 2018, Globocan 2019). The most common causes of HCC are related to alcohol abuse and chronic infection with hepatitis B and C viruses which are accompanied with inflamed and cirrhotic liver. Some other risk factors include non-alcoholic fatty liver disease and metabolic syndrome due to obesity or diabetes (Schlageter, Terracciano et al. 2014, Trojan, Zangos et al. 2016). HCC is characterized by high malignancy as well as fast progression, invasion and metastasis. HCC, mostly diagnosed in advanced stages, is highly resistant to antimitotic therapies (Sanchez, Gonzalez-Fernandez et al. 2018). Several substances have been applied in the HCC patients including sorafenib and tivantinib. Sorafenib was also applied in combination with radiation (RT-SOR) (Wild, Gandhi et al. 2013, Rebouissou, La Bella et al. 2017). All cancer therapies strategies have severe side effects which may impair the life quality of the patients and may lead to interruption of the treatment (Eriguchi, Levi et al. 2003, Innominato, Levi et al. 2010, Mandal, Biswas et al. 2010, Li 2019). Radiotherapy is rarely used in the management of the HCC due to lacking trail data which support the safety and efficacy of the radiotherapy and the increased risk of radiation-induced liver damage (RILD) which follows the hepatic radiotherapy (Ohri, Dawson et al. 2016, Chen 2019). An important question is whether the application of chronotherapy might improve the efficacy of HCC treatment and reduce its severe side effects.

Hepatocellular carcinoma markers

Ki67 and γ-H2AX are two important cell cycle components which can be used as markers to predict the response of HCC to antimitotic therapies, such as irradiation. Because Ki67 is expressed only in proliferating cells, it is one of the most widely used proliferation markers in cancer cells which is increased during the tumor development (Shi, Hu et al. 2015, Sun and Kaufman 2018). The proliferation rate changes during the day (Wood, Du-Quiton et al. 2006, Liu, Han et al. 2012, Ye, Yang et al. 2015) as a result of the circadian oscillation of the cell cycle molecules which either promote or inhibit cell cycle proliferation (e.g. CycD1 and c-Myc). The expression of the latter

molecules is subjected to the control of the circadian clock (Fu, Pelicano et al. 2002, You, Wood et al. 2005, Yang, Wood et al. 2009). In addition, Rebouissou *et al.* (2017) concluded that the expression of Ki67 can be considered as an important indicator for the response of HCC to antimitotic drugs (e.g. tivantinib). The G2/M phases are the most critical target phases for radiotherapy and in these phases normal cells express Ki67 (Shih, Shiozawa et al. 2003, Johnson, Chang-Claude et al. 2019).

γ-H2AX is a marker for DNA damage and repair (Kuo and Yang 2008). Upon DNA damage, DNA double strand breaks (DSBs) are formed which are characteristic for cancer cells due to mutated and unchecked cell cycles. DNA-DSBs are always followed by the phosphorylation of the H2AX histone and the formation of a new phosphorylated protein called γ-H2AX which starts the DNA repair process. After DNA repair, γ-H2AX is dephosphorylated (Sedelnikova and Bonner 2006, Kuo and Yang 2008). The DNA damage and repair process also follows a daily pattern which could be explained by the fact that DNA damage activates either ATM→Chk2 or ATR→Chk1 signaling pathways which are influenced by the circadian rhythm of the clock genes (e.g. *Per* and *Tim*) (Sancar, Lindsey-Boltz et al. 2010). In addition, some molecules which are involved in the DNA repair process (e.g. XPA) undergo circadian oscillation (Kang, Lindsey-Boltz et al. 2010, Corra, Salvadori et al. 2017).

It is well known that during the higher proliferation rate, the cells become more sensitive to DNA damage with cancer therapies (Shukla, Gupta et al. 2010, Rahn, Ray et al. 2011). So it is very important in cancer treatment protocols to take into consideration the circadian oscillation of cellular DNA repair molecules (e.g. γ-H2AX) as an indicator for the sensitivity of tumors and the surrounding healthy tissues to the treatment protocols. This can help to control the dose and the efficacy of the radiotherapy in localized targets (Kuo and Yang 2008). Recently, γ-H2AX was used to predict the efficacy of indolylquinoline derived substances and RT-SOR for therapy of HCC (Wild, Gandhi et al. 2013, Liu, Hsieh et al. 2016).

To evaluate any beneficial effect of antimitotic therapies on the HCC, it is necessary to clarify whether cell proliferation and DNA repair mechanisms in HCC cells follow a daily pattern and whether this pattern differs from that in the surrounding healthy liver (HL) tissue. These questions are addressed in the present thesis by immunohistochemical demonstration of Ki67 and γ-H2AX using two animal

models for HCC: 1) double transgenic c-myc/TGFα mice which were generated by crossing homozygous metallothionein/TGFα and albumin/c-myc single transgenic mice in CD1xB6CBA background in which hepatocarcinogenesis can be accelerated by $ZnCl_2$ in the drinking water (Thorgeirsson and Santoni-Rugiu 1996) and 2) transgenic *Per2::luc* mice on C57BL6/J background which were selected based on previous studies (Muller, Rodel et al. 2015). In these animals, luciferase is expressed under the control of *Per2* promoter, an important clock gene. This model allows for investigations of the on-line expression of the molecular clockwork via bioluminometry. HCC were induced by diethylnitrosamine (DEN) injection and phenobarbital in drinking water to accelerate tumor development.

Chronotherapy in oncology

The reaction of the tissue to exogenous stimuli (e.g. radiotherapy) and chemical drugs is influenced by the time of the day (Becciolini, Balzi et al. 1997, Scheving 2000). In addition, the efficacy and side effects of any antimitotic therapy depend on proper timing. Chemotherapy applied in the morning to mice bearing colon cancer was more effective than in the evening, with less side effects on the number of blood cells (Peters, Van Dijk et al. 1987). The time point, at which radiotherapy was applied, had an impact on the side effects in patients suffering from prostate and breast cancers (Noh, Choi et al. 2014, Hsu, Hou et al. 2016). Moreover, patients with cervical carcinoma, metastatic lung cancer and head-and-neck cancers revealed more severe mucositis when the radiotherapy was applied in the morning, afternoon and evening, respectively. The time-dependent relationship between mucositis and radiotherapy was explained by the fact that during these times of the day, the mucosal cells have a higher proliferation rate and during proliferation the cells become more sensitive to radiotherapy (Goyal, Shukla et al. 2009, Shukla, Gupta et al. 2010, Rahn, Ray et al. 2011). Thus, determination of the optimal time point for application of antimitotic therapies may help to improve the efficacy of HCC treatment. This hypothesis is also tested in the present thesis in which we investigated the effect of irradiation at four different time points of the day in transgenic *Per2::luc* mice bearing HCCs using the same biomarkers (Ki67 and γ-H2AX).

Circadian rhythm in oncology

The circadian system controls cell proliferation, apoptosis and DNA damage response as well as the sensitivity to antimitotic treatments (Zhou, Wang et al. 2016). Proliferation rate and DNA-damage are closely intertwined with the molecular circadian clockwork. This molecular circadian clockwork comprises clock genes which interact in positive and negative transcription–translation feedback loops (Schibler, Ripperger et al. 2003, Korf and von Gall 2013). In the positive loop, transcription factors CLOCK and BMAL1 heterodimerize and bind to the E-box of Period (*Per1* and *Per2*) and Cryptochrome (*Cry1* and *Cry2*), thus initiating their transcription. *Per* and *Cry* act as the negative feedback elements in the loop. PER and CRY are translated in the ribosomes and form PER/CRY heterodimers which translocate back to the nucleus to repress their own transcription by acting on the CLOCK/BMAL1 heterodimers. Another auxiliary loop is induced by CLOCK/BMAL1 heterodimers and activates transcription of two nuclear receptors, *Rev-erbα* and *Rorα*. REV-ERBα and RORα subsequently compete to bind receptor response elements (RREs) present in the *Bmal1* promoter to either repress or activate its expression, respectively. These autoregulatory feedback loops take approximately 24 hour to complete a cycle and represent circadian molecular clockwork (Schibler and Sassone-Corsi 2002, Schibler, Ripperger et al. 2003, Gallego and Virshup 2007, Korf and von Gall 2013). This circadian molecular clockwork is responsible for the regulation of many biological processes by controlling the expression of more than 3000, so-called clock-controlled genes (CCGs).

Bmal1-Clock heterodimers positively and negatively regulate the expression of *wee1* (anti-mitotic gene) and *c-Myc* (oncogene), respectively. Also, *Per2* and *Cry* play a very important role in the regulation of cell division by regulating the expression of *c-Myc* and *p21* genes (Fu, Pelicano et al. 2002, Antoch, Kondratov et al. 2005, Somade 2014). Thus, disruption or mutation of the molecular clockwork may lead to genomic instability and increase the cellular proliferation rate and thus provide favorable conditions for carcinogenesis (Huisman, Oklejewicz et al. 2015, Sanchez, Gonzalez-Fernandez et al. 2018). *Per2* mutation led to remarkable changes in the liver gene or protein expressions including *c-Myc* and *Wee1* which regulate cell proliferation (Mteyrek, Filipski et al. 2016). In addition, down-regulation of some clock genes may serve as potential prognostic factors for cancer development and this

down-regulation may be associated with more advanced cancer stages (Li 2019). The *Per2* expression was reported to be a potential novel prognostic marker for gastric cancer patients with a poor prognosis (Zhao, Zeng et al. 2014). Also, the ratio of PER2 to CRY1 is suggested to be a prognostic marker that predicts the survival outcomes of chronic lymphocytic leukemia patients (Morgan M. 2019). *Per1* and *Cry1* and *Clock*/*Bmal1* are the most commonly disrupted clock genes in endocrine and testicular tumors, respectively (Angelousi, Kassi et al. 2019). We have therefore investigated whether the circadian molecular clockwork is altered in HCC as compared with the surrounding HL.

An intact circadian clock was suggested to protect against irradiation-induced (IR-induced) toxicity. Human rectal tumor tissues revealed high expressions of *Per2* and *Cry2* and no change in the expressions of *Per1*, *Cry1* and *Bmal1* after treated with chemo-radiotherapy (Lu, Chu et al. 2015). In addition, clock-disrupted mouse models showed an increase in the IR-induced DNA damage and apoptosis (Dakup, Porter et al. 2020). So, there is a possible relation between disruption of the molecular clockwork and the sensitivity to the radiotherapy. To date little is known about the effects of radiotherapy on the molecular clockwork. Therefore, we analyzed whether the radiotherapy altered the circadian molecular clockwork in HCC and HL if the treatment was performed at different *Zeitgeber* time (ZT) points; ZT02 (defined as 2 hours after light on, early inactivity phase), ZT08 (late inactivity phase), ZT14 (defined as 2 hours after light off, early activity phase) and ZT20 (late activity phase).

Organotypic slice culture

Organotypic slice cultures (OSC) are made from primary tissue and maintain the three-dimensional structure as well as the functional extracellular matrix (Palma, Doornebal et al. 2019). OSC of normal liver were shown to be viable in culture conditions for several days and to keep a robust circadian rhythm (Yoo, Yamazaki et al. 2004, Muller, Rodel et al. 2015). Usage of OSC would allow much faster and more effective screening of any novel therapeutic strategy than experiments with whole animals and improve the animals' welfare. So in the present thesis, we have addressed the question of whether results obtained by *ex vivo* samples are comparable with those obtained by *in vitro* samples such as OSC. To evaluate whether OSC of liver and HCC represent adequate models to test novel anticancer therapies, we irradiated the

HCC and HL slices of *Per2::luc* mice at four different Circadian time (CT) points which approximately mimic the irradiated ZTs of the whole animals, CT02 (defined as 2 hours after medium change, early subjective day), CT08 (late subjective day), CT14 (early subjective night) and CT20 (late subjective night), and compared the *in vitro* results with *ex vivo* samples.

Possible side effects of radiotherapy

Tumor radiotherapy has dual effects because it not only affects the proliferation and the other biological processes of the tumor but also it can cause damage for the non-tumor tissues (Wang, Wang et al. 2018) and influence other biological systems in the body.

Irradiation triggers many biological events in the body including the inflammatory response. The early inflammatory response to the radiation is the release of the proinflammatory cytokines (e.g. Interleukin-1 (IL-1) and Tumor necrosis factor α (TNF-α)), chemokines (e.g. IL-8) and many other molecules which are involved in this mechanism. All these factors activate the blood circulating cells, granulocytes and monocytes, which build the first line of defense during the inflammation (Stone, Coleman et al. 2003, Crews, Sarkar et al. 2015, Uribe-Querol and Rosales 2015, Bray, Simmons et al. 2016). Many side effects which were reported after radiotherapy such as mucositis, diarrhea and lymphoedema were closely linked with the inflammatory immune response (Rahn, Ray et al. 2011, Harper and Talbot 2019).

It is well known that the main targets of the toxic effects of antimitotic therapies are the cells with high proliferation rate including hematopoietic cells (Antoch, Kondratov et al. 2005). Thus, hematopoiesis is one of the most sensitive systems in the body to the radiotherapy and reduction in the number of white and red blood cells is one of the most common side effects of the radiotherapy (Yang, Vaida et al. 1995, Wersal, Keller et al. 2019). Patients with testicular, ovarian, oral and prostate cancers showed depletion in the number of leukocytes, in particular lymphocytes, after radiotherapy (Campbell, Wiernik et al. 1976, Dovšak, Ihan et al. 2018, Sanguineti, Giannarelli et al. 2019). Leukopenia and lymphopenia were explained by the possible effects of the radiotherapy on the bone marrow and spleen cells (Sanguineti, Giannarelli et al. 2019). Therefore, we investigated the number of

blood cells of transgenic *Per2::luc* HCC bearing mice before and after irradiation at different ZTs to monitor possible acute side effects of the radiotherapy at each time point.

Cancer-related fatigue (CRF) is one of the most pronounced symptoms in cancer patients and one of the early chronic side effects of cancer treatment. Many cancer patients suffer from severe sleep problems, disrupted locomotor activity rhythm and cortisol levels and a decrease in life quality which accompany CRF, particularly after radiotherapy treatment. These symptoms persist for months to years even after the completion of cancer treatments. CRF is one of the key reasons for discontinuation of treatment by the patients (Fortner, Stepanski et al. 2002, Rich, Innominato et al. 2005, Bower, Ganz et al. 2006, Hofman, Ryan et al. 2007, Huang, Cheung et al. 2019).

Since sleep regulation involves two intertwined processes: the homeostatic regulation and output from the circadian system (Borbely 1982), CRF may partly depend on dysfunction/disruption of the circadian rhythm. In mammals and humans, the circadian rhythm is generated by the suprachiasmatic nucleus (SCN) of the hypothalamus and synchronized to the environmental rhythms by external cues called "*Zeitgebers*". The most prominent "*Zeitgeber*" is the external light-dark cycle, the photoperiod. Photoperiod stimuli are perceived by the retina and are transmitted to the SCN via the retinohypothalamic tract (RHT), which uses the glutamate and the neuropeptide pituitary adenylate cyclase-activating peptide (PACAP) as neurotransmitters. Activation of these neurotransmitters induces the activation of the extracellular signal-regulated kinase 1/2 (ERK 1/2) pathway which plays a very important role in the transmission of photic information to the core clockworks. In addition, phosphorylated ERK (p-ERK) interacts directly with some clock proteins (e.g. BMAL1) and regulates the activity of other transcription factors which regulate the expression of clock genes (e.g. CREB and its regulation for *Per1* expression) (Gau, Lemberger et al. 2002, Coogan and Piggins 2003, Mohawk, Green et al. 2012, Korf and von Gall 2013, Partch, Green et al. 2014). Via multiple output pathways, the circadian system controls a variety of overt body functions including the sleep-wake cycle, locomotor activity and hormone secretion (e.g. glucocorticoids).

We therefore analyzed how HCC development and radiotherapy treatment affect two important circadian outputs, spontaneous locomotor activity rhythms and serum corticosterone levels. The locomotor activity rhythm is a reliable marker for the output of the circadian system (Pfeffer, Wicht et al. 2015) and is considered as the main index which reflects the sleep-wake cycle and the general behavior in mammals (Galani, Duconseille et al. 2001, Sallam, Hassan et al. 2016). It can be readily determined by non-invasive techniques. Recording the locomotor activity patterns has been used to analyze possible dysfunctions of the circadian system in patients with cancer and after applying the cancer treatment protocols (Mormont and Levi 1997, Innominato, Giacchetti et al. 2012).

Rhythmic secretion of glucocorticoids is another important marker for circadian output. Glucocorticoids are also considered as the main regulators of stress responses and used as stress biomarkers. Stress is observed in many patients suffering from cancer and after radiotherapy. Under stress, the hypothalamus-pituitary-adrenal (HPA) axis is stimulated and induces glucocorticoid secretion (Gong, Miao et al. 2015, De la Roca-Chiapas, Barbosa-Sabanero et al. 2016). There is now growing evidence that the sleep disruption in cancer patients may be closely related to dysfunction of circadian rhythms including glucocorticoids rhythm (Huang, Cheung et al. 2019).

Aim of thesis

The main aim of the present thesis is to investigate, whether timing is essential in cancer treatment and to introduce the concept of chronotherapy to radiobiological cancer research. The efficacy and side effects of any antimitotic therapy may depend on proper timing and we tested this hypothesis to define the optimal time point at which HCC is increasingly susceptible, whilst the surrounding HL becomes increasingly resistant to the damaging effects of radiotherapy. To further elucidate the importance of timed irradiation in radiotherapy of the HCC, the following questions were addressed in our project: 1) Are HCC and the surrounding HL synchronized with regard to the proliferation, DNA repair mechanism and the expression of clock genes? 2) Is the molecular clockwork altered in the HCC as compared with the surrounding HL? 3) Does HCC and HL react differently with regard to proliferation, DNA repair and expression of clock genes, if irradiated at different time points? 4) Are *in vitro* samples (OSC) suitable models to assess the reaction of HCC and the surrounding HL to radiation and can they substitute *ex vivo* experiments with whole animals? 5) What is the optimal time point for irradiation in order to minimize the damage in HL and to maximize the damage in the HCC? 6) How does radiation affect the spontaneous locomotor activity rhythm, serum corticosterone levels and p-ERK immunoreaction in the SCN when irradiation was applied at different time points? 7) Do acute effects of radiation on the hematopoietic system depend on the time point at which the irradiation was applied?

References

Angelousi, A., E. Kassi, N. Nasiri-Ansari, H. S. Randeva, G. A. Kaltsas and G. P. Chrousos (2019). "Clock genes and cancer development in particular in endocrine tissues." Endocr Relat Cancer.

Antoch, M. P., R. V. Kondratov and J. S. Takahashi (2005). "Circadian clock genes as modulators of sensitivity to genotoxic stress." Cell Cycle **4**(7): 901-907.

Becciolini, A., M. Balzi, D. Fabbrica and C. S. Potten (1997). "The effects of irradiation at different times of the day on rat intestinal goblet cells." Cell Proliferation **30**(3-4): 161-170.

Borbely, A. A. (1982). "A two process model of sleep regulation." Hum Neurobiol **1**(3): 195-204.

Bower, J. E., P. A. Ganz, K. A. Desmond, C. Bernaards, J. H. Rowland, B. E. Meyerowitz and T. R. Belin (2006). "Fatigue in long-term breast carcinoma survivors: a longitudinal investigation." Cancer **106**(4): 751-758.

Bray, F. N., B. J. Simmons, A. H. Wolfson and K. Nouri (2016). "Acute and Chronic Cutaneous Reactions to Ionizing Radiation Therapy." Dermatol Ther (Heidelb) **6**(2): 185-206.

Campbell, A. C., G. Wiernik, J. Wood, P. Hersey, C. A. Waller and I. C. M. Maclennan (1976). "Characteristics of the lymphopenia induced by radiotherapy." Clinical and Experimental Immunology **23**(2): 200-208.

Chen, C. P. (2019). "Role of Radiotherapy in the Treatment of Hepatocellular Carcinoma." J Clin Transl Hepatol **7**(2): 183-190.

Coogan, A. N. and H. D. Piggins (2003). "Circadian and photic regulation of phosphorylation of ERK1/2 and Elk-1 in the suprachiasmatic nuclei of the Syrian hamster." J Neurosci **23**(7): 3085-3093.

Corra, S., R. Salvadori, L. Bee, V. Barbieri and M. Mognato (2017). "Analysis of DNA-damage response to ionizing radiation in serum-shock synchronized human fibroblasts." Cell Biol Toxicol **33**(4): 373-388.

Crews, F. T., D. K. Sarkar, L. Qin, J. Zou, N. Boyadjieva and R. P. Vetreno (2015). "Neuroimmune Function and the Consequences of Alcohol Exposure." Alcohol Res **37**(2): 331-341, 344-351.

Dakup, P. P., K. I. Porter, R. P. Gajula, P. N. Goel, Z. Cheng and S. Gaddameedhi (2020). "The circadian clock protects against ionizing radiation-induced cardiotoxicity." FASEB J **34**(2): 3347-3358.

De la Roca-Chiapas, J. M., G. Barbosa-Sabanero, J. A. Martinez-Garcia, J. Martinez-Soto, V. M. Ramos-Frausto, L. P. Gonzalez-Ramirez and K. Nowack (2016). "Impact of stress and levels of corticosterone on the development of breast cancer in rats." Psychol Res Behav Manag **9**: 1-6.

Dovšak, T., A. Ihan, V. Didanovič, A. Kansky, M. Verdenik and N. I. Hren (2018). "Effect of surgery and radiotherapy on complete blood count, lymphocyte subsets and inflammatory response in patients with advanced oral cancer." BMC Cancer **18**(1): 235.

Eriguchi, M., F. Levi, T. Hisa, H. Yanagie, Y. Nonaka and Y. Takeda (2003). "Chronotherapy for cancer." Biomedicine & Pharmacotherapy **57**: 92-95.

Fortner, B. V., E. J. Stepanski, S. C. Wang, S. Kasprowicz and H. H. Durrence (2002). "Sleep and quality of life in breast cancer patients." J Pain Symptom Manage **24**(5): 471-480.

Fu, L., H. Pelicano, J. Liu, P. Huang and C. Lee (2002). "The circadian gene Period2 plays an important role in tumor suppression and DNA damage response in vivo." Cell **111**(1): 41-50.

Galani, R., E. Duconseille, O. Bildstein and J. C. Cassel (2001). "Effects of room and cage familiarity on locomotor activity measures in rats." Physiol Behav **74**(1-2): 1-4.

Gallego, M. and D. M. Virshup (2007). "Post-translational modifications regulate the ticking of the circadian clock." Nat Rev Mol Cell Biol **8**(2): 139-148.

Gau, D., T. Lemberger, C. von Gall, O. Kretz, N. Le Minh, P. Gass, W. Schmid, U. Schibler, H. W. Korf and G. Schütz (2002). "Phosphorylation of CREB Ser142 regulates light-induced phase shifts of the circadian clock." Neuron **34**(2): 245-253.

Globocan (2019). "Liver cancer fact sheet".

Gong, S., Y. L. Miao, G. Z. Jiao, M. J. Sun, H. Li, J. Lin, M. J. Luo and J. H. Tan (2015). "Dynamics and correlation of serum cortisol and corticosterone under different physiological or stressful conditions in mice." PLoS One **10**(2): e0117503.

Goyal, M., P. Shukla, D. Gupta, S. S. Bisht, A. Dhawan, S. Gupta, M. C. Pant and N. S. Verma (2009). "Oral mucositis in morning vs. evening irradiated patients: a randomised prospective study." Int J Radiat Biol **85**(6): 504-509.

Harper, E. and C. J. Talbot (2019). "Is it Time to Change Radiotherapy: The Dawning of Chronoradiotherapy?" Clin Oncol (R Coll Radiol) **31**(5): 326-335.

Hofman, M., J. L. Ryan, C. D. Figueroa-Moseley, P. Jean-Pierre and G. R. Morrow (2007). "Cancer-related fatigue: the scale of the problem." Oncologist **12 Suppl 1**: 4-10.

Hsu, F. M., W. H. Hou, C. Y. Huang, C. C. Wang, C. L. Tsai, Y. C. Tsai, H. J. Yu, Y. S. Pu and J. C. Cheng (2016). "Differences in toxicity and outcome associated with circadian variations between patients undergoing daytime and evening radiotherapy for prostate adenocarcinoma." Chronobiol Int **33**(2): 210-219.

Huang, T.-W., D. S. T. Cheung, X. Xu, E.-W. Loh, J.-H. Lai, W.-W. Su, S.-S. Wu and C.-C. Lin (2019). "Relationship between diurnal cortisol profile and sleep quality in patients with Hepatocellular Carcinoma." Biological Research for Nursing **22**(1): 139-147.

Huisman, S. A., M. Oklejewicz, A. R. Ahmadi, F. Tamanini, J. N. Ijzermans, G. T. van der Horst and R. W. de Bruin (2015). "Colorectal liver metastases with a disrupted circadian rhythm phase shift the peripheral clock in liver and kidney." Int J Cancer **136**(5): 1024-1032.

IARC (2018). "Latest global cancer data: Cancer burden rises to 18.1 million new cases and 9.6 million cancer deaths in 2018." PRESS RELEASE **N° 263**

Innominato, P. F., S. Giacchetti, G. A. Bjarnason, C. Focan, C. Garufi, B. Coudert, S. Iacobelli, M. Tampellini, X. Durando, M. C. Mormont, J. Waterhouse and F. A. Levi (2012). "Prediction of overall survival through circadian rest-activity monitoring during chemotherapy for metastatic colorectal cancer." Int J Cancer **131**(11): 2684-2692.

Innominato, P. F., F. A. Levi and G. A. Bjarnason (2010). "Chronotherapy and the molecular clock: Clinical implications in oncology." Adv Drug Deliv Rev **62**(9-10): 979-1001.

Johnson, K., J. Chang-Claude, A. M. Critchley, C. Kyriacou, S. Lavers, T. Rattay, P. Seibold, A. Webb, C. West, R. P. Symonds, C. J. Talbot and R. Consortium (2019). "Genetic Variants Predict Optimal Timing of Radiotherapy to Reduce Side-effects in Breast Cancer Patients." Clin Oncol (R Coll Radiol) **31**(1): 9-16.

Kang, T. H., L. A. Lindsey-Boltz, J. T. Reardon and A. Sancar (2010). "Circadian control of XPA and excision repair of cisplatin-DNA damage by cryptochrome and HERC2 ubiquitin ligase." Proc Natl Acad Sci U S A **107**(11): 4890-4895.

Korf, H.-W. and C. von Gall (2013). Circadian Physiology. Neuroscience in the 21st Century: From Basic to Clinical. D. W. Pfaff. New York, NY, Springer New York**:** 1813-1845.

Kuo, L. J. and L. Yang (2008). "γ-H2AX – A Novel Biomarker for DNA Double-strand Breaks" in vivo **22**: 305-310.

Li, H. X. (2019). "The role of circadian clock genes in tumors." Onco Targets Ther **12**: 3645-3660.

Liu, C. Y., C. H. Hsieh, S. H. Kim, J. P. Wang, Y. L. Ni, C. L. Su, C. F. Yao and K. Fang (2016). "An indolylquinoline derivative activates DNA damage response and apoptosis in human hepatocellular carcinoma cells." Int J Oncol **49**(6): 2431-2441.

Liu, S. L., Y. Han, Y. Zhang, C. Y. Xie, E. H. Wang, Y. Miao, H. Y. Li, H. T. Xu and S. D. Dai (2012). "Expression of metastasis-associated protein 2 (MTA2) might predict proliferation in non-small cell lung cancer." Target Oncol **7**(2): 135-143.

Lu, H., Q. Chu, G. Xie, H. Han, Z. Chen, B. Xu and Z. Yue (2015). "Circadian gene expression predicts patient response to neoadjuvant chemoradiation therapy for rectal cancer." Int J Clin Exp Pathol **8**(9): 10985-10994.

Mandal, A. S., N. Biswas, K. M. Karim, A. Guha, S. Chatterjee, M. Behera and K. Kuotsu (2010). "Drug delivery system based on chronobiology--A review." J Control Release **147**(3): 314-325.

Mohawk, J. A., C. B. Green and J. S. Takahashi (2012). "Central and peripheral circadian clocks in mammals." Annu Rev Neurosci **35**: 445-462.

Morgan M., S. D., Chloe-Anne Martinez , Bernadette Kerr, Peter A. Cistulli and Kristina M. Cook (2019). The Cancer Clock Is (Not) Ticking: Links between Circadian Rhythms and Cancer, Clocks&Sleep.

Mormont, M. C. and F. Levi (1997). "Circadian-system alterations during cancer processes: a review." Int J Cancer **70**(2): 241-247.

Mteyrek, A., E. Filipski, C. Guettier, A. Okyar and F. Levi (2016). "Clock gene Per2 as a controller of liver carcinogenesis." Oncotarget **7**(52): 85832-85847.

Muller, M. H., F. Rodel, U. Rub and H. W. Korf (2015). "Irradiation with X-rays phase-advances the molecular clockwork in liver, adrenal gland and pancreas." Chronobiol Int **32**(1): 27-36.

Noh, J. M., D. H. Choi, H. Park, S. J. Huh, W. Park, S. W. Seol, B. K. Jeong, S. J. Nam, J. E. Lee and W. H. Kil (2014). "Comparison of acute skin reaction following morning versus late afternoon radiotherapy in patients with breast cancer who have undergone curative surgical resection." J Radiat Res **55**(3): 553-558.

Ohri, N., L. A. Dawson, S. Krishnan, J. Seong, J. C. Cheng, S. K. Sarin, M. Kinkhabwala, M. M. Ahmed, B. Vikram, C. N. Coleman and C. Guha (2016). "Radiotherapy for Hepatocellular Carcinoma: New Indications and Directions for Future Study." J Natl Cancer Inst **108**(9).

Palma, E., E. J. Doornebal and S. Chokshi (2019). "Precision-cut liver slices: a versatile tool to advance liver research." Hepatol Int **13**(1): 51-57.

Partch, C. L., C. B. Green and J. S. Takahashi (2014). "Molecular architecture of the mammalian circadian clock." Trends Cell Biol **24**(2): 90-99.

Peters, G. J., J. Van Dijk, J. C. Nadal, C. J. Van Groeningen, J. Lankelma and H. M. Pinedo (1987). "Diurnal variation in the therapeutic efficacy of 5-fluorouracil against murine colon cancer." In Vivo **1**(2): 113-117.

Pfeffer, M., H. Wicht, C. von Gall and H. W. Korf (2015). "Owls and larks in mice." Front Neurol **6**: 101.

Rahn, D. A., 3rd, D. K. Ray, D. J. Schlesinger, L. Steiner, J. P. Sheehan, J. M. O'Quigley and T. Rich (2011). "Gamma knife radiosurgery for brain metastasis of nonsmall cell lung cancer: is there a difference in outcome between morning and afternoon treatment?" Cancer **117**(2): 414-420.

Rebouissou, S., T. La Bella, S. Rekik, S. Imbeaud, A. L. Calatayud, N. Rohr-Udilova, Y. Martin, G. Couchy, P. Bioulac-Sage, B. Grasl-Kraupp, L. de Koning, N. Ganne-Carrie, J. C. Nault, M. Ziol and J. Zucman-Rossi (2017). "Proliferation Markers Are Associated with MET Expression in Hepatocellular Carcinoma and Predict Tivantinib Sensitivity In Vitro." Clin Cancer Res **23**(15): 4364-4375.

Rich, T., P. F. Innominato, J. Boerner, M. C. Mormont, S. Iacobelli, B. Baron, C. Jasmin and F. Levi (2005). "Elevated serum cytokines correlated with altered behavior, serum cortisol rhythm, and dampened 24-hour rest-activity patterns in patients with metastatic colorectal cancer." Clin Cancer Res **11**(5): 1757-1764.

Sallam, A. E.-D., S. A. Hassan, E. Hassaneen and E. M. Ali (2016). "Environmental stress of mobile phone EM radiation on locomotor activity and melatonin circadian rhythms of rats." Biological Rhythm Research **47**(4): 597-607.

Sancar, A., L. A. Lindsey-Boltz, T. H. Kang, J. T. Reardon, J. H. Lee and N. Ozturk (2010). "Circadian clock control of the cellular response to DNA damage." FEBS Lett **584**(12): 2618-2625.

Sanchez, D. I., B. Gonzalez-Fernandez, I. Crespo, B. San-Miguel, M. Alvarez, J. Gonzalez-Gallego and M. J. Tunon (2018). "Melatonin modulates dysregulated circadian clocks in mice with diethylnitrosamine-induced hepatocellular carcinoma." Journal of Pineal Research **65**(3).

Sanguineti, G., D. Giannarelli, M. G. Petrongari, S. Arcangeli, A. Sangiovanni, B. Saracino, A. Farneti, A. Faiella, M. Conte and G. Arcangeli (2019). "Leukotoxicity after moderately Hypofractionated radiotherapy versus conventionally fractionated dose escalated radiotherapy for localized prostate Cancer: a secondary analysis from a randomized study." Radiation Oncology **14**(1): 23.

Scheving, L. A. (2000). "Biological clocks and the digestive system." Gastroenterology **119**(2): 536-549.

Schibler, U., J. Ripperger and S. A. Brown (2003). "Peripheral circadian oscillators in mammals: time and food." J Biol Rhythms **18**(3): 250-260.

Schibler, U. and P. Sassone-Corsi (2002). "A web of circadian pacemakers." Cell **111**(7): 919-922.

Schlageter, M., L. M. Terracciano, S. D'Angelo and P. Sorrentino (2014). "Histopathology of hepatocellular carcinoma." World J Gastroenterol **20**(43): 15955-15964.

Sedelnikova, O. A. and W. M. Bonner (2006). "GammaH2AX in cancer cells: a potential biomarker for cancer diagnostics, prediction and recurrence." Cell Cycle **5**(24): 2909-2913.

Shi, W., J. F. Hu, S. Z. Zhu, X. Y. Shen, X. Y. Zhang, C. Q. Yang, H. J. Gao and H. Zhang (2015). "Expression of MTA2 and Ki-67 in hepatocellular carcinoma and their correlation with prognosis." International Journal of Clinical and Experimental Pathology **8**(10): 13083-13089.

Shih, H. C., T. Shiozawa, K. Kato, T. Imai, T. Miyamoto, J. Uchikawa, T. Nikaido and I. Konishi (2003). "Immunohistochemical expression of cyclins, cyclin-dependent kinases, tumor-suppressor gene products, Ki-67, and sex steroid receptors in endometrial carcinoma: positive staining for cyclin A as a poor prognostic indicator." Hum Pathol **34**(5): 471-478.

Shukla, P., D. Gupta, S. S. Bisht, M. C. Pant, M. L. Bhatt, R. Gupta, K. Srivastava, S. Gupta, A. Dhawan, D. Mishra and M. P. Negi (2010). "Circadian variation in radiation-induced intestinal mucositis in patients with cervical carcinoma." Cancer **116**(8): 2031-2035.

Somade, O. (2014). "Role of circadian clock genes in the regulation of cell cycle processes." romanian journal of biochemistry **51**: 151-178.

Stone, H. B., C. N. Coleman, M. S. Anscher and W. H. McBride (2003). "Effects of radiation on normal tissue: consequences and mechanisms." Lancet Oncol **4**(9): 529-536.

Sun, X. and P. D. Kaufman (2018). "Ki-67: more than a proliferation marker." Chromosoma **127**(2): 175-186.

Thorgeirsson, S. S. and E. Santoni-Rugiu (1996). "Transgenic mouse models in carcinogenesis: interaction of c-myc with transforming growth factor alpha and hepatocyte growth factor in hepatocarcinogenesis." Br J Clin Pharmacol **42**(1): 43-52.

Trojan, J., S. Zangos and A. A. Schnitzbauer (2016). "Diagnostics and Treatment of Hepatocellular Carcinoma in 2016: Standards and Developments." Visc Med **32**(2): 116-120.

Uribe-Querol, E. and C. Rosales (2015). "Neutrophils in Cancer: Two Sides of the Same Coin." Journal of Immunology Research **2015**: 983698.

Wang, J. S., H. J. Wang and H. L. Qian (2018). "Biological effects of radiation on cancer cells." Mil Med Res **5**(1): 20.

Wersal, C., A. Keller, C. Weiss, F. Giordano, Y. Abo-Madyan, B. Tuschy, M. Suetterlin, F. Wenz and E. Sperk (2019). "Long-term changes in blood counts after intraoperative radiotherapy for breast cancer—single center experience and review of the literature." Translational Cancer Research **8**: 1882-1903.

Wild, A. T., N. Gandhi, S. T. Chettiar, K. Aziz, R. P. Gajula, R. D. Williams, R. Kumar, K. Taparra, J. Zeng, J. A. Cades, E. Velarde, S. Menon, J. F. Geschwind, D. Cosgrove, T. M. Pawlik, A. Maitra, J. Wong, R. K. Hales, M. S. Torbenson, J. M. Herman and P. T. Tran (2013). "Concurrent versus sequential sorafenib therapy in combination with radiation for hepatocellular carcinoma." PLoS One **8**(6): e65726.

Wood, P. A., J. Du-Quiton, S. You and W. J. Hrushesky (2006). "Circadian clock coordinates cancer cell cycle progression, thymidylate synthase, and 5-fluorouracil therapeutic index." Mol Cancer Ther **5**(8): 2023-2033.

Yang, F. E., F. Vaida, L. Ignacio, A. Houghton, J. Nauityal, H. Halpern, H. Sutton and S. Vijayakumar (1995). "Analysis of weekly complete blood counts in patients receiving standard fractionated partial body radiation therapy." Int J Radiat Oncol Biol Phys **33**(3): 617-617.

Yang, X., P. A. Wood, C. M. Ansell, D. F. Quiton, E. Y. Oh, J. Du-Quiton and W. J. Hrushesky (2009). "The circadian clock gene Per1 suppresses cancer cell proliferation and tumor growth at specific times of day." Chronobiol Int **26**(7): 1323-1339.

Ye, H., K. Yang, X. M. Tan, X. J. Fu and H. X. Li (2015). "Daily rhythm variations of the clock gene PER1 and cancer-related genes during various stages of carcinogenesis in a golden hamster model of buccal mucosa carcinoma." Oncotargets and Therapy **8**.

Yoo, S. H., S. Yamazaki, P. L. Lowrey, K. Shimomura, C. H. Ko, E. D. Buhr, S. M. Siepka, H. K. Hong, W. J. Oh, O. J. Yoo, M. Menaker and J. S. Takahashi (2004). "PERIOD2::LUCIFERASE real-time reporting of circadian dynamics reveals persistent circadian oscillations in mouse peripheral tissues." Proc Natl Acad Sci U S A **101**(15): 5339-5346.

You, S., P. A. Wood, Y. Xiong, M. Kobayashi, J. Du-Quiton and W. J. Hrushesky (2005). "Daily coordination of cancer growth and circadian clock gene expression." Breast Cancer Res Treat **91**(1): 47-60.

Zhao, H., Z. L. Zeng, J. Yang, Y. Jin, M. Z. Qiu, X. Y. Hu, J. Han, K. Y. Liu, J. W. Liao, R. H. Xu and Q. F. Zou (2014). "Prognostic relevance of Period1 (Per1) and Period2 (Per2) expression in human gastric cancer." Int J Clin Exp Pathol **7**(2): 619-630.

Zhou, D., Y. Wang, L. Chen, L. Jia, J. Yuan, M. Sun, W. Zhang, P. Wang, J. Zuo, Z. Xu and J. Luan (2016). "Evolving roles of circadian rhythms in liver homeostasis and pathology." Oncotarget **7**(8): 8625-8639.

Publications

The present thesis consists of three manuscripts in support of the focus of this dissertation

I. **Soha A. Hassan,** Christian Schmithals, Maike von Harten, Albrecht Piiper, Horst-Werner Korf, Charlotte von Gall (2020). "Time-dependent changes in proliferation, DNA damage and clock gene expression in hepatocellular carcinoma and healthy liver of a transgenic mouse model". The main aim of this work was to investigate whether cell proliferation and DNA repair mechanisms in HCC tissue follow a daily pattern and whether this pattern differs from that in the surrounding HL in HCC mouse model. We further investigated the circadian molecular clockwork in HCC and the surrounding HL. The results obtained from *ex vivo* samples were compared with those obtained by *in vitro* OSC to evaluate whether OSC of liver and HCC represent adequate models to test novel anticancer therapies.

II. **Soha A. Hassan**, Amira A. H. Ali, Dennis Sohn, Ulrich Flögel, Reiner U. Jänicke, Horst-Werner Korf, Charlotte von Gall. "Does timing matter in radiotherapy of hepatocellular carcinoma? An experimental study in mice". Here the main aim was to introduce the concept of chronotherapy to HCC treatment by identifying the optimal time point at which the HCC is highly sensitive, whilst the surrounding HL is highly resistant to DNA damage by radiotherapy using HCC mouse model. Ki67 as a marker for proliferation rate and γ-H2AX as a marker for DNA-DSBs were investigated before and after therapeutic irradiation at four different time points of the day in OSC and *ex vivo* samples. OSC model was used to investigate whether the model is suitable to test this chronotherapeutic approach. In *ex vivo* samples, core clock genes and complete blood counts were also analyzed before and after irradiation to investigate the possible effects of irradiation at different ZTs on molecular clockwork and hematopoietic system.

III. Soha A. Hassan, Amira A. H. Ali, Mona Yassine, Dennis Sohn, Martina Pfeffer, Reiner U. Jänicke, Horst-Werner Korf, Charlotte von Gall. "Relationship between locomotor activity rhythm and corticosterone levels during HCC development, progression and treatment in a mouse model." In this manuscript, we determined whether appropriate timing of radiotherapy of HCC would help to reduce severe side effects related to the chronic fatigue syndrome. To this end, we evaluated how tumor development and irradiation treatment affect two important circadian outputs, spontaneous locomotor activity rhythms and corticosterone levels in HCC mouse model. In addition, p-ERK immunoreaction in the SCN, as a marker for rhythmic SCN neuronal activity, was investigated.

Time-dependent changes in proliferation, DNA damage and clock gene expression in hepatocellular carcinoma and healthy liver of a transgenic mouse model

Soha A. Hassan, Christian Schmithals, Maike von Harten, Albrecht Piiper, Horst-Werner Korf*, Charlotte von Gall

* Corresponding author

Status of publication: The manuscript was published in the *International Journal of Cancer* in July 2020.

Impact factor: 5.145

Contribution to the publication: Concept/design, performance of all experiments, acquisition, analysis and interpretation of data, and writing of the manuscript.

Received: 17 March 2020 | Revised: 3 July 2020 | Accepted: 13 July 2020

DOI: 10.1002/ijc.33228

Check for updates

TUMOR MARKERS AND SIGNATURES

IJC International Journal of Cancer

Time-dependent changes in proliferation, DNA damage and clock gene expression in hepatocellular carcinoma and healthy liver of a transgenic mouse model

Soha A. Hassan[1,2] | Christian Schmithals[3] | Maike von Harten[3] | Albrecht Piiper[3] | Horst-Werner Korf[4,5] | Charlotte von Gall[1]

[1]Institute of Anatomy II, Medical Faculty, Heinrich-Heine-University, Düsseldorf, Germany

[2]Zoology Department, Faculty of Science, Suez University, Suez, Egypt

[3]Department of Medicine 1, University Hospital Frankfurt, Frankfurt, Germany

[4]Institute of Anatomy I, Medical Faculty, Heinrich-Heine-University, Düsseldorf, Germany

[5]Institute of Anatomy II, Goethe University, Frankfurt, Germany

Correspondence
Horst-Werner Korf, Institute of Anatomy I, Medical Faculty, Heinrich-Heine-University, Universitätsstr. 1, 40225 Düsseldorf, Germany.
Email: korf@uni-duesseldorf.de

Abstract

Hepatocellular carcinoma (HCC) is highly resistant to anticancer therapy and novel therapeutic strategies are needed. Chronotherapy may become a promising approach because it may improve the efficacy of antimitotic radiation and chemotherapy by considering timing of treatment. To date little is known about time-of-day dependent changes of proliferation and DNA damage in HCC. Using transgenic c-myc/transforming growth factor (TGFα) mice as HCC animal model, we immunohistochemically demonstrated Ki67 as marker for proliferation and γ-H2AX as marker for DNA damage in HCC and surrounding healthy liver (HL). Core clock genes (*Per1*, *Per2*, *Cry1*, *Cry2*, *Bmal 1*, *Rev-erbα* and *Clock*) were examined by qPCR. Data were obtained from samples collected ex vivo at four different time points and from organotypic slice cultures (OSC). Significant differences were found between HCC and HL. In HCC, the number of Ki67 immunoreactive cells showed two peaks (ex vivo: ZT06 middle of day and ZT18 middle of night; OSC: CT04 and CT16). In ex vivo samples, the number of γ-H2AX positive cells in HCC peaked at ZT18 (middle of the night), while in OSC their number remained high during subjective day and night. In both HCC and HL, clock gene expression showed a time-of-day dependent expression ex vivo but no changes in OSC. The expression of *Per2* and *Cry1* was significantly lower in HCC than in HL. Our data support the concept of chronotherapy of HCC. OSC may become useful to test novel cancer therapies.

KEYWORDS

clock genes, hepatocellular carcinoma, Ki67, transgenic c-myc/TGFα mice, γ-H2AX

1 | INTRODUCTION

Hepatocellular carcinoma (HCC) ranks fourth among cancer-related mortalities worldwide with a mortality rate of 8.2% (782 000 deaths) and with high new incidence cases (about 841 080) in 2018.[1] The most common causes of HCC are related to alcohol abuse and chronic infection with hepatitis B and C viruses which are accompanied with inflamed and cirrhotic liver. Some other risk factors include non-alcoholic fatty liver disease and hepatic manifestation of the metabolic syndrome due to obesity or diabetes.[2,3] HCC, mostly diagnosed in advanced stages, is highly resistant to antimitotic therapy. Several substances have been applied in the HCC patients including sorafenib

Abbreviation: CT, circadian time; DNA-DSBs, DNA-double-strand breaks; HCC, hepatocellular carcinoma; LD, light-dark; HL, healthy liver; OSC, organotypic slice culture; ZT, Zeitgeber time.

This is an open access article under the terms of the Creative Commons Attribution License, which permits use, distribution and reproduction in any medium, provided the original work is properly cited.
© 2020 The Authors. *International Journal of Cancer* published by John Wiley & Sons Ltd on behalf of Union for International Cancer Control.

and tivantinib. Sorafenib was also applied in combination with radiation (RT-SOR).[4,5] However, these therapies have substantial side effects. The limited success of these therapies may in part be due to therapy in a phase in which the tumors are not particularly susceptible and determination of the optimal time point for therapies (chronotherapy) may improve their efficacy.[6] Ki67 and γ-H2AX are good markers to predict the response of HCC therapies. Ki67 is one of the most important cell proliferation markers which is increased during the tumor development. It is expressed in the S phase and G2/M phases of the cell cycle. Its expression changes during the day and is regulated by the circadian clock.[7-9] Because Ki67 is expressed only in proliferating cells, it is one of the most widely used proliferation markers in cancer cells.[10,11] γ-H2AX is a marker for DNA damage and repair. Upon DNA damage, DNA double-strand breaks (DSBs) are formed which are characteristic for cancer cells due to mutated and unchecked cell cycles. DNA-DSBs are always followed by the phosphorylation of H2AX histone and the formation of a new phosphorylated protein called γ-H2AX which starts the DNA repair process. After DNA is repaired, γ-H2AX is dephosphorylated.[12,13] γ-H2AX can be used as a marker of radio-sensitivity of cancer and the normal surrounding tissues, their ability to recover from damage and the efficacy of the cellular repair process. This helps to control the dosage, the effectiveness and frequency of radiation therapy in localized target.[12]

To evaluate any beneficial effect of chronotherapy, it is necessary to clarify whether cell proliferation and DNA repair mechanisms in HCC cells follow a diurnal pattern and whether this pattern differs from that in healthy liver (HL) tissue. These questions are addressed in the present study in an animal model for HCC, double transgenic c-myc/TGFα mice[14] by immunohistochemical demonstration of Ki67 and γ-H2AX.

Cell cycle and proliferation are closely intertwined with the molecular circadian clockwork and there is increasing evidence that cancer development and progression may be associated with dysfunction or mutation of this molecular clockwork. We have therefore investigated whether the circadian molecular clockwork is altered in HCC as compared to healthy liver tissue. The molecular circadian clockwork comprises clock genes which interact in positive and negative transcription-translation feedback loops.[15,16] Briefly, the expression of *Per* (*Per1* and *Per2*) and *Cry* (*Cry1* and *Cry2*) genes is activated by heterodimers of the transcription factors CLOCK/BMAL1 which act as the positive elements in the loop while dimers of PER/CRY form the negative loop.[16] The molecular circadian clockwork ticks in all nucleated cells and governs many physiological processes by controlling the expression of more than 3000, so-called clock-controlled genes.

Finally, we have addressed the question whether results obtained by ex vivo samples are compared to those obtained by in vitro samples such as organotypic slice cultures (OSC) to evaluate whether OSC of liver and HCC represent adequate models to test novel anticancer therapies. Previous studies have shown that OSC which maintain the three-dimensional structure of the tissue and a functional extracellular matrix maintain the circadian rhythms for several days.[17] Usage of OSC would allow much faster and more effective screening of any novel therapeutic strategy than experiments with whole animals.

What's new?

The acquisition of therapeutic resistance in hepatocellular carcinoma (HCC) is a major obstacle in chemotherapy-based approaches to HCC treatment. Therapeutic resistance may be attributed in part to the phase of tumor development at the time of therapy. Here, assessment of timing of antimitotic therapies in an HCC animal model reveals time-of-day dependent changes in tumor cell proliferation and DNA damage. In addition, clock gene expression was altered in HCC, suggesting a link to tumor development and growth. The results indicate that the efficacy of antimitotic therapies depends on proper timing and that this time dependency should be evaluated further.

2 | MATERIALS AND METHODS

2.1 | Experimental animals

The experiments described in our study were conducted according to accepted standards of humane animal care and were consistent with federal guidelines and Directive 2010/63/EU of the European Union. They were approved by the Regierungspräsidium Darmstadt (Gen. Nr. FU 1067). All experiments were performed with male c-myc/TGFα bitransgenic mice. The animals were generated by crossing homozygous metallothionein/TGFα and albumin/c-myc single transgenic mice in CD13B6CBA background in which hepatocarcinogenesis can be accelerated by zinc in the drinking water.

Food and water containing $ZnCl_2$ were supplied *ad libitum*. All animals were kept under normal light-dark (LD) cycle (12:12). The development and growth of HCCs was controlled by MRI as described recently.[18]

2.2 | Ex vivo investigations

Twelve animals were used for immunohistochemical and 12 animals for real-time PCR analyses. All animals investigated had either single or multiple tumors (Table 1). The animals were sacrificed at 4 different *Zeitgeber* time points: ZT00 (light on), ZT06, ZT12 (light off) and ZT18. For immunohistochemical investigations, the animals (n = 3/ZT) were anesthetized by a mixture of ketamine (100 mg/kg body weight, Rotexmedica, Trittau, Germany) and xylazine (10 mg/kg body weight, Rompun 2%, Bayer Leverkusen, Germany) through intraperitoneal injection and then perfused transcardially with 0.9% sodium chloride solution for 1 minute followed by approximately 100 mL 4% paraformaldehyde (PFA) in 0.1 M phosphate-buffered saline (PBS, pH 7.4) for 15 minutes. Perfusion during the night was performed under dim red light. Healthy liver tissues and tumors were excised and post-fixed separately in 4% PFA in PBS for 2 hours, cryoprotected with gradually increasing concentrations of sucrose (10%, 20% and 30%) and cryosectioned separately into 12 μm thick serial sections. For qPCR

TABLE 1 Number, size and volume of tumors in each mouse investigated ex vivo for qPCR, immunocytochemistry or in slice preparations (OSC)

qPCR Mouse				
Mouse ID	Number of tumors	Size diameters (cm)	Tumor volume (cm^3)	Time point
500254/	1	0.85 × 1.03	0.3721	ZT00
500255R	1	1.0 × 0.76	0.2888	ZT00
500232/	6	0.65 × 0.99; 1.07 × 0.69; 0.16 × 0.19; 0.32 × 0.31; 0.27 × 0.21; 0.37 × 0.38	0.5136	ZT00
500204RR	2	1.19 × 0.89; 1.09 × 0.69	0.7308	ZT06
500200/	4	0.63 × 0.65; 0.62 × 0.66; 0.81 × 0.94; 1.32 × 1.65	2.002	ZT06
500210/	5	0.98 × 0.77; 0.51 × 0.63; 0.28 × 0.31; 0.26 × 0.3; 0.45 × 0.49	0.4444	ZT06
500228L	3	1.68 × 1.11; 0.31 × 0.38; 0.61 × 0.5	1.1295	ZT12
500242/	2	0.64 × 1.26; 0.27 × 0.42	0.2734	ZT12
500253L	2	1.16 × 1.26; 0.91 × 0.95	1.2411	ZT12
500230R	3	0.43 × 0.32; 0.73 × 1.12	0.3204	ZT18
500229/	3	0.35 × 0.49; 0.36 × 0.29; 0.2 × 0.17	0.0480	ZT18
500209RR	10	0.4 × 0.74; 0.66 × 0.48; 0.34 × 0.41; 0.4 × 0.43; 0.38 × 0.42; 0.58 × 0.5; 0.39 × 0.44; 0.97 × 0.74; 1.36 × 0.8; 0.66 × 0.74	1.193	ZT18
Immunostaining				
Mouse ID	Number of tumors	Size diameters (cm)	Tumor volume (cm^3)	Time point
463663L	1	1.2 × 0.61	0.2233	ZT00
463665RR	3	0.25 × 0.36; 0.22 × 0.26; 0.23 × 0.27	0.0247	ZT00
466832RL	2	0.2 × 0.32; 0.32 × 0.51	0.0325	ZT00
463664RL	1	1.34 × 0.68	0.3098	ZT06
466835R	4	0.70 × 0.69; 0.29 × 0.35; 0.32 × 0.37; 0.32 × 0.44	0.2228	ZT06
469617L	2	0.36 × 0.36; 0.24 × 0.21	0.0286	ZT06
463666LL	1	1.13 × 0.58	0.1901	ZT12
466836L	5	0.56 × 0.87; 0.64 × 0.44; 0.18 × 0.3; 0.27 × 0.23; 0.18 × 0.19	0.2134	ZT12
470729R	1	0.49 × 0.4	0.0392	ZT12
463662R	1	0.35 × 0.3	0.0158	ZT18
463667/	3	0.36 × 0.21; 0.45 × 0.3; 0.2 × 0.26	0.0334	ZT18
469615/	2	0.46 × 0.76; 1.37 × 1.5	1.6217	ZT18
OSC				
Mouse ID	Number of tumors	Size diameters (cm)	Tumor volume (cm^3)	
500166/	5	0.28 × 0.29; 0.34 × 0.29; 0.56 × 0.53; 0.87 × 0.83; 0.21 × 0.2	0.4082	
500146L	2	0.79 × 0.97; 0.44 × 0.51	0.3427	
500150R	4	0.75 × 0.44; 0.46 × 0.46; 0.55 × 0.39; 0.37 × 0.46	0.1946	
500158/	2	1.26 × 1.14; 0.81 × 0.8	1.0779	
500174L	2	0.94 × 0.7; 0.53 × 0.41	0.2748	
500176/	2	0.38 × 0.34; 0.87 × 0.61	0.1838	
500155R	1	0.86 × 0.67	0.1930	

Note: Time point indicates killing of the animals.

investigations, the animals (n = 3/ZT) were decapitated at ZT00 (light on), ZT06, ZT12 (light off) and ZT18 and healthy liver tissue and tumors were excised separately, frozen rapidly in liquid nitrogen and stored at −80°C until further use. The experiments during the night were performed under dim red light.

2.3 | In vitro investigations of organotypic slice cultures

For in vitro investigations, six animals were sacrificed at 10:00 AM (ZT04) and healthy liver tissue and tumors were freshly excised under

sterilized conditions and kept in cold storage solution (MACS tissue storage solution, Miltenyi Biotec, Bergisch Gladbach, Germany). Organotypic slice cultures (OSC) were prepared using a Krumdieck tissue chopper (TSE Systems, Bad Homburg, Germany). Healthy liver tissue and tumors were sliced separately in ice-cold sterilized Dulbecoo's phosphate-buffered saline (DPBS) (Gibco by Life Technologies, Paisley, UK). The slices (250 μm thick) were transferred to cell culture inserts (0.4 μm pores, Falcon, Durham, North Carolina) which were put in six-well plates filled with 1 mL prewarmed culture medium modified after.[19] The medium consisted of DMEM, supplemented with 10% fetal bovine serum, 100 U/mL penicillin, 0.1 mg/mL streptomycin, 10 mmol/L HEPES, 1 mg/mL insulin, 8 mg/mL ascorbic acid and 20 mmol/L sodium pyruvate. All slices were cultured under constant conditions of 37°C and 5% CO_2 for 24 hours. The slices from healthy liver tissue and tumors were harvested at four different circadian time (CT) points; CT04, CT10, CT16 and CT22. CT00 is defined as the onset of the former light phase (6:00 AM). Slices to be used for immunohistochemistry were fixed in 4% PFA in PBS for 12 hours. The fixed slices were cryoprotected with gradually increasing concentrations of sucrose (15 and 30%) for at least 24 hours and then cryosectioned separately into 10 μm thick serial sections. The unfixed slices were quickly frozen on liquid nitrogen and stored at −80°C for qPCR investigations.

2.4 | Immunofluorescence staining

Cell proliferation (Ki67) and DNA-DSBs (γ-H2AX) were investigated in ex vivo and OSC samples of healthy liver and tumors of c-myc/TGFα mice harvested at different ZTs and CTs. To reduce nonspecific staining, sections were preincubated in normal goat serum (1:20) diluted in PBS with 0.3% Triton (PBST) for 1 hour at room temperature. Sections were then incubated with primary antibodies against Ki67 (1:200, KI6891C01, DCS, Hamburg, Germany) or against γ-H2A.X (1:100, #2577, Cell Signaling Technology, Frankfurt am Main, Germany) diluted in 1% bovine serum albumin (BSA) in PBST at room temperature overnight. On the next day, sections were incubated with the secondary goat antirabbit antibodies diluted in PBST (1:250, Alexa 568 for Ki67 or Alexa 488 for γ-H2AX, Life Technologies, San Diego, California) for 1 hour in darkness at room temperature. Finally, all sections were stained with Hoechst nucleus dye diluted in PBS (1:10 000) for 5 minutes in darkness at room temperature. The stained sections were covered by fluorescent mounting media (Dako, Glostrup, Denmark). To verify the results from the immunostaining, negative controls were incubated with the secondary antibodies only.

2.5 | Data acquisition

For the quantitative analysis of the number of cells which are positively stained with Ki67 or γ-H2AX, six representative images from each animal and each time point were taken using a confocal laser microscope (Olympus Fluo view SC20, Japan) at 20× objective. For each type of staining, the microscope settings were kept constant. The number of positive cells was counted manually in a total area = 409.6 mm^2 using Photoshop CS3 program (v10, Adobe, San Jose, California) by an investigator not familiar with the experimental protocol.

2.6 | Real-time PCR

Total RNA from healthy liver and tumor tissue was extracted using RNeasy Plus Universal Mini Kit (QIAGEN, Hilden, Germany). RNA purity and concentration were measured using a Nano-Drop spectrophotometer. Then cDNA was synthesized from total RNA (1 μg) using Revert Aid First Strand cDNA Synthesis Kit (Thermo Scientific, Vilnius, Lithuania). Relative expression of mRNA for target genes was measured using quantitative real-time PCR (qRT-PCR; Step One Plus; Applied Biosystems), SYBR GREEN (Kapa Abi-Prism) and specific primers for clock genes (all Sigma Aldrich, Table 2). All PCR amplificates were examined by conventional PCR and gel analyses. Expression of target genes was normalized to β-actin. Relative mRNA expression of genes was finally calculated by use of the Pfaffl method.[20]

2.7 | Statistical analysis

Statistics were calculated by using Graph Pad Prism 8 software. The results were expressed as mean ± SE of the mean (SEM). The significant differences for circadian effect in healthy liver and tumor were tested by RM One-Way analysis of variance (ANOVA) for OSC

TABLE 2 qPCR list of primers

Gene	Sequence
mPer2 F	5′-CCAAACTGCTTGTTCCAGGC-3′
mPer2 R	5′-ACCGGCCTGTAGGATCTTCT-3′
mCry1 F	5′-CTT CTG TCT GAT GAC CAT GAT GA-3′
mCry1 R	5′-CCC AGG CCT TTC TTT CCA A-3′
mCry2 F	5′-AGG GCT GCC AAG TGC ATC AT-3′
mCry2 R	5′-AGG AAG GGA CAG ATG CCA ATA G-3′
mClock F	5′-CAC CGA CAA AGA TCC CTA CTG AT-3′
mClock R	5′-TGA GAC ATC GCT GGC TGT GT-3′
mPer1 F	5′-TGG CTC AAG TGG CAA TGA GTC-3′
mPer1 R	5′-GGC TCG AGC TGA CTG TTC ACT-3′
β-Actin F	5′-GGCTGTATTCCCCTCCATGC-3′
β-Actin R	5′-CCAGTTGGTAACAATGCCATGT-3′
Rev-erb α F	5′-GGT GCG CTT TGC ATC GTT-3′
Rev-erb α R	5′-GGT TGT GCG GCT CAG GAA-3′
Bmal F	5′-GTA GAT CAG AGG GCG ACA GC-3′
Bmal R	5′-CCT GTG ACA TTC TGC GAG GT-3′

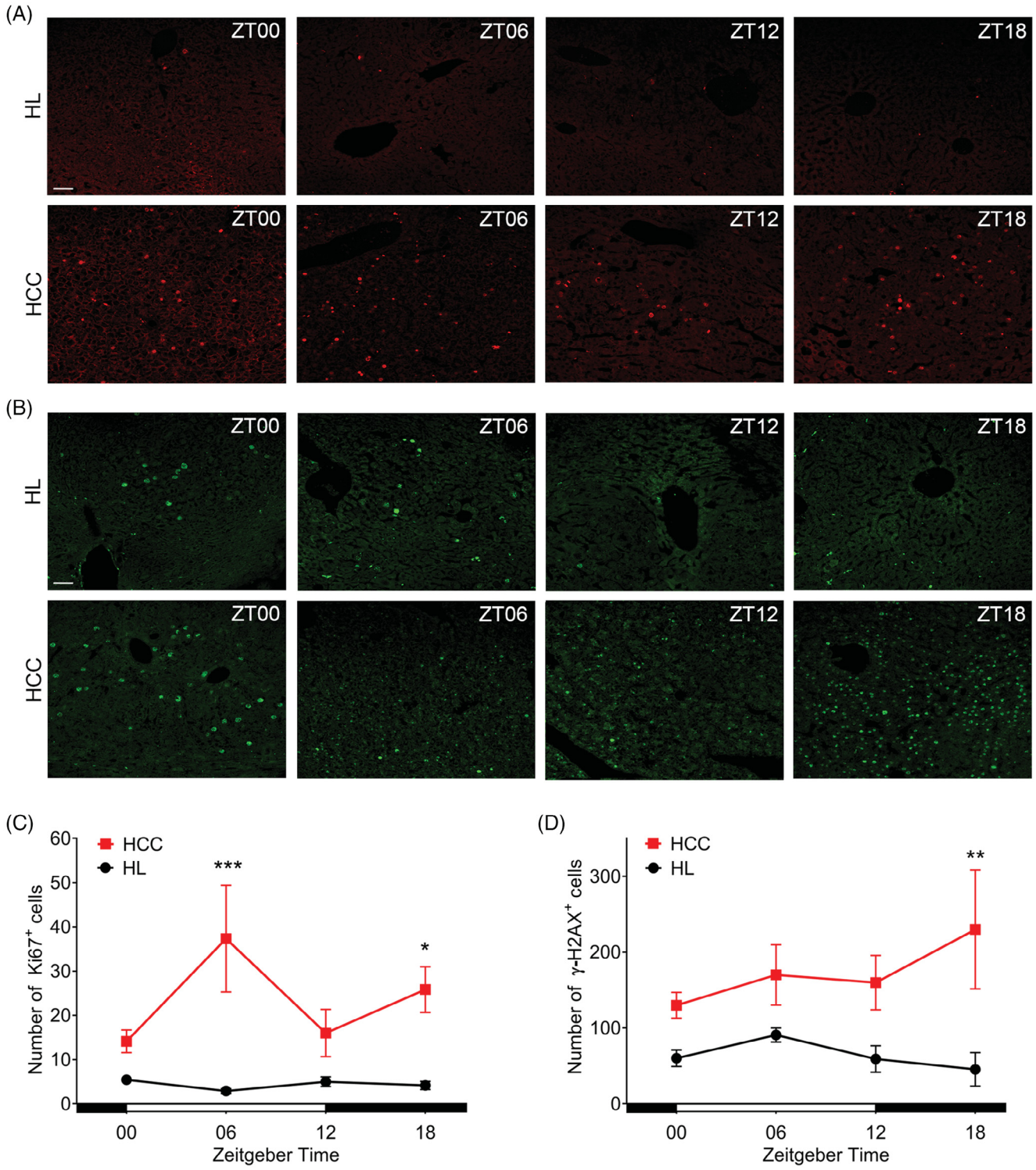

FIGURE 1 Ex vivo analyses of Ki67 and γ-H2AX in hepatocellular carcinoma (HCC) and surrounding healthy liver (HL) of c-myc/TGFα mice. The mice (n = 3 mice per time point) were killed at different *Zeitgeber* time (ZT) points, ZT00, ZT06, ZT12 and ZT18. A, Representative photomicrographs of Ki67 immunoreaction in HCC and HL at different ZTs. B, Representative γ-H2AX immunoreaction in HCC and HL at different ZTs. C, Number of Ki67 immunoreactive cells in HCC (red) and HL (black). D, Number of γ-H2AX immunoreactive cells in HCC (red) and HL (black). Plotted are the mean numbers ± SEM of immunoreactive cells. White and black bars indicate day and night, respectively. $^{*}P < .05$, $^{**}P < .01$, $^{***}P < .001$ differences between HCC and HL. Scale bars, 50 μm [Color figure can be viewed at wileyonlinelibrary.com]

samples and Ordinary One-Way analysis of variance (ANOVA) for ex vivo samples followed by Tukey's test for multiple comparisons between different time points. Two-Way analysis of variance (ANOVA) was used to validate differences according to time and tissue followed by Sidak's test for multiple comparisons between groups. The results were regarded as significant at $P < .05$.

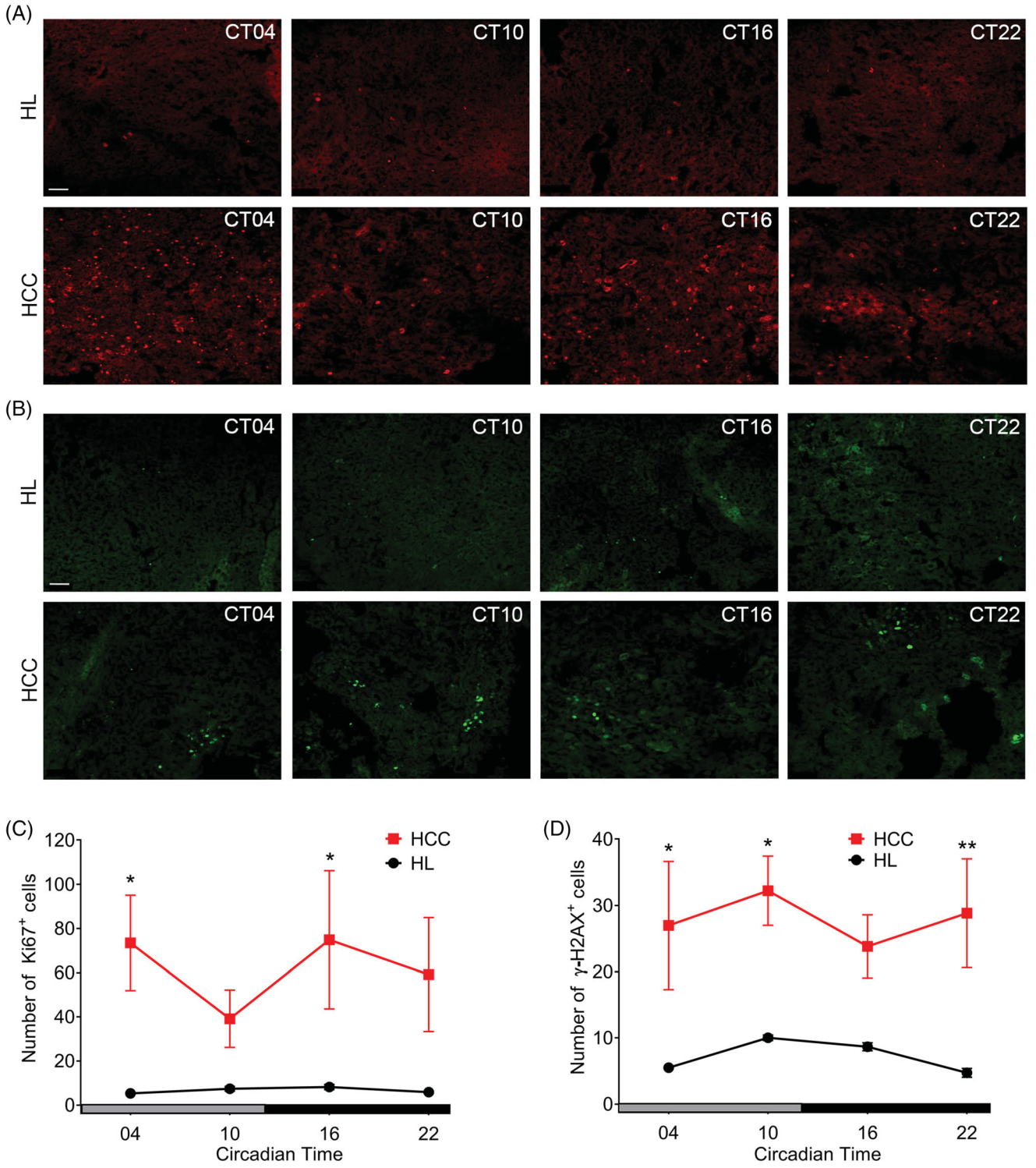

FIGURE 2 In vitro analyses of Ki67 and γ-H2AX in hepatocellular carcinoma (HCC) and the surrounding healthy liver (HL) of OSC from c-myc/TGFα mice. The slices (n = 6 per time point) were collected at different circadian time (CT) points. A, Representative photomicrographs of Ki67 immunoreaction in HCC and HL at different CTs. B, Representative γ-H2AX immunoreaction in HCC and HL at different CTs. C, Number of Ki67 immunoreactive cells in HCC (red) and HL (black). D, Number of γ-H2AX immunoreactive cells in HCC (red) and HL (black). Plotted are the mean numbers ± SEM of immunoreactive cells. Gray and black bars indicate the former day and night, respectively. *P < .05, **P < .01 differences between HCC and HL. Scale bars, 50 μm [Color figure can be viewed at wileyonlinelibrary.com]

3 | RESULTS

3.1 | Investigation of Ki67 and γ-H2AX immunoreactivity in HCC and surrounding HL

These investigations were performed in both, ex vivo samples and OSC. In ex vivo samples, the number of Ki67 immunoreactive cells was very low in healthy liver and did not change significantly at the four time points investigated. As expected, the number of Ki67 immunoreactive cells was higher in HCC than in HL (Figure 1A). In HCC, the number of Ki67 immunoreactive cells showed a maximum at midday (ZT06) and second, smaller peak at midnight (ZT18) and a minimum in the morning (ZT00; Figure 1C). The differences in the number of proliferating Ki67 immunoreactive cells between HCC and HL were very highly significant at ZT06 ($P < .001$) and significant at ZT18 ($P < .05$) as shown by

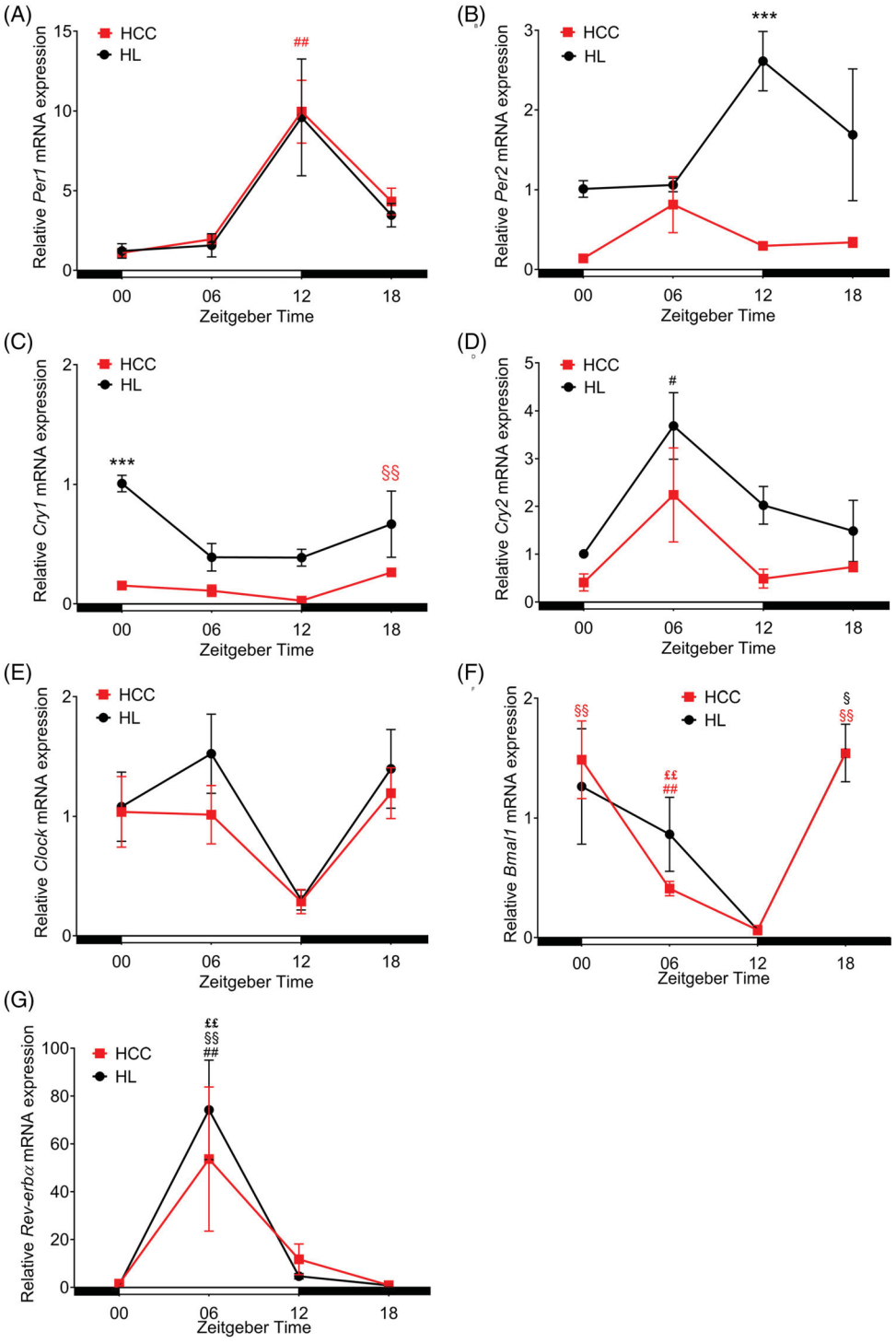

FIGURE 3 Ex vivo analyses of clock genes expression in hepatocellular carcinoma (HCC, red) and the surrounding healthy liver (HL, black) of c-myc/TGFα mice by real time qPCR. The mice (n = 3 mice per time point) were killed at different *Zeitgeber* time points. A, Relative expression of *Per1* in HCC and HL. B, Relative expression of *Per2* in HCC and HL. C, Relative expression of *Cry1* in HCC and HL. D, Relative expression of *Cry2* in HCC and HL. E, Relative expression of *Clock* in HCC and HL. F, Relative expression of *Bmal 1* in HCC and HL. G, Relative expression of *Rev-erbα* in HCC and HL. Plotted are the mean relative mRNA expression ± SEM of clock genes. White and black bars indicate day and night, respectively. ***$P < .001$ differences between HCC and HL. #$P < .05$; ##$P < .01$ differences between this ZT and ZT00. §$P < .05$; §§$P < .01$ differences between this ZT and ZT12. ££$P < .01$ differences between this ZT and ZT18 [Color figure can be viewed at wileyonlinelibrary.com]

two-way ANOVA followed by Sidak's multiple comparisons test (Figure 1C).

As a marker for DNA-DSBs repair, γ-H2AX immunoreactivity was investigated in the same ex vivo samples. The number of γ-H2AX immunoreactive cells was higher in HCC than in HL (Figure 1B). In HCC, the number of γ-H2AX immunoreactive cells showed a peak at midnight (ZT18). At ZT18, the difference between HCC and HL was highly significant ($P < .01$, Figure 1D).

Ki67 and γ-H2AX immunoreactivities were also investigated in OSC of HL and HCC of c-myc/TGFα mice. The OSC were cultured for 24 hours and thereafter fixed at four time points (CT04, CT10, CT16 and CT22). The number of Ki67 immunoreactive cells was higher in HCC than in HL (Figure 2A). Two-way ANOVA showed that the difference between HCC and HL was significant at CT04 and CT16 ($P < .05$, Figure 2C). The number of γ-H2AX immunoreactive cells was higher in HCC than in the surrounding HL. The differences in the number of γ-H2AX immunoreactive cells between HL and HCC were significant at CT04 and CT10 ($P < .05$) and highly significant at CT22 ($P < .01$; Figure 2D).

3.2 | Investigations of Clock genes expression in HCC and surrounding HL

Expression of clock genes *Per1*, *Per2*, *Cry1*, *Cry2* and *Clock* was investigated in HCC and HL using qPCR in both, ex vivo samples and OSC. In addition, expression of *Bmal 1 and Rev-erb α* was analyzed in the ex vivo samples.

In ex vivo samples, the relative expression of *Per1* showed a peak at ZT12 in HL which tended to be different from ZT00 ($P = .058$) and ZT06 ($P = .07$). A peak at ZT12 was also observed in HCC which was significantly different from the values at ZT00 and ZT06 ($P < .01$) and at ZT18 ($P < .05$; Figure 3A). The relative expression of *Per1* did not differ significantly between HL and HCC at all time points investigated ($P > .1$, Figure 3A).

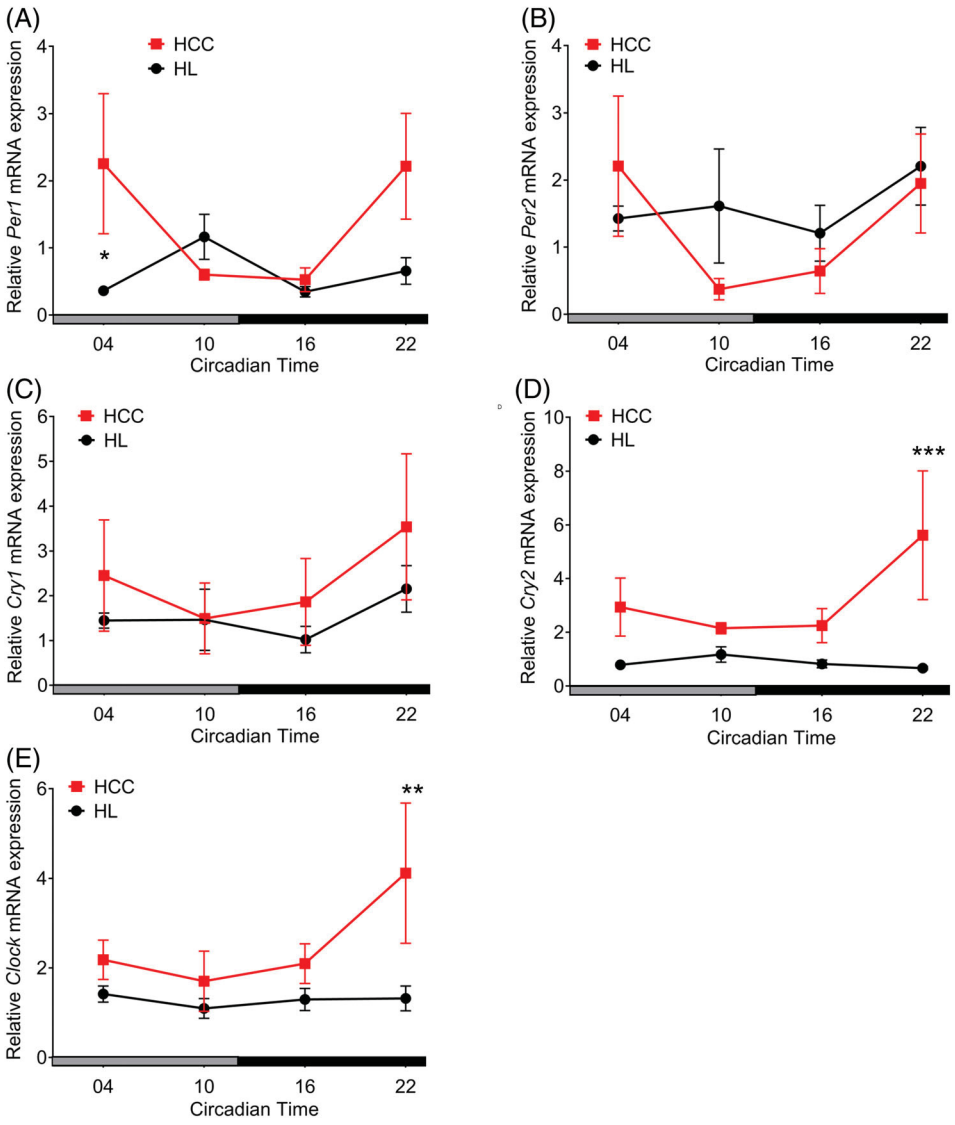

FIGURE 4 In vitro analyses of clock genes expression in hepatocellular carcinoma (HCC, red) and the surrounding healthy liver (HL, black) of OSC from c-myc/TGFα mice. The slices (n = 6 per time point) were collected at different circadian time points. A, Relative expression of *Per1* in HCC and HL. B, Relative expression of *Per2* in HCC and HL. C, Relative expression of *Cry1* in HCC and HL. D, Relative expression of *Cry2* in HCC and HL E, Relative expression of *Clock* in HCC and HL. Plotted are the mean relative mRNA expression ± SEM of clock genes. Gray and black bars indicate the former day and night, respectively. *$P < .05$, **$P < .01$ and ***$P < .001$ differences between HCC and HL [Color figure can be viewed at wileyonlinelibrary.com]

The relative expression of *Per2* in HL did not change significantly between day and night (Figure 3B). The relative expression of *Per2* was decreased in HCC as compared to the surrounding HL and this difference was highly significant at ZT12 ($P < .001$, Figure 3B).

The relative expression of *Cry1* in HL showed a maximum at ZT00 which tended to be different from the values at ZT06 and ZT12 ($P = .09$). In contrast, the HCC showed a peak at ZT18 which was significantly different from the values at ZT12 ($P < .01$) and ZT06 ($P < .05$; Figure 3C). The relative expression of *Cry1* was lower in HCC than in HL and the two-way ANOVA showed that this difference was significantly different at ZT00 ($P < .001$) and tended to be significant at ZT18 ($P = .09$, Figure 3C).

The relative expression of *Cry2* in HL showed a peak at (ZT06) which was significantly different from the values at ZT00 ($P < .05$) and tended to be different from those at ZT18 ($P = .06$). The relative expression of *Cry2* in HCC showed no significant changes during the day ($P > .1$, Figure 3D). The relative expression of *Cry2* was lower in HCC than the HL although the difference between HCC and HL was not significant at all investigated time points as shown by two-way ANOVA ($P > .1$, Figure 3D).

The relative expression of *Clock* changed during the day in the HCC and the surrounding HL. The values at ZT12 tended to be different from those at ZT06 ($P = .056$) and ZT18 ($P = .09$) in the HL and at ZT18 ($P = .08$) (Figure 3E) in the HCC. No significant changes were detected comparing the relative expression of *Clock* in HL and the HCC at the all investigated time points using the two-way ANOVA test ($P > .1$, Figure 3E).

The relative expression of *Bmal 1* in HL and HCC revealed a peak at (ZT18) which significantly differed from the values at ZT12 ($P < .05$ and $P < .01$; respectively). In HCC, ZT18 also showed a significant difference from ZT06 ($P < .01$). The value at ZT00 was significantly different from ZT06 and ZT12 ($P < .01$, Figure 3F). The relative expression of *Bmal* did not differ significantly between HL and HCC at all time points investigated ($P > .1$, Figure 3F).

The relative expression of *Rev-erb* α in HL showed a maximum at ZT06 which was significantly different from the values at ZT00, ZT12 and ZT18 ($P < .01$, Figure 3G). A maximum at ZT06 was also observed in HCC but it did not differ significantly from the other ZTs. No significant differences were detected comparing the relative expression of *Rev-erb* α in HL and HCC at all time points investigated. In the OSC, the relative expression of *Per1*, *Per2*, *Cry1*, *Cry2* and *Clock* showed a trend to daily variation in HCC and HL but the differences were not significant between day and night ($P > .1$, Figure 4). The relative expression was significantly higher in HCC than in HL for *Per1* at CT04 ($P < .05$), for *Cry2* at CT22 ($P < .001$) and for *Clock* at CT22 ($P < .01$; Figure 4, two-way ANOVA followed by Sidak's multiple comparisons test).

4 | DISCUSSION

An important topic in oncology is whether timing plays a role in antimitotic therapy. Taking this topic into consideration we have addressed three questions in the present study: (a) Do cell proliferation and DNA damage repair mechanisms show a distinct temporal pattern that would help to determine the optimal time point(s) for antimitotic therapy? (b) Does the expression of clock genes differ between normal and tumor tissue? (c) Are organotypic slice cultures an appropriate model to determine the optimal time point(s) for antimitotic therapies? The investigations were performed with a well-established animal model for hepatocellular carcinomas, the double transgenic c-myc/TGFα mice.

4.1 | Do cell proliferation and DNA damage repair mechanisms show a distinct temporal pattern that would help to determine the optimal time point(s) for antimitotic therapy?

Markers which reflect cell proliferation and DNA damage repair mechanisms are used for early detection of tumors, prediction of tumor development and assessment of the tumor response to therapy.[13] We have assessed cell proliferation by means of immunohistochemical demonstration of Ki67, a nuclear antigen expressed in proliferating cells. As biomarker for DNA damage and repair,[10,13] we have investigated γ-H2AX.

Our investigations of ex vivo samples revealed that the number of Ki67 immunoreactive cells was much higher in the HCC than in the surrounding HL. Lin et al[21] reported that Wee1 (one of the cell cycle mitotic inhibitor) was decreased, while Cyclin B and CDC2 (cell cycle control genes) and cell cycle- related proteins (eg, cyclin A) were overexpressed in the HCCs as compared to healthy, noncancerous liver tissue. This disturbance in the expression of cell cycle regulators could explain the higher number of proliferating rate (Ki67) in HCC as compared to the surrounding HL.[21]

In HCC, the number of Ki67 immunoreactive cells showed a maximum at midday (ZT06) and second, smaller peak at midnight (ZT18). These results are in agreement with a study by You et al[22] who showed that mammary tumors had two daily growth rate peaks, one minor at mid-sleep and one major peak at mid-activity. Two proliferation peaks were also observed in other fast-growing tumors.[9,23] In an early study, fast and slow growing hepatomas showed two mitotic activity peaks, one during the light phase and the other during dark phase.[24] It is well known that the expression of cell cycle regulators which either promote or inhibit cell proliferation are affected by the circadian clockwork. In mammary tumor, the expression of some known clock-controlled cell cycle genes which promote cell proliferation, such as CycD1 and C-Myc as well as cancer cell mitosis showed two peaks during the day, one at mid-day and the other at the midnight,[22,25] whereas only one peak was found in healthy tissue.

A highly relevant result of our ex vivo studies was that the difference in number of proliferating Ki67 immunoreactive cells between the HCC and the HL was significant at ZT06 (midday) and at ZT18 (midnight). Since it is well known that highly proliferating cells become more sensitive to DNA damage with cancer therapies,[26,27] we conclude that midday and midnight may be considered as optimal time

points to apply antimitotic therapies to HCC with minimum side effects on the surrounding HL. This assumption now needs to be confirmed in further experiments. Since the two peaks occurred at midday and midnight, the findings in nocturnal species (mouse) might be easily transferred to diurnal species (eg, primates).

We then investigated γ-H2AX, a histone which accumulates in the damaged sites of DNA-DSBs in ex vivo samples. The number of γ-H2AX immunoreactive cells was higher in the HCC than in the surrounding HL. This conforms to previous investigations by Kim et al[28] and Matsuda et al[29] who showed that γ-H2AX was significantly increased in different human liver diseases including chronic hepatitis, HBV-related liver cirrhosis and HBV-related HCC as compared to normal and noncancerous tissues. Increased levels of γ-H2AX were also found in human tumors of the urinary bladder, breast, lung and colon.[30,31]

As shown by our study the number of γ-H2AX immunoreactive cells showed a trend to daily variation in the HCC and the surrounding HL. The mechanism behinds these changes remain to be elucidated. One possibility is that ATM → Chk2 signaling pathway which is mainly activated by double-strand breaks is subjected to the circadian rhythm of the clock genes.[32] Other publications also reported that cellular responses to DNA damage and repair process are influenced by the circadian rhythm. XPA, one of the DNA repair protein, was shown to be controlled by the circadian clock in the mouse brain, liver and skin.[33-35] Kang et al[34] found that the activity of nucleotide excision repair (NER) is highest in the afternoon/evening hours and lowest in the night/early morning hours in mouse brain. Thus, it is very important in cancer treatment protocols to take into consideration the circadian oscillation of cellular DNA repair molecules.

4.2 | Does the expression of clock genes differ between healthy and tumor tissue?

Cell cycle and proliferation are closely intertwined with the molecular circadian clockwork and there is increasing evidence that cancer development and progression may be associated with dysfunction or mutation of this molecular clockwork. We therefore investigated the expression of seven core clock genes, *Per1*, *Per2*, *Cry1*, *Cry2*, *Bmal 1*, *Rev-erbα* and *Clock*, in HL and HCC at four different time points. Relative mRNA expression of all seven clock genes was shown to change between day and night in HL of c-myc/TGFα bitransgenic mice. Similar patterns were found in HL of non-transgenic mice.[36] Notably, mRNA expression of *Per1*, *Cry2*, *Bmal 1*, *Rev-erbα* and *Clock* in the HCC had the same daily patterns as in the HL with similar peaks. In line with these results, Yang et al[37] reported that the daily expression of core clock genes maintains circadian rhythms within normal and tumor tissues of mice and concluded that the circadian clock remains functional in tumors. Two studies on buccal mucosal carcinogenesis showed that the daily rhythmic mRNA expression of *Per1* and *Per2* was similar in normal buccal mucosa and carcinoma stages and the acrophase occurred at approximately the same time.[8,38]

Notably, in our study, the peaks of mRNA expression of *Per2* and *Cry1* differed between the HCC and the surrounding HL and the expression of *Per2*, *Cry1* and *Cry2* was lower in the HCC than the surrounding HL. Lowered expression of *Per2* and *Cry2* was also observed in human HCC[21,39] and the amplitude of *Cry1* and *Cry2* were decreased in mouse livers treated with diethylnitrosamine and in human colorectal liver metastasis.[40,41] Downregulation of different core clock genes was also reported in gastric, colorectal, pancreatic, prostate, breast, lung cancer, chronic lymphocytic leukemia, colorectal liver metastasis and HCC.[39-42]

Downregulation of clock genes may result from a hypoxic microenvironment which is a common feature in most solid tumors. Although HCC is one of the most hypervascularized types of tumors, it contains hypoxic regions due to rapid cell proliferation and the formation of aberrant blood vessels. Hypoxia can activate HIF-1α and HIF-1β and the overexpression of these transcription factors may contribute to the disturbed expression of clock genes in HCC cells. HIF also controls the expression of glycolytic enzymes which are responsible for acidic tumor environment, and this acidity is thought to act on the tumor cellular clocks.[21,43,44] Downregulation of clock genes may also relate to the overexpression of factors that play an important role in the methylation of gene promoters which lead to inhibition of gene expressions as well as phosphorylation and degradation of clock genes. Thus, EZH2 and CK1ε gene expression levels were strongly increased in HCC and colorectal liver metastasis, as compared to noncancerous tissues.[21,42,43]

Our data showed no changes in the expression of the *Bmal 1*, *Rev-erbα* and *Clock* gene in the HCC as compared to the surrounding HL. The same results were reported also for *Bmal1* and *Clock* in the human HCC.[21,45] The reason for this is unclear and further studies are needed to clarify whether downregulation of some clock genes is associated with more advanced cancer stages.[46]

The *Per2* gene appears to be a functionally more relevant in the mammalian circadian clock than the *Per1* gene.[47] Lower expression of *Per2* was shown to elicit more profound effects on the tumor growth, both in vitro and in vivo than lower expression of *Per1*.[25] In gastric cancer, the *Per2* expression was reported to be a potential prognostic factor and lower expression of *Per2* might help identify gastric cancer patients with a poor prognosis. Also, in chronic lymphocytic leukemia, the ratio between PER2 and CRY1 is suggested to be a prognostic marker that predicts the survival outcomes of patients.[43] In line with these results, *Per2* and *Cry1* may play a more important role for cell cycle disruption and HCC growth than the other core clock genes investigated here.

4.3 | Are organotypic slice cultures an appropriate model to determine the optimal time point(s) for anticancer therapies?

OSC is a model which is made from primary tissue and maintains the three-dimensional structure as well as the extracellular matrix.[48] OSC of normal liver was shown to be viable in culture conditions for several days and to keep a robust circadian rhythm.[17,49] The present study with OSC which includes HCC and the surrounding HL showed

that the number of Ki67 and γ-H2AX immunoreactive cells was much higher in the HCC than in the HL as was also observed in ex vivo samples. The number of Ki67 immunoreactive cells showed two peaks which occurred at CT04 and CT16 and thus slightly differed from the time points which were observed in the ex vivo samples (ZT06 and ZT18). Notably, also the expression pattern and amplitudes of the clock genes differed between the OSC and ex vivo samples. This difference may be due to the lack of entrainment signals which under in vivo conditions are transmitted derived from the master oscillator of the circadian system, the suprachiasmatic nucleus, to the periphery via neuronal pathways or the blood stream. It is well known that temperature can act as physical synchronizer and resetting cue for circadian peripheral oscillators.[50] The fact that the temperature was kept constant in our culture experiments may contribute to the differences between OSC and ex vivo samples, although previous studies using identical, constant culture conditions[17,49] have shown that OSC kept a robust circadian rhythm under constant temperature. The stress generated by the dissection process and the initiation of the culture may also contribute to these observed differences. The results suggest that OSC may be helpful to establish therapeutic strategies, but it remains to be established whether are suited to determine the optimal time points of antimitotic therapies.

In conclusion, our study with an experimental mouse model for hepatocellular carcinoma showed significant differences in proliferation rate as well as DNA damage and repair mechanisms between the HCC and the HL. The observation that the proliferation rate in the HCC showed two distinct peaks indicates that the efficacy of antimitotic therapies depends on the timing. Future studies in oncology should consider this time dependency and determine the optimal time point(s) for anticancer therapy for each tumor entity. Since γ-H2AX expression was higher in the HCC than in the HL, it can be used as a marker to determine HCC sensitivity to the antimitotic treatment. Since expressions of *Per2* and *Cry1* were significantly lower and had different daily variation patterns in the HCC and the HL, these two clock genes might be closely linked to development and growth of the HCC. Overall, OSC may become a suitable model to develop and test anticancer strategies; however, future studies are needed to prove whether they could substitute for whole animal studies with regard to determination of the optimal time points for therapy.

ACKNOWLEDGEMENTS

S. A. H. is supported by German Egyptian Research Long-term Scholarship (GERLS) Program of the DAAD. We are grateful to Prof Nürnberger (Institute of Anatomy II, Goethe University, Frankfurt am Main, Germany) for continuous support and advice. We thank Snorri Thorgeirsson (National Cancer Institute, NIH, Bethesda) for providing the mice transgenic for c-myc and TGFα. We thank Hanna Bellert, Ralf Fassbender, Angelika Hallenberger and Ursula Lammersen for excellent technical support. Open access funding enabled and organized by Projekt DEAL.

CONFLICT OF INTEREST

The authors have no conflict of interest.

DATA AVAILABILITY STATEMENT

The data will be made available upon reasonable request. https://www.researchgate.net/profile/Horst-Werner_Korf.

ETHICS STATEMENT

The experiments described in our study were conducted according to accepted standards of humane animal care and were consistent with federal guidelines and Directive 2010/63/EU of the European Union. They were approved by the Regierungspräsidium Darmstadt (Gen. Nr. FU 1067).

ORCID

Horst-Werner Korf https://orcid.org/0000-0002-5051-0303

REFERENCES

1. IARC. Latest global cancer data: cancer burden rises to 18.1 million new cases and 9.6 million cancer deaths in 2018. No. 263. Press Release; 2018.
2. Trojan J, Zangos S, Schnitzbauer AA. Diagnostics and treatment of hepatocellular carcinoma in 2016: standards and developments. *Visc Med*. 2016;32:116-120.
3. Schlageter M, Terracciano LM, D'Angelo S, Sorrentino P. Histopathology of hepatocellular carcinoma. *World J Gastroenterol*. 2014;20:15955-15964.
4. Wild AT, Gandhi N, Chettiar ST, et al. Concurrent versus sequential sorafenib therapy in combination with radiation for hepatocellular carcinoma. *PLoS One*. 2013;8:e65726.
5. Rebouissou S, La Bella T, Rekik S, et al. Proliferation markers are associated with MET expression in hepatocellular carcinoma and predict Tivantinib sensitivity in vitro. *Clin Cancer Res*. 2017;23:4364-4375.
6. Ballesta A, Innominato PF, Dallmann R, Rand DA, Levi FA. Systems Chronotherapeutics. *Pharmacol Rev*. 2017;69:161-199.
7. Liu SL, Han Y, Zhang Y, et al. Expression of metastasis-associated protein 2 (MTA2) might predict proliferation in non-small cell lung cancer. *Target Oncol*. 2012;7:135-143.
8. Ye H, Yang K, Tan XM, Fu XJ, Li HX. Daily rhythm variations of the clock gene PER1 and cancer-related genes during various stages of carcinogenesis in a golden hamster model of buccal mucosa carcinoma. *Onco Targets Ther*. 2015;8:1419-1426.
9. Wood PA, Du-Quiton J, You S, Hrushesky WJ. Circadian clock coordinates cancer cell cycle progression, thymidylate synthase, and 5-fluorouracil therapeutic index. *Mol Cancer Ther*. 2006;5:2023-2033.
10. Shi W, Hu JF, Zhu SZ, et al. Expression of MTA2 and Ki-67 in hepatocellular carcinoma and their correlation with prognosis. *Int J Clin Exp Pathol*. 2015;8:13083-13089.
11. Sun X, Kaufman PD. Ki-67: more than a proliferation marker. *Chromosoma*. 2018;127:175-186.
12. Kuo LJ, Yang L. γ-H2AX—a novel biomarker for DNA double-strand breaks. *In Vivo*. 2008;22:305-310.
13. Sedelnikova OA, Bonner WM. GammaH2AX in cancer cells: a potential biomarker for cancer diagnostics, prediction and recurrence. *Cell Cycle*. 2006;5:2909-2913.
14. Thorgeirsson SS, Santoni-Rugiu E. Transgenic mouse models in carcinogenesis: interaction of c-myc with transforming growth factor alpha and hepatocyte growth factor in hepatocarcinogenesis. *Br J Clin Pharmacol*. 1996;42:43-52.
15. Schibler U, Ripperger J, Brown SA. Peripheral circadian oscillators in mammals: time and food. *J Biol Rhythms*. 2003;18:250-260.
16. Korf H-W, von Gall C. Circadian physiology. In: Pfaff DW, ed. *Neuroscience in the 21st Century: From Basic to Clinicaled*. New York, NY: Springer; 2013:1813-1845.

17. Muller MH, Rodel F, Rub U, Korf HW. Irradiation with X-rays phase-advances the molecular clockwork in liver, adrenal gland and pancreas. *Chronobiol Int*. 2015;32:27-36.
18. Schmithals C, Koberle V, Korkusuz H, et al. Improving drug penetrability with iRGD leverages the therapeutic response to Sorafenib and doxorubicin in hepatocellular carcinoma. *Cancer Res*. 2015;75:3147-3154.
19. Verrill C, Davies J, Millward-Sadler H, Sundstrom L, Sheron N. Organotypic liver culture in a fluid-air interface using slices of neonatal rat and adult human tissue—a model of fibrosis in vitro. *J Pharmacol Toxicol Methods*. 2002;48:103-110.
20. Pfaffl MW. Quantification strategies in real-time PCR. In: Bustin SA, ed. *A-Z of quantitative PCR*. La Jolla, CA: International University Line (IUL); 2004:87-112.
21. Lin YM, Chang JH, Yeh KT, et al. Disturbance of circadian gene expression in hepatocellular carcinoma. *Mol Carcinog*. 2008;47:925-933.
22. You S, Wood PA, Xiong Y, Kobayashi M, Du-Quiton J, Hrushesky WJ. Daily coordination of cancer growth and circadian clock gene expression. *Breast Cancer Res Treat*. 2005;91:47-60.
23. Kobayashi M, Wood PA, Hrushesky WJM. Circadian chemotherapy for gynecological and genitourinary cancers. *Chronobiol Int*. 2009;19:237-251.
24. Echave Llanos JM, Nash RE. Mitotic circadian rhythm in a fast-growing and a slow-growing hepatoma: mitotic rhythm in hepatomas. *J Natl Cancer Inst*. 1970;44:581-585.
25. Yang X, Wood PA, Ansell CM, et al. The circadian clock gene Per1 suppresses cancer cell proliferation and tumor growth at specific times of day. *Chronobiol Int*. 2009;26:1323-1339.
26. Shukla P, Gupta D, Bisht SS, et al. Circadian variation in radiation-induced intestinal mucositis in patients with cervical carcinoma. *Cancer*. 2010;116:2031-2035.
27. Rahn DA 3rd, Ray DK, Schlesinger DJ, et al. Gamma knife radiosurgery for brain metastasis of nonsmall cell lung cancer: is there a difference in outcome between morning and afternoon treatment? *Cancer*. 2011;117:414-420.
28. Kim H, Oh BK, Roncalli M, et al. Large liver cell change in hepatitis B virus-related liver cirrhosis. *Hepatology*. 2009;50:752-762.
29. Matsuda Y, Wakai T, Kubota M, et al. DNA damage sensor gamma-H2AX is increased in preneoplastic lesions of hepatocellular carcinoma. *ScientificWorldJournal*. 2013;2013:597095.
30. Bartkova J, Bakkenist CJ, Rajpert-De Meyts E, et al. ATM activation in normal human tissues and testicular cancer. *Cell Cycle*. 2005;4:838-845.
31. Gorgoulis VG, Vassiliou LV, Karakaidos P, et al. Activation of the DNA damage checkpoint and genomic instability in human precancerous lesions. *Nature*. 2005;434:907-913.
32. Sancar A, Lindsey-Boltz LA, Kang TH, Reardon JT, Lee JH, Ozturk N. Circadian clock control of the cellular response to DNA damage. *FEBS Lett*. 2010;584:2618-2625.
33. Corra S, Salvadori R, Bee L, Barbieri V, Mognato M. Analysis of DNA-damage response to ionizing radiation in serum-shock synchronized human fibroblasts. *Cell Biol Toxicol*. 2017;33:373-388.
34. Kang TH, Lindsey-Boltz LA, Reardon JT, Sancar A. Circadian control of XPA and excision repair of cisplatin-DNA damage by cryptochrome and HERC2 ubiquitin ligase. *Proc Natl Acad Sci U S A*. 2010;107:4890-4895.
35. Gaddameedhi S, Selby CP, Kaufmann WK, Smart RC, Sancar A. Control of skin cancer by the circadian rhythm. *Proc Natl Acad Sci U S A*. 2011;108:18790-18795.
36. Huisman SA, Oklejewicz M, Ahmadi AR, et al. Colorectal liver metastases with a disrupted circadian rhythm phase shift the peripheral clock in liver and kidney. *Int J Cancer*. 2015;136:1024-1032.
37. Yang X, Wood PA, Oh EY, Du-Quiton J, Ansell CM, Hrushesky WJ. Down regulation of circadian clock gene period 2 accelerates breast cancer growth by altering its daily growth rhythm. *Breast Cancer Res Treat*. 2009;117:423-431.
38. Tan XM, Ye H, Yang K, et al. Circadian variations of clock gene Per2 and cell cycle genes in different stages of carcinogenesis in golden hamster buccal mucosa. *Sci Rep*. 2015;5:9997.
39. Mteyrek A, Filipski E, Guettier C, Okyar A, Levi F. Clock gene Per2 as a controller of liver carcinogenesis. *Oncotarget*. 2016;7:85832-85847.
40. Deng F, Yang K. Current status of research on the period family of clock genes in the occurrence and development of cancer. *J Cancer*. 2019;10:1117-1123.
41. Huisman SA, Ahmadi AR, JN IJ, Verhoef C, van der Horst GT, de Bruin RW. Disruption of clock gene expression in human colorectal liver metastases. *Tumour Biol*. 2016;37:13973-13981.
42. Oshima T, Takenoshita S, Akaike M, et al. Expression of circadian genes correlates with liver metastasis and outcomes in colorectal cancer. *Oncol Rep*. 2011;25:1439-1446.
43. Morgan M, Dvuchbabny S, Martinez C-A, Kerr B, Cistulli PA, Cook KM. The cancer clock is (not) ticking: links between circadian rhythms and cancer. *Clocks & Sleep*. 2019;1:435-458.
44. Yu C, Yang SL, Fang X, Jiang JX, Sun CY, Huang T. Hypoxia disrupts the expression levels of circadian rhythm genes in hepatocellular carcinoma. *Mol Med Rep*. 2015;11:4002-4008.
45. Yang SL, Yu C, Jiang JX, Liu LP, Fang X, Wu C. Hepatitis B virus X protein disrupts the balance of the expression of circadian rhythm genes in hepatocellular carcinoma. *Oncol Lett*. 2014;8:2715-2720.
46. Li HX. The role of circadian clock genes in tumors. *Onco Targets Ther*. 2019;12:3645-3660.
47. Zhao H, Zeng ZL, Yang J, et al. Prognostic relevance of Period1 (Per1) and Period2 (Per2) expression in human gastric cancer. *Int J Clin Exp Pathol*. 2014;7:619-630.
48. Palma E, Doornebal EJ, Chokshi S. Precision-cut liver slices: a versatile tool to advance liver research. *Hepatol Int*. 2019;13:51-57.
49. Yoo SH, Yamazaki S, Lowrey PL, et al. PERIOD2::LUCIFERASE real-time reporting of circadian dynamics reveals persistent circadian oscillations in mouse peripheral tissues. *Proc Natl Acad Sci USA*. 2004;101:5339-5346.
50. Buhr ED, Yoo SH, Takahashi JS. Temperature as a universal resetting cue for mammalian circadian oscillators. *Science*. 2010;330:379-385.

How to cite this article: Hassan SA, Schmithals C, von Harten M, Piiper A, Korf H-W, von Gall C. Time-dependent changes in proliferation, DNA damage and clock gene expression in hepatocellular carcinoma and healthy liver of a transgenic mouse model. *Int. J. Cancer*. 2021;148:226–237. https://doi.org/10.1002/ijc.33228

Does timing matter in radiotherapy of hepatocellular carcinoma? An experimental study in mice

Soha A. Hassan, Amira A. H. Ali, Dennis Sohn, Ulrich Flögel, Reiner U. Jänicke, Horst-Werner Korf*, Charlotte von Gall

* Corresponding author

Status of publication: The manuscript has been published as an online open-access *preprint* (doi: 10.20944/preprints202101.0603.v1) and resubmitted to *Cancers* after consideration the reviewers' comments.

Impact factor: 6.126

Contribution to the publication: Concept/design, performance of all experiments, acquisition, analysis and interpretation of data, and writing of the manuscript.

Title:

Does timing matter in radiotherapy of hepatocellular carcinoma? An experimental study in mice

Authors:

Soha A. Hassan[1,2], Amira A. H. Ali[1], Dennis Sohn[3], Ulrich Flögel[4], Reiner U. Jänicke[3], Horst-Werner Korf[5], Charlotte von Gall[1]

1 Institute of Anatomy II, Medical Faculty, Heinrich-Heine-University, Universitätstrasse 1, 40225 Düsseldorf, Germany.
2 Zoology Department, Faculty of Science, Suez University, Suez 43111, Egypt.
3 Laboratory of Molecular Radiooncology, Clinic and Policlinic for Radiation Therapy and Radiooncology, Medical Faculty of Heinrich-Heine-University, Universitätstrasse 1, 40225 Düsseldorf, Germany.
4 Department of Molecular Cardiology, Heinrich-Heine-University, Universitätstrasse 1, 40225 Düsseldorf, Germany.
5 Institute of Anatomy I, Medical Faculty, Heinrich-Heine-University, Universitätsstr. 1, 40225 Düsseldorf, Germany.

Correspondence: Prof. Horst-Werner Korf, korf@uni-duesseldorf.de

Simple Summary: Hepatocellular carcinoma (HCC), which is mostly diagnosed in advanced stage, is highly resistant to antimitotic therapies. External beam radiotherapy is rarely used in HCC treatment due to the increased risk of radiation-induced liver damage which follows hepatic radiotherapy. To date, it is unknown if this side effect can be reduced if the radiotherapy applied at the proper timing. Our study aims to introduce the concept of chronotherapy to radiobiological cancer research by defining the optimal time point at which the HCC is more radiosensitive, whilst the surrounding NTL is more radioresistant to the damaging effects. Our results from *Per2::luc* mice bearing HCCs irradiated at four time points during the day allowed us to define ZT20 (late activity phase) as an optimal time point to apply radiotherapy since at this ZT ratio between efficacy of tumor treatment and side effects was maximal. Translation studies are now required to clarify whether these findings can be confirmed for HCC patients.

Abstract: This study investigates whether a chronotherapeutic treatment of hepatocellular carcinoma (HCC) may improve treatment efficacy and mitigate side effects on non-tumoral liver (NTL). HCC was induced in *Per2::luc* mice which were

irradiated at four time points of the day. Proliferation and DNA-double strand breaks were investigated in irradiated and non-irradiated organotypic slice culture (OSC) and *ex vivo* samples by detection of Ki67 and γ-H2AX. OSC proved useful to determine dose-dependent effects on proliferation and DNA damage but appeared unsuited to test the chronotherapeutic approach. Irradiation of *ex vivo* samples was most effective at the proliferation peaks in HCC at ZT02 (early inactivity phase) and ZT20 (late activity phase). Irradiation effects on NTL were minimal at ZT20. *Ex vivo* samples revealed disruption in daily variation and down-regulation of all investigated clock genes except *Per1* in non-irradiated HCC as compared with NTL. Irradiation affected rhythmic clock gene expression in NTL and HCC at all ZTs except at ZT20 (late activity phase). Irradiation at ZT20 had no effect on total leukocyte numbers. Our results indicate ZT20 as the optimal time point for irradiation of HCC in mice at which the ratio between efficacy of tumor treatment and toxic side effects was maximal. Translational studies are now needed to evaluate whether the late activity phase is the optimal time point for irradiation of HCC in man.

Keywords: Clock genes; Hepatocellular carcinoma; Ki67; Radiotherapy; Transgenic *Per2::luc* mice; γ-H2AX.

1. Introduction

Hepatocellular carcinoma (HCC) occupies the fourth rank of cancer death causes worldwide with a mortality rate of 8.2% (782 000 deaths) and 841 080 new cases in 2018 [1,2]. HCC is characterized by high malignancy as well as fast progression, invasion and metastasis. Moreover, HCC is highly resistant to antimitotic therapies [3]. Chemotherapies (e.g. sorafenib and tivantinib) and chemotherapy in combination with radiation (e.g. RT-Sorafenib) are the most commonly applied protocols in HCC patients [4,5]. However, these therapies have severe side effects which impair life quality of the patients and may lead to interruption of the treatment [6-9].

Radiotherapy is rarely used in the management of the HCC due to lacking trail data which supports the safety and efficacy of the radiotherapy and the increased risk of radiation-induced liver damage (RILD) which follows the hepatic radiotherapy [10,11]. Thus, an important question is whether the application of chronotherapy might improve the efficacy of radiotherapy for HCC.

In a recent study with a mouse model of HCC (double transgenic c-myc/TGFα mice), we have shown significant time of day-dependent differences in proliferation rate as well as DNA damage and repair mechanisms between the HCC and the surrounding non-tumoral liver (NTL) [12]. These results suggest that the efficacy and side effects of any antimitotic therapy for HCC may depend on proper timing and that determination of the optimal time point for application of antimitotic therapies may help to improve the efficacy of HCC treatment. Such a chronotherapeutic approach has been taken in humans for other tumors such as bone and brain metastases, breast, rectal and cervical cancers but not for HCC [13]. To test the potential value of a chronotherapeutic approach, we investigated the effect of irradiation at four different *Zeitgeber* time (ZT) points in mice bearing HCCs. As an experimental animal model, *Per2::luc* mice were selected based on previous studies [14]. In order to evaluate the response to radiotherapy, Ki67 was used as a marker for proliferation and γ-H2AX as a marker for DNA-double strand breaks (DSBs) in HCC and NTL. Ki67 is expressed during the G2/M phase of the cell cycle, which is the most critical target phase for radiotherapy [15,16]. In HCC, the expression of Ki67 is established as an indicator for the response to antimitotic drugs (e.g. tivantinib) [5]. In addition, it is well known that during proliferation cells become more sensitive to DNA damage induced by cancer therapies [17,18]. Thus, γ-H2AX, a histone which accumulates in the damaged sites of DNA-DSBs to start the DNA repair process [19,20], is used as an indicator for the sensitivity of tumors and the surrounding healthy tissues to the treatment protocols and helps to control the dose and the efficacy of radiotherapy [19]. In HCC, γ-H2AX was recently used as a marker to predict the efficacy of a combined sorafenib treatment with radiation (RT-SOR) and indolylquinoline derivative substances [4,21].

In contrast to experiments with whole animals, the usage of organotypic slice cultures (OSC) allows a faster and more effective screening of any novel therapeutic strategy and also improves animal welfare. In our previous study, we concluded that OSC from HCC and NTL may be helpful model to test and establish novel therapeutic strategies [12]. To investigate whether OSC is suitable to determine the optimal time points of radiotherapy, OSC slices were irradiated with two different doses (2 and 10 Gy) at 4 different circadian time (CT) points and Ki67 and γ-H2AX immunoreactive cells were analyzed.

Cell cycle, proliferation rate and DNA damage repair mechanism as well as the sensitivity to antimitotic treatments are controlled by the molecular clockwork [22-25] which is based on clock genes that interact through positive and negative transcription-translation feedback loops [26,27]. The transcription factors CLOCK and BMAL1 represent the positive elements in the loops and activate the expression of *Per* (*Per1* and *Per2*) and *Cry* (*Cry1* and *Cry2*) genes which form PER/CRY complexes representing the negative elements [27]. This molecular clockwork controls the expression of more than 3000 so-called clock-controlled genes and, thus, rhythmic cell and organ functions. Disruption of the molecular clockwork or down-regulation of clock gene expression leads to genomic instability which increases the cellular proliferation rate and thus promotes carcinogenesis [3,9,28]. In our previous study, expression of *Per2* and *Cry1* was significantly lower and showed an altered rhythm in HCC [12]. To date, little is known about the time-of-day dependent effects of radiotherapy on the molecular clockwork. Therefore, we analyzed whether radiotherapy at different ZTs affects the molecular clockwork in HCC and NTL.

Hematopoiesis is one of the most sensitive systems in the body to radiotherapy and reduction of white and red blood cells is one of the most common side effects of the radiotherapy [29,30]. Thus, blood cells of mice with HCC with and without irradiation at different ZTs were analyzed as an additional readout for the side effects of the radiotherapy.

2. Results

2.1. Ki67 and γ-H2AX in OSCs of HCC and NTL without and with irradiation with two different doses at four different CTs (in vitro)

In non-irradiated OSCs, the number of Ki67+ cells was very low and not different among the four CTs in NTL ($p > 0.05$, Fig. 1A, C). In HCC, the number of Ki67+ cells was significantly higher ($p < 0.0001$) as compared with NTL and showed a peak at CT02 which, however, did not differ from the values at the other CTs ($p > 0.05$, Fig. 1B, D).

Irradiation with 2 or 10 Gy had no effect on the number of Ki67+ cells at all CTs in NTL ($p > 0.05$, Fig. 1A, C). In HCC, irradiation with 2 Gy elicited no changes in the number of Ki67+ cells at any CT ($p > 0.05$, Fig. 1B, D). In contrast, after irradiation with a dose of 10 Gy at CT02, the number of Ki67+ cells was significantly

lower as compared with the respective non-irradiated HCC ($p < 0.05$). Irradiation with 10 Gy had no effect on the number of Ki67+ cells at any other time point (Fig. 1B, D).

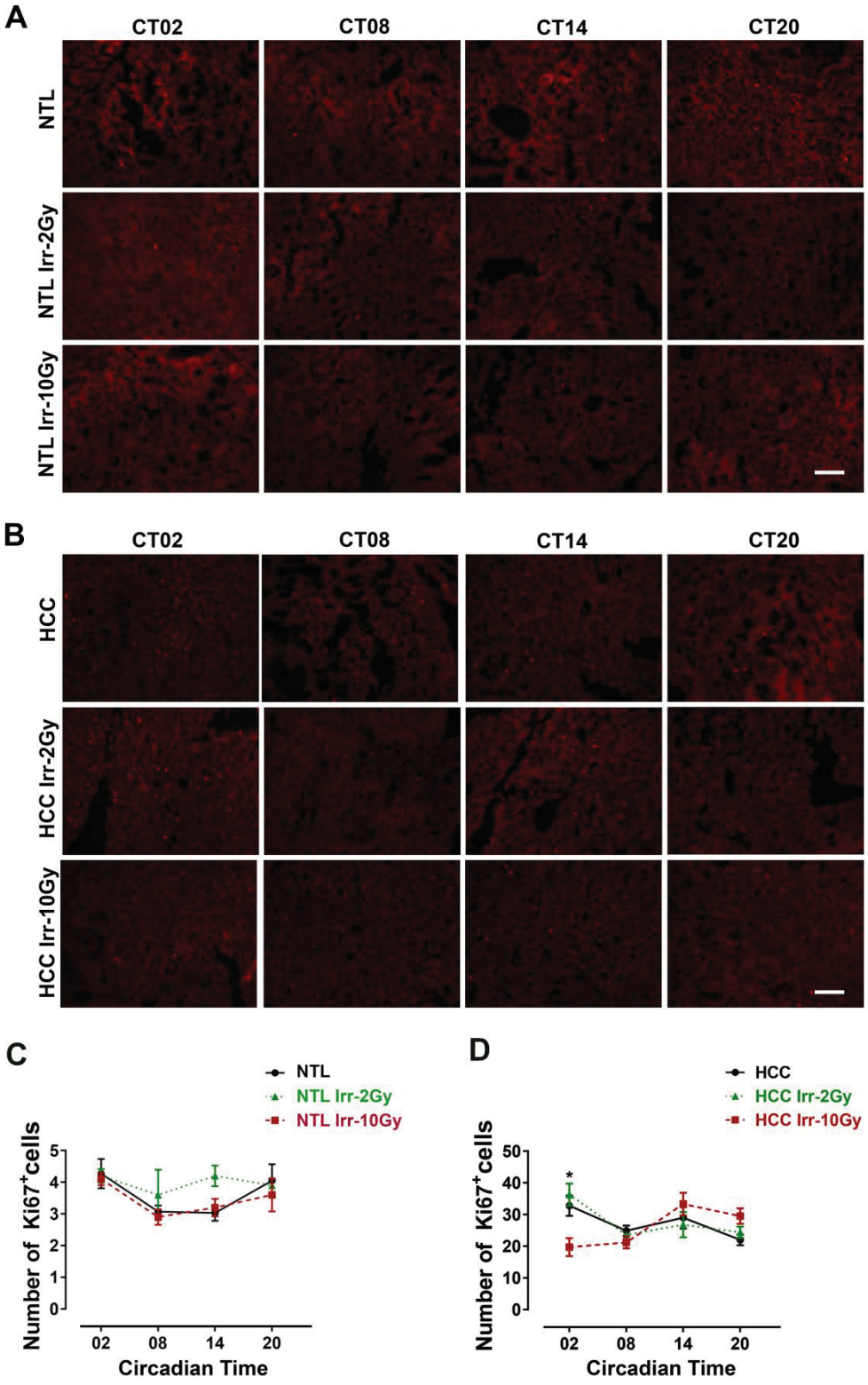

Fig. 1 Ki67 in organotypic slice cultures (OSCs) of hepatocellular carcinoma (HCC) and surrounding non-tumoral liver (NTL) with or without irradiation. At different circadian times (CT00= medium change), OSCs were irradiated (Irr) with a dose of 2 Gy or 10 Gy (n=5/time point in each dose) or handled similarly but not irradiated. 48 hours later, OSCs were collected at the same CTs. Representative photomicrographs of Ki67 immunoreaction in NTL (**A**) and HCC (**B**). Quantification of Ki67 immunoreactive (+) cells in NTL (**C**) and HCC (**D**). Plotted are the mean numbers ± SEM of immunoreactive (+) cells. *: $p < 0.05$ differences between the non-irradiated and irradiated OSCs with a dose of 10 Gy. Scale bars, 100 µm.

In non-irradiated NTL, the number of γ-H2AX+ cells was low and showed a peak at CT02 (Fig. 2C). In HCC, the number of γ-H2AX+ cells was significantly higher in the HCC as compared with NTL (Fig. 2B, D, $p < 0.0001$), and higher at CT14 ($p < 0.05$) and CT20 ($p < 0.01$) as compared with CT08 (Fig. 2D).

In NTL, irradiation with either 2 or 10 Gy resulted in a time-dependent increase in the number of γ-H2AX+ cells (Fig. 2A, C). The strongest effects were observed at CT02 (39.3% and 60.2%, respectively) and CT14 (24% and 27.7%, respectively) ($p < 0.0001$). A smaller effect of irradiation with 2 and 10 Gy was observed at CT08 with a significant increase of 18.4% and 14.5%, respectively ($p < 0.01$). Irradiation at CT20 had no effect on the number of γ-H2AX+ cells ($p > 0.05$). In HCC, the number of γ-H2AX+ cells was further increased after irradiation with 2 or 10 Gy at CT02 (24.8% and 58.4%, respectively) and CT08 (19.3% and 20.2 %, respectively) as compared with non-irradiated HCC ($p < 0.0001$). At CT14, only irradiation with 10 Gy resulted in a significant increase in the number of γ-H2AX+ cells as compared with non-irradiated HCC (17%, $p < 0.001$). At CT20, irradiation had no effect on the number of γ-H2AX+ cells ($p > 0.05$, Fig. 2B, D).

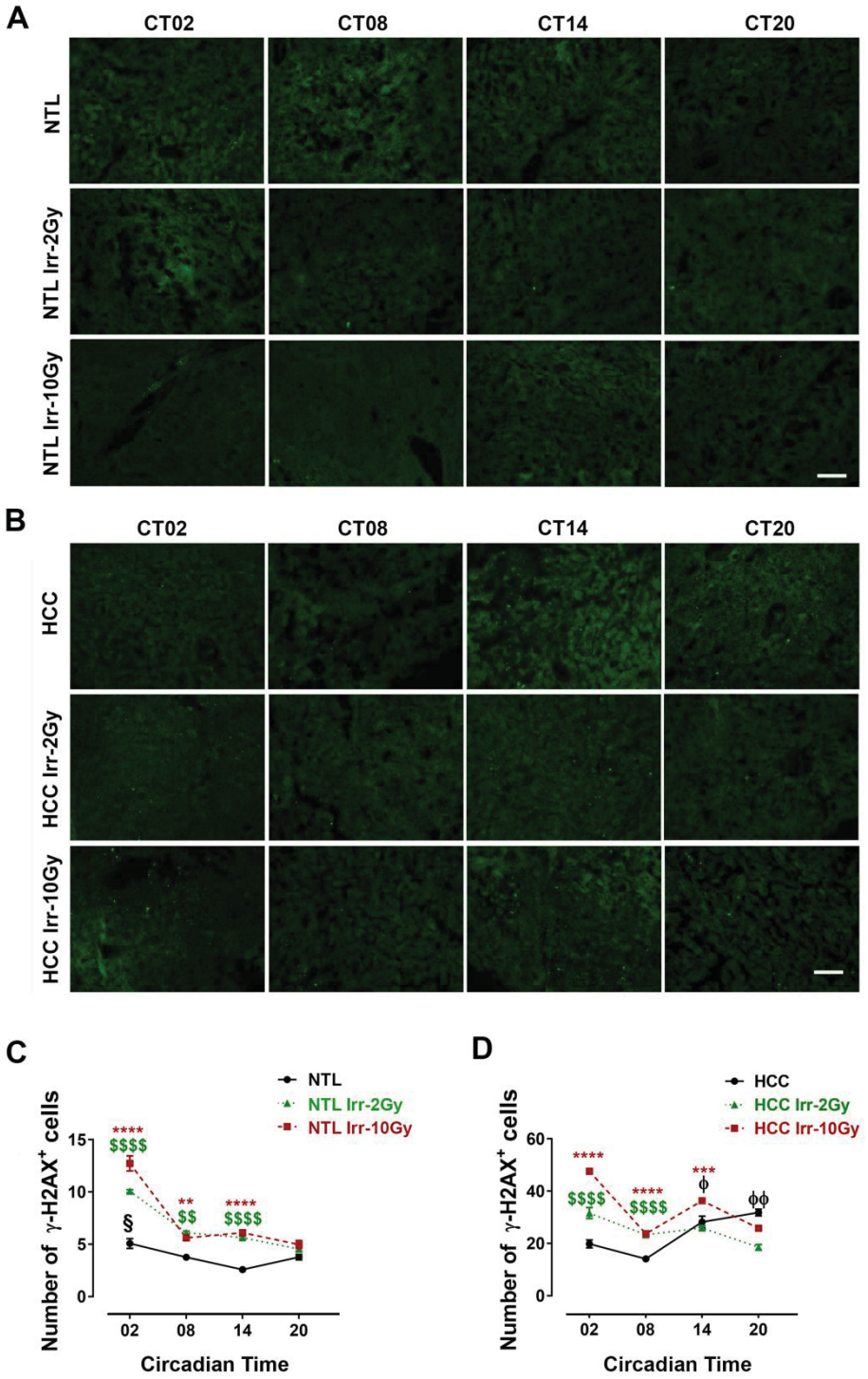

Fig. 2 γ-H2AX in organotypic slice cultures (OSCs) of hepatocellular carcinoma (HCC) and surrounding non-tumoral liver (NTL) with or without irradiation. At different circadian times (CT00= medium change), OSCs were irradiated (Irr) with a dose of 2 Gy or 10 Gy (n=5/time point in each dose) or handled similarly but not irradiated. 48 hours later, OSCs were collected at the same CTs. Representative photomicrographs of γ-H2AX immunoreaction in NTL (**A**) and HCC (**B**). Quantification of γ-H2AX immunoreactive (+) cells NTL (**C**) and HCC (**D**). Plotted are the mean numbers ± SEM of immunoreactive (+) cells. §: *p <0.05* differences between this CT and CT14. φ: *p <0.05*; φφ: *p <0.01* differences between this CT and CT08.**: *p <0.01*; ***: *p <0.001*; ****: *p <0.0001* differences between the non-irradiated and irradiated OSCs with a dose of 10 Gy. $$: *p <0.01*; $$$$: *p <0.0001* differences between the non-irradiated and irradiated OSCs with a dose of 2 Gy. Scale bars, 100 µm.

2.2. *Ki67 and γ-H2AX in HCC and NTL in mice without and with irradiation (10 Gy) at four different ZTs (ex vivo)*

In non-irradiated NTL, the number of Ki67+ cells showed one peak during the light phase (ZT02) which was significantly different from the trough at the early dark phase (ZT14, $p < 0.001$) (Fig. 3A, C). In HCC, the number of Ki67+ cells was higher than in NTL at all ZTs (ZT02, 14, 20, $p < 0.0001$; ZT08, $p < 0.01$), but in contrast to the NTL, the number of Ki67+ cells showed two peaks, one during the early light phase (ZT02, $p < 0.05$) and the second in the late dark phase (ZT20, $p < 0.01$) as compared with the trough at ZT08 (Fig. 3D).

Irradiation (10 Gy) resulted in a decrease in the number of Ki67+ cells. In NTL, the highest effect of irradiation was observed after irradiation during the light phase, when Ki67 expressions were high without irradiation (ZT02, 89.8%; ZT08, 60.6%, $p < 0.0001$). During the dark phase, irradiation had little effects (ZT14, 20%; ZT20, 32.6%, $p < 0.05$) (Fig. 3A, C). In HCC, irradiation resulted in a significant decrease in Ki67+ cells at all ZTs (ZT02, 72.3%; ZT08, 37.7%; ZT14, 67.1%; with the strongest decrease observed at ZT20, 94.3%) (Fig. 3B, D).

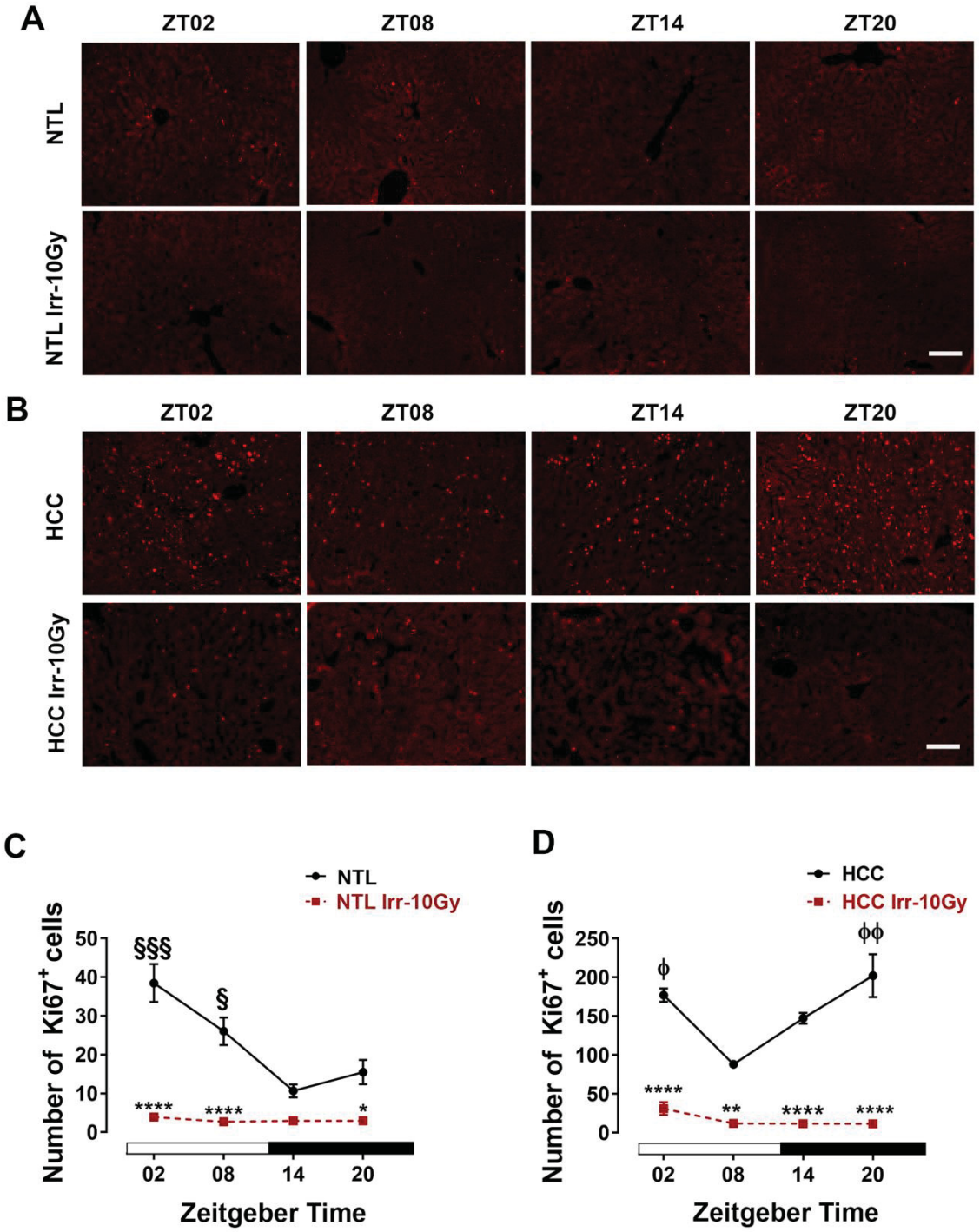

Fig. 3 Ki67 in *ex vivo* samples of hepatocellular carcinoma (HCC) and non-tumoral liver (NTL) with or without irradiation. At different *Zeitgeber* times (ZT00= the onset of the light phase), mice were irradiated (Irr-10Gy) (n= 3/time point) or handled similarly but not irradiated. 48 hours later, mice were sacrificed at the same ZTs. Representative photomicrographs of Ki67 immunoreaction in NTL (**A**) and HCC (**B**). Quantification of Ki67 immunoreactive (+) cells in NTL (**C**) and HCC (**D**). Plotted are the mean numbers ± SEM of immunoreactive (+) cells. White and black bars indicate the light and dark phases, respectively. §: $p < 0.05$; §§§: $p < 0.001$ differences between this ZT and ZT14. φ: $p < 0.05$; φφ: $p < 0.01$ differences between this ZT and ZT08. *: $p < 0.05$; **: $p < 0.01$; ****: $p < 0.0001$ differences between the non-irradiated and irradiated group. Scale bars, 100 µm.

In non-irradiated NTL, the number of γ-H2AX+ cells showed a peak in the early light phase (ZT02) which was significantly different from the trough at the early dark phase (ZT14) ($p < 0.0001$, Fig. 4A, C). In non-irradiated HCC, the number of γ-H2AX+ cells was significantly higher at ZT02 and ZT20 ($p < 0.0001$) as compared with NTL. The HCC revealed two peaks, one at ZT02 and a second at ZT20. The two peaks were significantly different from the minimum at ZT08 ($p < 0.05$, Fig. 4D).

Irradiation led to an increase in the number of γ-H2AX+ cells at all four ZTs in HCC and NTL as compared with non-irradiated samples. As compared with non-irradiated NTL, the number of γ-H2AX+ cells in NTL was higher when the animals were irradiated at ZT02 and ZT14 (90.7% and 80%, respectively; $p < 0.0001$) than at ZT08 (47.9%, $p < 0.001$) and ZT20 (32.2%, $p < 0.05$; Fig. 4A, C and Fig. S1). In irradiated HCC, the number of γ-H2AX+ cells was significantly increased ($p < 0.01$) as compared with the non-irradiated HCC at all ZTs (Fig. 4B, D).

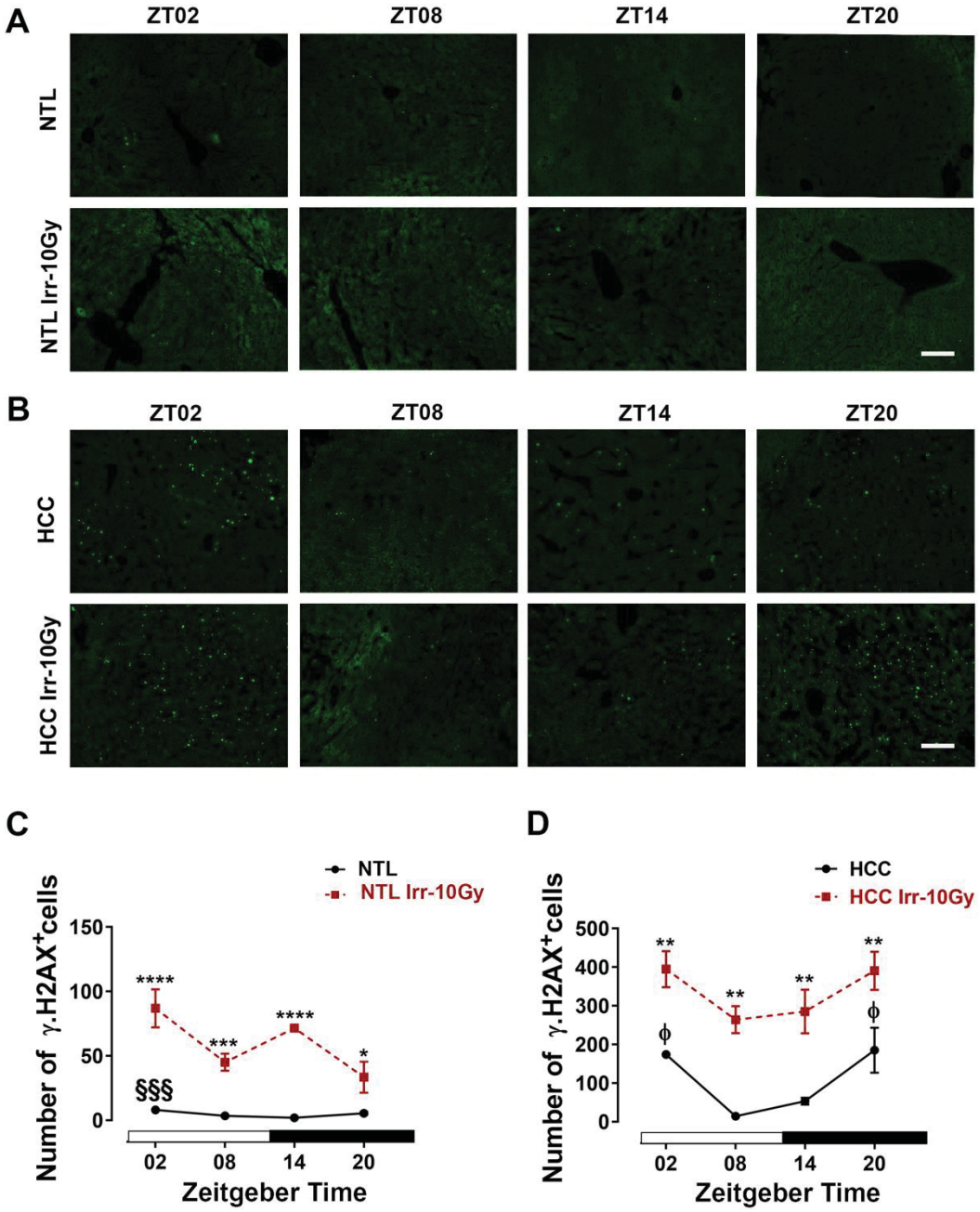

Fig. 4 γ-H2AX in *ex vivo* samples of hepatocellular carcinoma (HCC) and non-tumoral liver (NTL) with or without irradiation. At different *Zeitgeber* times (ZT00= the onset of the light phase), mice were irradiated (Irr-10Gy) (n= 3/time point) or handled similarly but not irradiated. 48 hours later, mice were sacrificed at the same ZTs. Representative photomicrographs of γ-H2AX immunoreaction in NTL (**A**) and HCC (**B**). Quantification of γ-H2AX immunoreactive (+) cells in NTL (**C**) and HCC (**D**). Plotted are the mean numbers ± SEM of immunoreactive (+) cells. White and black bars indicate the light and dark phases, respectively. §§§: $p < 0.001$ differences between this ZT and ZT14. φ: $p < 0.05$ differences between this ZT and ZT08. *: $p < 0.05$; **: $p < 0.01$; ***: $p < 0.001$; ****: $p < 0.0001$ differences between the non-irradiated and irradiated group. Scale bars, 100 µm.

2.3. Clock gene expression in HCC and NTL in mice without and with irradiation (10 Gy) at four different ZTs (ex vivo)

The relative expression of *Per1* in non-irradiated NTL and HCC showed a peak at ZT14 which was significantly different from the value at ZT02 ($p < 0.05$). There were no differences between HCC and NTL among ZTs ($p > 0.05$). The relative expression of *Per1* did not differ when the irradiated NTL and HCC were compared with the non-irradiated samples at all irradiated ZTs ($p > 0.05$, Fig. 5A, B).

The relative expression of *Per2* in non-irradiated NTL and HCC was higher at ZT14 and ZT20 as compared with ZT08 ($p < 0.05$). At ZT02, the relative expression of *Per2* was lower in HCC than in NTL ($p < 0.05$). When the mice were irradiated at ZT14, the relative expression of *Per2* was significantly increased in both the NTL and the HCC ($p < 0.001$; $p < 0.01$, Fig. 5C, D).

The relative expression of *Cry1* showed a peak at ZT02 in non-irradiated NTL which was significantly different from the value at ZT14 ($p < 0.05$, Fig. 5E). In non-irradiated HCC, the relative expression of *Cry1* was not different among the ZTs (Fig. 5F) and was significantly lower as compared with non-irradiated NTL at ZT02 ($p < 0.01$). Irradiation had no effect on the relative expression of *Cry1* in HCC or NTL ($p > 0.05$, Fig. 5E, F).

The relative expression of *Cry2* had a peak at ZT02 in non-irradited NTL which showed a tendancy to be significantly differefnt from the value at ZT20 ($p = 0.08$, Fig. 5G). In non-irradiated HCC, the relative expression of *Cry2* was not different among the ZTs (Fig. 5H). At ZT02, the relative expression of *Cry2* was lower in HCC than in NTL ($p < 0.01$). When the mice were irradiated at ZT14, the relative expression of *Cry2* was increased in HCC as compared with the non-irradiated HCC ($p < 0.05$, Fig. 5H).

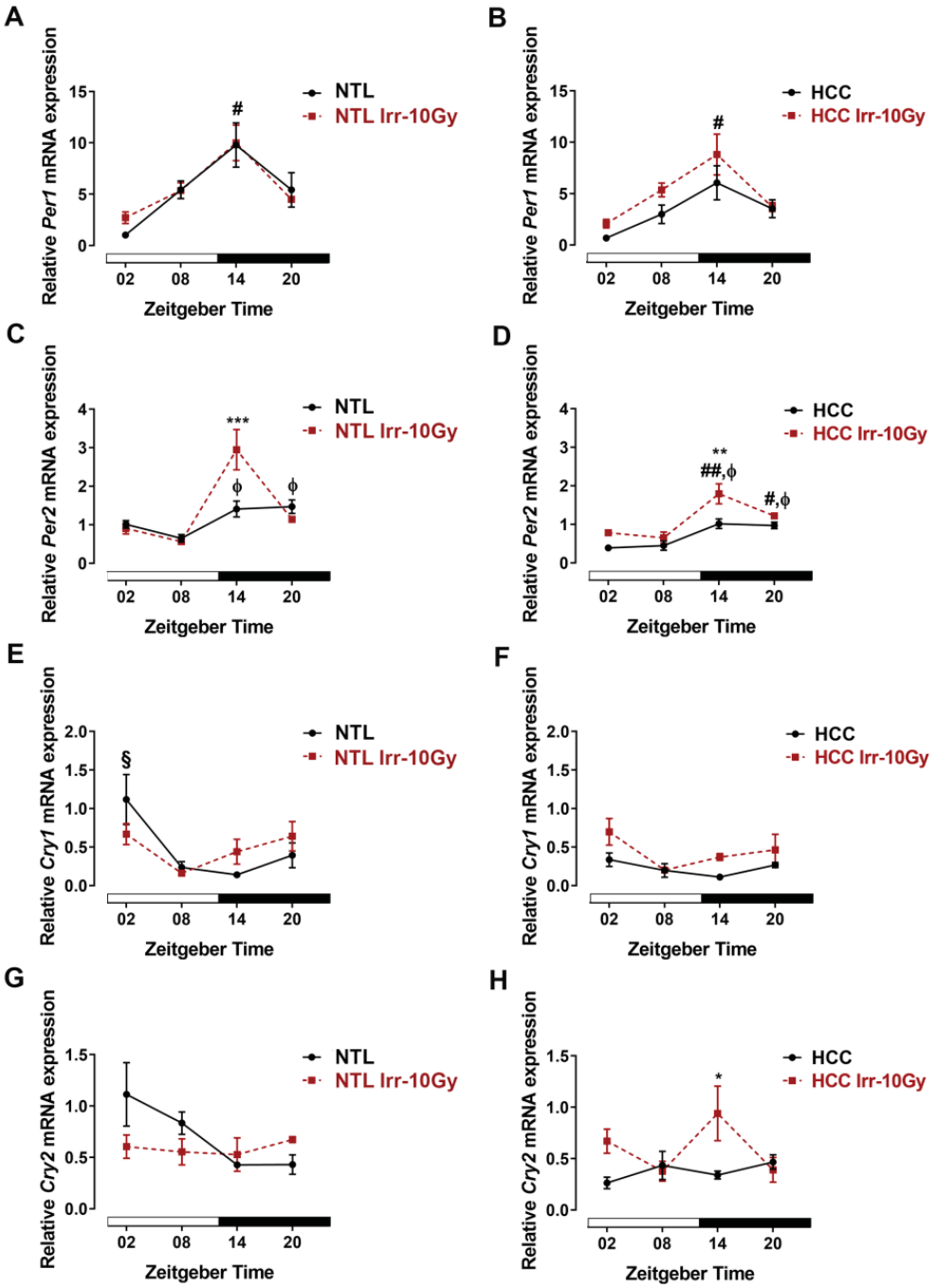

Fig. 5 Clock gene expressions in *ex vivo* samples of hepatocellular carcinoma (HCC, left panel) and surrounding non-tumoral liver (NTL, right panel) without or with irradiation (Irr-10Gy). At different *Zeitgeber* times (ZT00= the onset of the light phase), mice were irradiated (n= 3/time point) or handled similarly but not irradiated. 48 hours later, mice were sacrificed at the same ZTs. Relative expression of *Per1* in NTL (**A**) and HCC (**B**). Relative expression of *Per2* in NTL (**C**) and HCC (**D**). Relative expression of *Cry1* in NTL (**E**) and HCC (**F**). Relative expression of *Cry2* in NTL (**G**) and HCC (**H**). Plotted are the mean relative mRNA expressions ± SEM. White and black bars indicate the light and dark phases, respectively. #: $p < 0.05$; ##: $p < 0.01$ differences between this ZT and ZT02. φ: $p < 0.05$ differences between this ZT and ZT08. §: $p < 0.05$ differences between this ZT and ZT14. *: $p < 0.05$; **: $p < 0.01$; ***: $p < 0.001$ differences between the non-irradiated and irradiated group.

The relative expression of *Clock* in non-irradiated NTL showed a peak at ZT08 which was significantly different from ZT14 and ZT20 ($p < 0.05$, Fig. 6A). In non-irradiated HCC, the relative expression of *Clock* was not different among the ZTs ($p > 0.05$, Fig. 6B) and was lower at ZT02 ($p < 0.01$) and ZT08 ($p < 0.001$) as compared with NTL. In NTL irradiated at ZT02 ($p < 0.01$) and ZT08 ($p < 0.001$), the relative expression of *Clock* was reduced as compared with the non-irradiated NTL (Fig. 6A).

The relative expression of *Bmal1* in non-irradiated NTL showed a peak at ZT02 which was significantly different from ZT14 ($p < 0.01$) and ZT20 ($p < 0.05$, Fig. 6C). In non-irradiated HCC, the relative expression of *Bmal1* was not different among the ZTs ($p > 0.05$, Fig. 6B) and was lower at ZT02 as compared with NTL ($p < 0.01$). After irradiation at ZT02, the relative expression of *Bmal1* was decreased in irradiated NTL and increased in HCC as compared with non-irradiated samples ($p < 0.05$, Fig. 6C, D).

The relative expression of *Rev-erbα* showed a peak at (ZT08) in non-irradiated NTL ($p < 0.001$) and HCC ($p < 0.05$) which differed from ZT20 (Fig. 6E, F). At ZT08, the relative expression of *Rev-erb α* was lower in HCC than in NTL ($p < 0.0001$). Irradiation of the mice had no effect on the relative expression of *Rev-erbα* ($p > 0.05$, Fig. 6E, F).

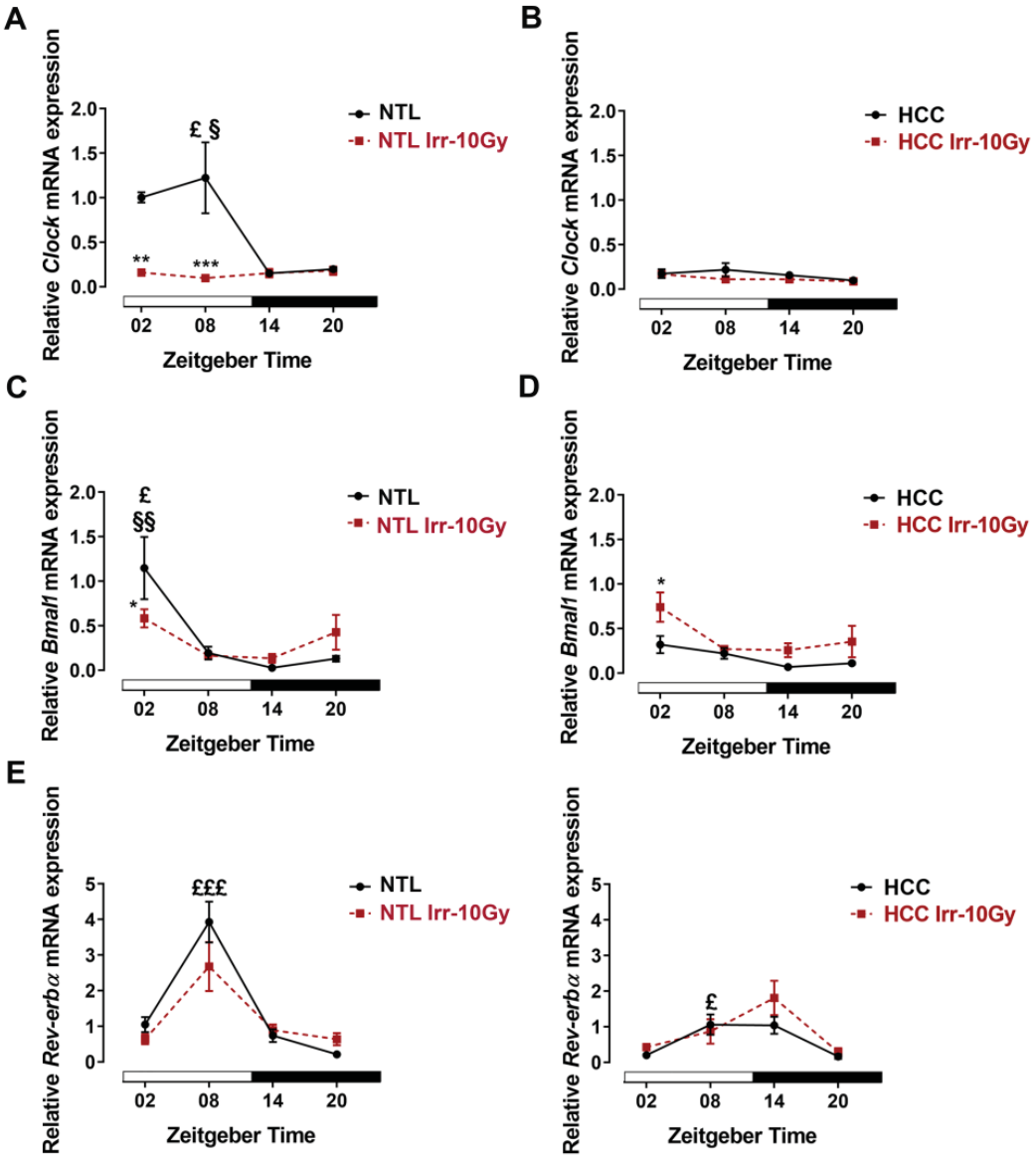

Fig. 6 Clock gene expressions in *ex vivo* samples of hepatocellular carcinoma (HCC, left panel) and non-tumoral liver (NTL, right panel) without or with irradiation (Irr-10Gy). At different *Zeitgeber* times (ZT00= the onset of the light phase), mice were irradiated (n= 3/time point) or handled similarly but not irradiated. 48 hours later, mice were sacrificed at the same ZTs. Relative expression of *Clock* in NTL (**A**) and HCC (**B**). Relative expression of *Bmal1* in NTL (**C**) and HCC (**D**). Relative expression of *Rev-erbα* in NTL (**E**) and HCC (**F**). Plotted are the mean relative mRNA expressions ± SEM. White and black bars indicate the light and dark phases, respectively. §: $p < 0.05$; §§: $p < 0.01$ differences between this ZT and ZT14. £: $p < 0.05$; £££: $p < 0.001$ differences between this ZT and ZT20. *: $p < 0.05$; **: $p < 0.01$; ***: $p < 0.001$ differences between the non-irradiated and irradiated group.

2.4. Blood cell counts in mice without and with irradiation (10 Gy) at four different ZTs (ex vivo)

Control mice showed a daily variation in the total number of leukocytes with higher levels during the light phase than during the dark phase (Fig. 7A). In the non-irradiated HCC group, there was no significant daily variation of leukocytes and at ZT20 the leukocytes number was significantly higher as compared with the control group ($p < 0.05$, Fig. 7A). In the irradiated group, the number of leukocytes at ZT02 ($p < 0.05$) and ZT08 ($p < 0.01$) was significantly decreased (Fig. 7A).

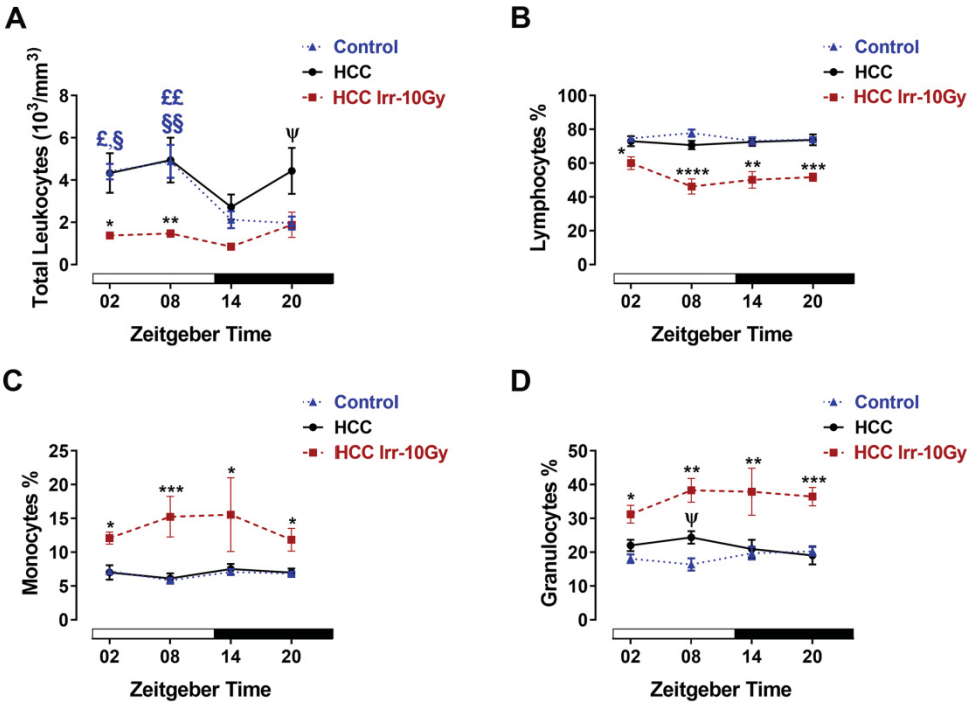

Fig. 7 Blood cell analysis in control and hepatocellular carcinoma (HCC) bearing mice without and with irradiation. At different *Zeitgeber* times (ZT00= the onset of the light phase), mice were irradiated (Irr) with a dose of 10 Gy (n= 3-6/time point) or handled similarly but not irradiated. 48 hours later, mice were sacrificed and the blood was collected at the same ZTs. (**A**) Total leukocytes numbers. (**B**) Lymphocyte percentage. (**C**) Monocyte percentage. (**D**) Granulocyte percentage. Plotted are the mean numbers ± SEM. White and black bars indicate the light and dark phases, respectively. §: $p < 0.05$; §§: $p < 0.01$ differences between this ZT and ZT14. £: $p < 0.05$; ££: $p < 0.01$ differences between this ZT and ZT20. *: $p < 0.05$; **: $p < 0.01$; ***: $p < 0.001$; ****: $p < 0.0001$ differences between non-irradiated and irradiated animals. ψ: $p < 0.05$ differences between control and non-irradiated animals.

There were no differences in the percentages of leukocyte types in both the control group and the HCC mice (Fig. 7B-D). However, at ZT08, the percentage of the granulocytes was higher in HCC mice as compared with the control group ($p < 0.05$, Fig. 7D). Irradiation at any time point resulted in a decrease in percentage of lymphocytes and an increase in the percentage of both monocytes and granulocytes as compared with the non-irradiated HCC mice (Fig. 7B-D). There were no differences in the number of erythrocytes, platelets and the hemoglobin concentration in control, non-irradiated, and irradiated mice (Supplementary Figure S2 A-C).

3. Discussion

This study with a newly developed mouse model for hepatocellular carcinoma (HCC) addresses the question of whether timed application of radiotherapy may increase the efficacy of hepatocellular carcinoma treatment in mice which was raised from our recent findings in double transgenic c-myc/TGFα [12]. Irradiation was performed at four different time points. Readouts for treatment efficacy and side effects were proliferation, DNA-DSBs, clock gene expression and blood cell counts.

As a first step, time- and dose-dependent effects were analyzed in OSC of NTL and HCC either irradiated at 4 different circadian time (CT) points (CT02, CT08, CT14 and CT20) with two different doses (2 and 10 Gy) or left without irradiation. Irradiation with 2 Gy or 10 Gy affected DNA-DSBs: as compared with the non-irradiated slices, the number of γ-H2AX+ cells was increased in both NTL and HCC irradiated at CT02, 08 and 14. This indicates a similar time- and dose-dependent effect of irradiation on DNA-DSBs in healthy tissue and tumor. With regard to proliferation in non-irradiated HCC, the number of Ki67+ cells revealed two peaks (CT02 and CT14) which correspond to the two peaks previously observed also in double transgenic c-myc/TGFα mice [12]. After irradiation of HCC and NTL slices with a dose of 2 Gy at the different CTs, the number of Ki67+ cells did not differ from those in the non-irradiated groups. Thus, the low dose of irradiation does not affect proliferation in HCC. In contrast, irradiation with 10 Gy elicited a strong antiproliferative effect: HCC slices irradiated with a dose of 10 Gy at CT02 (the proliferation peak) showed a decrease in the number of Ki67+ cells as compared with the non-irradiated HCC. Notably, irradiation with 10 Gy at this CT did not affect the proliferation rate in NTL. Dose-dependent antiproliferative effects were also found in

other *in vitro* models of cancer. Irradiation of DU 145 cells (a human prostate cancer cell line) inhibited their proliferation only when given in high doses (10 and >20 Gy), while a dose of 2 Gy was ineffective [31]. A dose of 10 Gy was also shown to cause disruption in the mitotic stage and initiation of cell apoptosis in HeLa cells, a cervical cancer cell line [32].

Since the *in vitro* data showed antiproliferative effects of irradiation only at a dose of 10 Gy, we used this dose for our *ex vivo* analyses with whole animals which were irradiated at 4 different *Zeitgeber* time (ZT) points (ZT02, ZT08, ZT14 and ZT20) or left without irradiation. As in OSC, the number of Ki67+ cells was much higher in non-irradiated HCC than in NTL. Both tissues showed a daily variation in the number of Ki67+ cells but the pattern was different. The non-irradiated NTL showed one peak at ZT02, whilst the non-irradiated HCC showed two peaks, a maximum at the late activity phase (ZT20) and a second peak in the early inactivity phase (ZT02). This is in contrast to the time course in OSCs. Two proliferation peaks were also observed in double transgenic c-myc/TGFα [12] and thus seem to be a characteristic feature of fast-growing tumors [33,34]. A difference in proliferation peaks between tumor and surrounding non-tumoral tissue was also observed in other tumors [35,36]. The daily variations of cell proliferation in HCC and the NTL result from the circadian oscillation of the cell cycle molecules which either promote or inhibit cell cycle proliferation (e.g. CycD1 and c-Myc) [33,36,37].

Whole-body irradiation experiments on rodents (i.e. mice and rats) proved that response of the tumors and adjacent host tissues to radiotherapy is influenced by the time of the day. Thus, applying the radiotherapy at the proper timing can improve the efficacy of the radiotherapy on tumors to the maximum and reduce its high cytotoxicity effects (low tolerance) on the adjacent host tissues [38]. Patients with metastatic lung cancer head-and-neck cancers, and cervical carcinoma revealed less toxicity (i.e. mucositis) when the radiotherapy was applied in the morning and evening, respectively [17,18,39].

Our results showed that irradiation resulted in a decrease in the number of Ki67+ cells in both NTL and HCC at all-time points. Importantly, the effect was most pronounced when the radiotherapy was applied at the time points of the proliferation peaks which were different between the HCC and NTL. Notably, irradiation at ZT20

had a low antiproliferative effect on NTL (32.6%) but had the highest anti-proliferative effect on the HCC (94.3%).

In the *ex vivo* samples without irradiation, the number of γ-H2AX+ cells was much higher in HCC than in NTL, consistent with the *in vitro* data and with our previous findings [12]. Both tissues showed a daily variation in γ-H2AX immunoreaction. NTL showed only one peak at ZT02 while HCC showed an additional peak at ZT20. The increase of γ-H2AX+ cells in HCC during the second half of the dark phase is consistent with our previous findings [12]. Notably, the time courses of Ki67 and γ-H2AX run largely parallel in both tissues, indicating an interconnection of the two cell cycle components in both non-tumoral tissue and tumor.

In both HCC and NTL, irradiation resulted in an increase in the number of γ-H2AX+ cells. The effect of irradiation on DNA damage was time-dependent. In NTL, it was highest at ZT02 and ZT14, intermediate at ZT08 and lowest at ZT20. In HCC, the effect of irradiation was similar at all ZTs. Importantly, radiotherapy treatment during the late activity phase (ZT20) had the lowest effect on DNA-DSBs damage in NTL and caused effective damage in HCC. The increase in the number of γ-H2AX+ cells after irradiation confirms that the irradiation induces the DNA-DSBs repairing mechanism [40] and that X-rays as well as ionizing radiotherapy contribute to the γ-H2AX response [19].

At this point, results obtained *in vitro* and *ex vivo* should be compared in order to evaluate whether OSC could substitute or at least supplement experiments with whole animals. Our study reveals that *in vitro* experiments may be useful to determine the dosage, because the effects of irradiation were dose-dependent and found only at a dose of 10 Gy but not of 2 Gy. However, with regard to the time course of proliferation, DNA-DSBs and radiosensitivity there were substantial differences between *in vitro* and *ex vivo* samples. The time-dependent changes observed in *ex vivo* samples of both non-irradiated HCC and NTL could not be detected in the OSC and also the time points at which irradiation elicited maximal effects on proliferation and DNA-DSBs differed between *ex vivo* and *in vitro* samples. These differences can be explained by: 1) the cell cycle components are regulated by molecular clockwork which in turn is entrained by signals which are generated from the central rhythm

generator in the SCN and transmitted to peripheral organs, such as the liver via the autonomic innervation or the blood stream. However, OSC lack these connections. 2) The impact of daily changes in body temperature which is considered a resetting cue for the peripheral clocks including the liver [41] is missing in OSC which were kept at constant temperature throughout the whole experiments. Thus, under the conditions used in our study, OSC are not suited to test chronotherapeutic approaches. Future studies are needed to test whether stronger external synchronization signals, such as timed melatonin and/or glucocorticoid application would increase the chronotherapeutic value of OSC.

Disruption or mutation of clock genes is associated with genomic instability and increased proliferation rate, both favorable conditions for carcinogenesis [3,28]. Thus, we analysed the expression of seven core clock genes in the HCC and the surrounding NTL of non-irradiated and irradiated animals. In NTL, all clock genes showed a time-dependent variation consistent with our previous observations [12]. In HCC, *Per1*, *Per2*, and *Rev-erbα* showed a similar time course, although *Rev-erbα* showed reduced amplitude, indicating that rhythmic expression of these clock genes is regulated similarly in the tumor and the non-tumoral liver. The molecular clockwork in liver is controlled by many different rhythmic cues such as food intake, glucocorticoids, insulin and body temperature [26,27,41-43]. These rhythmic cues might also regulate the rhythmic expression of clock genes in the tumor. However, expression of the other clock genes, *Cry1*, *Cry2*, *Clock*, and *Bmal1* showed a time-dependent decrease in HCC as compared with the NTL. Transcription of *Wee1* which inhibits the entry into mitosis through inhibiting Cdk1, a key player in cell cycle regulation, is activated by CLOCK/BMAL1 and repressed by PER/CRY [44]. Thus, down-regulation of *Cry1*, *Cry2*, *Clock* and *Bmal1* might be linked with the enhanced proliferation in HCC. Clock gene expression is differently altered in various tumors [45-50] for multiple reasons. One major reason for clock gene dysregulation is a lack of tumor vascularization with many consequences such as a lack of access to circadian resetting cues in the blood and hypoxia [51]. Chronic hypoxia leads to an activation of transcription factors such as HIF-1α and HIF-1β, which bind to hypoxia response elements in the promoter region of target genes [51,52]. In the HCC cell line, PLC/PRF/5, experimental hypoxia led to altered clock gene expression [53]. In

addition, hyper-methylation of clock gene promoter regions is discussed as possible reasons for clock gene dysregulation in tumors [49,51,53].

To date, little is known about the effects of radiotherapy on the molecular clockwork which controls several rhythmic cell functions and thus affecting tolerability and efficacy of anticancer treatments [6,54,55]. Clock genes regulate DNA damage checkpoint responses, DNA repair mechanisms, and apoptosis in response to ionizing radiation in the healthy tissue [56]. Mice with mutations/deletion in the clock genes, *Clock/Bmal1* and *Per1/2*, showed enhanced chemotherapy- or gamma radiation-induced toxicity in the healthy tissue [57,58] and *Per2* mutant mice are more prone to develop cancer induced by gamma radiation or chronic nitrosamine treatment [36,46]. An effect of gamma irradiation on clock gene expression in liver has been reported before in OSC [14] and with the whole animals [14,36], however the experiments with the whole animals were only performed at one time point of irradiation (ZT10) and during the acute phase, up to 15 h after irradiation [36]. Most remarkably, the clock gene expression pattern in the tumor predicts the response of tumor patients to chemo-radiotherapy [55], emphasizing the role of the molecular clockwork in the efficacy of cancer treatment. Thus, we analyzed the effect of irradiation on clock gene expression in NTL and HCC. In NTL, irradiation resulted in a down-regulation in expression of the transcriptional activators *Clock* (ZT02, 08) and *Bmal1* (ZT02) and an up-regulation in expression of the transcriptional repressor *Per2* (ZT14). Importantly, irradiation at ZT20 had no effect on clock gene expression in NTL. This is consistent with a low impact of irradiation on proliferation and DNA-DSBs in NTL at this time point.

Hematopoiesis is one of the most sensitive systems in the body to radiotherapy and reduction of white and red blood cells are one of the most common side effects of radiotherapy [29,30]. Thus, we analyzed the number of blood cells in control and HCC bearing mice with and without irradiation at different ZTs to monitor time-dependent acute side effects of radiotherapy.

The control mice showed significant daily variations in the number of leukocytes with a peak at the light phase and a trough at the dark phase while the number of erythrocytes and the hemoglobin concentration was not significantly different among time points. This is consistent with an earlier study in C57BL/6 mice

[59]. In HCC bearing mice, the number of leukocytes was increased during the late dark phase (ZT20) and the percentage of granulocytes was increased at ZT08. Our previos data (submitted paper [60]) showed that corticosterone levels are increased at ZT08 in the HCC bearing mice. Glucocorticoids are known to increase granulocytosis [61]. Thus, the increase in glucocorticoids may account for the change in leukocyte number and composition. While irradiation had no effect on hemoglobin concentration, erythrocyte or platelet numbers, it caused a significant reduction in the total number of leukocytes. Irradiation when applied at ZT02 and ZT08 caused a significant depletion in the total number of leukocytes conforming to data on white blood cell counts in patients [62,63]. Notably, irradiation at ZT14 and ZT20 had no effect on the total leukocyte number, thus, these time points might be preferable for radiotherapy in terms of reducing this severe side effect.

Irrespective of the time of irradiation, the percentage of lymphocytes was significantly decreased, while the percentage of the other types of leucocytes were increased. Consistently, antimitotic therapy led to a dramatic decrease in the number of circulating lymphocytes independent of a functional molecular clockwork [57]. We could find recently, that irradiation of HCC bearing mice resulted in a strong increase in corticosterone levels (submitted paper [60]). Lymphocyte apoptosis is enhanced by glucocorticoids [64,65] and the decrease in lymphocytes might be a consequence of increased corticosterone levels after irradiation recently demonstrated (submitted paper [60]). In contrast, the increased percentages of granulocytes and monocytes, which build the first line of defense during the inflammation, may be due to the release of the proinflammatory cytokines (e.g. IL-1 and TNF-α), chemokines (e.g. IL-8) and factors participating in the early inflammatory response to the radiation [62,66,67].

As expected, no effect was observed in number of erythrocytes 2 days after irradiation because of the fact that the erythrocytes survive for 120 days and the reduction in number of erythrocytes after radiotherapy is considered one of the long-term side effects.

4. Material and method

4.1. Experimental animals and HCC induction

Male transgenic *Per2::luc* mice on a C57BL6/J background were used according to accepted standards of humane animal care and federal guidelines and Directive 2010/63/EU of the European Union. All experiments were approved by the Regierungspräsidium Darmstadt and the Landesamt für Natur, Umwelt und Verbraucherschutz NRW (Reference number: AZ 81-02.04.2018-A146). At the age of 2 weeks, the mice were injected intraperitoneally between ZT02 and ZT04 with a single dose of diethylnitrosamine (DEN) (10 mg/kg body weight, Sigma Aldrich, St. Louis, USA) to induce HCC. Phenobarbital (PB) (Luminal, Desitin, Hamburg, Germany) was chronically administered via the drinking water with a concentration of 0.05% to accelerate the HCC induction. Food and water containing PB were supplied ad libitum. All mice were kept under the standard light-dark (LD) cycle (12:12). ZT00 defines the onset of the light phase. All experiments during the dark phase were performed under dim red light. At the age of 7-10 months, HCC presented either as a single big tumor or as multiple smaller tumors (Supplementary Figure S3). Tumor development was screened via magnetic resonance imaging and post mortem inspection.

4.2. Magnetic resonance imaging (MRI)

For MRI, mice were anesthetized with 1.5% isoflurane in a water-saturated gas mixture of 20% oxygen in nitrogen applied at a rate of 75 mL/min by manually restraining the animal and placing its head in an in-house-built nose cone. Respiration was monitored with a pneumatic pillow positioned at the animal's back. Vital function was acquired by using an M1025 system (SA Instruments, Stony Brook, NY) to synchronize data acquisition with respiratory motion. Throughout the experiments mice were breathing spontaneously at a rate of ~100 min-1 and were kept at 37 °C. Animals were placed within the resonator so that in z-direction (30 mm) the field of view (FOV) covered the abdomen from just below the diaphragm down to the pelvis.

Data were recorded on a Bruker AvanceIII 9.4 Tesla Wide Bore (89 mm) nuclear magnetic resonance (MR) spectrometer (Bruker, Rheinstetten, Germany) operating at a frequency of 400.13 MHz for 1H. Experiments were carried out using a Bruker microimaging unit (Micro 2.5) equipped with actively shielded gradient sets

(capable of 1.5 T/m maximum gradient strength and 150 µs rise time at 100% gradient switching), a linear 1H 25-mm birdcage resonator, and Paravision 5.1 as operating software.

Liver tumors were determined by acquisition of images with a respiratory-gated 2D 1H multi-slice fast low angle snapshot (FLASH) gradient-echo sequence exploiting the native tissue contrast between non-tumoral and tumor tissue (see supplementary Figure S4). Data were taken from a field-of-view of 25.6×25.6 mm^2 with a spatial resolution of 100×100 μm^2 (TE, 1.62 ms; TR, 111.52 ms; slices, 16; slice thickness, 1 mm; averages, 1, acquisition time, 15 s).

4.3. Irradiation of organotypic slice cultures (OSC)

Mice with HCC were sacrificed at ZT02. The liver was dissected under sterile conditions and stored quickly in ice-cold storage solution (MACS tissue storage solution, Miltenyi Biotec, Bergisch Gladbach, Germany). NTL and HCCs were sliced separately into 600µm thick sections using a Krumdieck tissue chopper (TSE Systems, Bad Homburg, Germany) and kept in ice-cold sterilized Dulbecoo's phosphate buffered saline (DPBS) (Gibco by Life Technologies, Paisley, UK). Then the slices were transferred to cell culture inserts (0.4 µm pores, Falcon, Durham, USA) which were inserted in 6 well plates filled with 1 ml pre-warmed culture medium modified according to previously published protocol [68]. The medium consisted of DMEM, supplemented with 10% fetal bovine serum, 100 U/ml penicillin, 0.1 mg/ml streptomycin, 10 mmol/l HEPES, 1 mg/ml insulin, 8 mg/ml ascorbic acid and 20 mmol/l sodium pyruvate. The slices from the NTL and HCCs of each mouse were randomly divided into three groups, one non-irradiated and two for irradiation with different doses, and placed in twelve different plates. All slices were cultured in an incubator under constant conditions of 37° C and 5% CO_2. On the next day, at 05:00 am, the medium was changed and this time point was defined as CT00 as medium change resets the molecular clockwork in cell culture [69]. 2 hours after the medium change (CT02), the plates were removed from the culturing conditions and transferred to the irradiation lab in a cooler to reduce the possible changes in the ambient temperature. The slices were irradiated at four different CTs (CT02, CT08, CT14 and CT20) with two different doses, 2 Gy (at 175 kV and 15 mA, for about 2 min) and 10 Gy (at 175 kV and 15 mA, for about 10 min), using Gulmay RS225 X-

ray system (X-Strahl, Camberley, UK). Non-irradiated slices were transported to the irradiation lab but did not receive irradiation. Within one hour after irradiation, the slices were returned to regular culturing conditions. 48 hours after irradiation, the slices were harvested at the same CTs used for irradiation. For immunohistochemistry, the slices were fixed in 4% paraformaldehyde (PFA) in phosphate buffered saline (0.1 M PBS, pH 7.4) for 12 hours and then cryoprotected with gradually increasing concentrations of sucrose in PBS (15% and 30%). Then the slices were cut into 10 µm thick serial sections using a cryostat (Leica CM, Wetzlar, Germany).

4.4. Irradiation of mice and ex vivo analyses

Forty-eight HCC bearing mice (7-10 month old) were used for *ex vivo* investigations and randomly divided into 2 groups: the first group comprised 24 animals which were irradiated with a dose of 10 Gy (irradiated group) at four different ZTs (ZT02, ZT08, ZT14 and ZT20). The second group comprised 24 mice with HCC which were transported to the irradiation lab together with the animals of the irradiated group at the same ZTs but they were not subjected to irradiation (non-irradiated group) to omit the effect of transportation.

For irradiation, the mice were deeply anesthetized by intraperitoneal injection with a mixture of ketamine (100 mg/kg body weight, Inresa, Freiburg, Germany) and xylazine (10 mg/kg body weight, Rompun 2%, Bayer Leverkusen, Germany) then the whole animal's body irradiated with a dose of 10 Gy by fixing the animals on a styrofoam plate so that their ventral side was exposed to the irradiation source. Exposure with 10 Gy irradiation was performed as described above (OSCs).

48 hours later, the irradiated and non-irradiated mice (n= 6/ZT in each group) were sacrificed at the same ZTs used for irradiation. Blood was collected from the right atrium in EDTA blood tubes and quickly mixed to avoid coagulation. In addition, the blood cells were analyzed in a control group which did not receive any treatment. The complete blood counts (CBC) were measured automatically using Scil Vet abc, animal blood count machine (Scil, Viernheim, Germany).

Each group of mice was randomly divided into two subgroups (n=3/ZT) which were used for either immunohistochemistry or real-time PCR analysis. For immunofluorescence, the animals were anesthetized as mentioned above and then

perfused transcardially with NaCl (0.9%) for 1 min followed by approximately 100 ml 4% PFA in PBS for 15 min. Perfusion during the night was performed under dim red light. NTL and HCCs were excised and separated by a scalpel. Then the tissues were post-fixed for 2 hours in 4% PFA in PBS, cryoprotected with gradually increasing concentrations of sucrose in PBS (10%, 20%, and 30%) and cut into 12 µm thick serial frozen sections using a cryostat.

For real-time PCR, the mice were sacrificed and NTL and HCCs were freshly dissected, rapidly snap frozen in liquid nitrogen and stored at -80° C until further use. The experimental design is shown in Supplementary Figure S5.

4.5. Immunofluorescence

Sections from OSC and *ex vivo* samples were incubated with normal goat serum (1:20) diluted in PBS with 0.3% Triton (PBST) for 1 hour at room temperature (RT) to minimize non-specific staining. Then the sections were incubated with the primary antibodies against Ki67 (1:200, #KI6891C01, DCS, Hamburg, Germany) or against γ-H2AX (1:200, #2577, Cell Signaling Technology, Frankfurt am Main, Germany) overnight at RT. The primary antibodies were diluted in 1% bovine serum albumin (BSA) in PBST. On the next day, sections were incubated with secondary goat anti rabbit antibodies (Alexa Fluor 568 for Ki67 or Alexa Fluor 488 for γ-H2AX) in PBS (1:250, Life Technologies, San Diego, CA, USA) for 1 hour in darkness at RT. For negative control, the primary antibodies were omitted and sections were only incubated with the secondary antibodies. For nuclear staining, all sections were incubated with Hoechst dye diluted in PBS (1:10000) for 10 min in darkness at RT. The sections were then covered with fluorescent mounting media (Fluoromount-G, Southern Biotech, Germany).

Sections were analyzed using Keyence BZ-X800 series microscope (Keyence, Osaka, Japan) using x20 objective and the settings were kept constant for each staining. Six representative images at least from each animal/time point/group were analyzed and averaged. The number of immunoreactive (+) cells was counted by an investigator blind to the treatment. The number of positive cells was counted manually in each image in a total area= 0.4 mm^2.

4.6. Real-time PCR

Total RNA from *ex vivo* samples was extracted using RNeasy Plus Universal Mini Kit (QIAGEN, Hilden, Germany). Total RNA concentration and purity were measured using a Nano-Drop spectrophotometer. Revert Aid First Strand cDNA Synthesis Kit (Thermo Scientific, Vilnius, Lithuania) was used for the synthesis of the cDNA from 1 µg RNA. Primers for the clock genes *Per1*, *Per2*, *Cry1*, *Cry2*, *Clock*, *Bmal1,* and *Rev-erbα* (Sigma Aldrich, Germany, Table 1) and the housekeeping gene, β-actin, were validated using conventional PCR and gel electrophoresis. Real-time PCR was performed using Step One Plus (Applied Biosystems) and SYBR GREEN (Kapa Abi-Prism). The relative mRNA expression of the clock genes, normalized to the housekeeping gene, was calculated according to Pfaffl method [70].

Table (1): List of primer sequences used in qPCR**.**

Gene	Primer sequence
β-Actin F	**5′ –GGCTGTATTCCCCTCCATGC- 3′**
β-Actin R	**5′ –CCAGTTGGTAACAATGCCATGT- 3′**
mPer1 F	**5′ –TGG CTC AAG TGG CAA TGA GTC - 3′**
mPer1 R	**5′ –GGC TCG AGC TGA CTG TTC ACT - 3′**
mPer2 F	**5′ –CCAAACTGCTTGTTCCAGGC- 3′**
mPer2 R	**5′ –ACCGGCCTGTAGGATCTTCT - 3′**
mCry1 F	**5′ – CTT CTG TCT GAT GAC CAT GAT GA- 3′**
mCry1 R	**5′ – CCC AGG CCT TTC TTT CCA A- 3′**
mCry2 F	**5′ – AGG GCT GCC AAG TGC ATC AT- 3′**
mCry2 R	**5′ – AGG AAG GGA CAG ATG CCA ATA G- 3′**
mClock F	**5′ – CAC CGA CAA AGA TCC CTA CTG AT- 3′**
mClock R	**5′ – TGA GAC ATC GCT GGC TGT GT- 3′**
Bmal F	**5′ –GTA GAT CAG AGG GCG ACA GC- 3′**
Bmal R	**5′ –CCT GTG ACA TTC TGC GAG GT- 3′**
Rev-erbα F	**5′ –GGT GCG CTT TGC ATC GTT- 3′**
Rev-erbα R	**5′ –GGT TGT GCG GCT CAG GAA- 3′**

4.7. Statistical analysis

Statistics were calculated using Graph Pad Prism 8 software. For *in vitro* experiments, repeated measure analysis of variance (ANOVA) was used. For *ex vivo* experiments, ordinary one-way ANOVA followed by *Tukey's* test for multiple comparisons among different time points was performed. Effect of time and treatment was analyzed by two-way ANOVA followed by *Sidak's* test for multiple comparisons. The results were represented as mean ± standard error of the mean (SEM) and were regarded as significant at $p < 0.05$.

5. Conclusions

Our study showed time-dependent effects of radiotherapy on proliferation rate, DNA damage/repair, clock gene expression, and white blood cells. The late activity phase (ZT20) might be the most favorable time to apply radiotherapy in nocturnal mice as the effects on the tumor are high and the side effects on the surrounding NTL and on the total leukocyte number are lowest at this time point. Moreover, at this time point irradiation had no effect on clock gene expression in NTL. Translational studies are required now to clarify whether also in humans the late activity phase (ZT08) would be the optimal time point to apply radiotherapy for HCC patients. The comparison between *in vitro* (OSC) data and *ex vivo* results from whole animals shows that *in vitro* experiments may be useful to determine the dosage, because the effects of irradiation were dose-dependent. However, with regard to the time course of proliferation, DNA-DSBs and radiosensitivity, there were substantial differences between *in vitro* and *ex vivo* samples. Thus, under the conditions used in our study, OSC is of limited value. While they may help to determine dose-dependent effects, they are not suited to design chronotherapeutic approaches. Adding resetting cues to the medium (e.g. melatonin and dexamethasone) or changes the temperature conditions during the incubation of the culture might improve the value of the OSC to test the chronotherapeutic strategies.

Author Contributions: Soha A. Hassan: concept/design, acquisition, analysis and interpretation of data and drafting of the manuscript. Amira A. H. Ali: acquisition of data and organization of figures. Dennis Sohn: acquisition of data. Ulrich Flögel: acquisition of data. Reiner U. Jänicke: critical revision of the manuscript. Horst-

Werner Korf: concept/design, acquisition and interpretation of data, supervision and drafting of the manuscript. Charlotte von Gall: data interpretation and drafting of the manuscript. All authors have read and approved the manuscript.

Funding: S. A. H. is supported by German Egyptian Research Long-term Scholarship (GERLS) Program of the DAAD. We acknowledge support by the Heinrich-Heine-University Düsseldorf for open access funding.

Institutional Review Board Statement: Animals were used according to accepted standards of humane animal care and federal guidelines and Directive 2010/63/EU of the European Union. All experiments were approved by the Regierungspräsidium Darmstadt and the Landesamt für Natur, Umwelt und Verbraucherschutz NRW (Reference number: AZ 81-02.04.2018-A146).

Acknowledgments: We thank Dr. Julia Hesse (Department of Molecular Cardiology, Heinrich-Heine-University, Düsseldorf, Germany) for facilitating the *in vitro* experiments in her department. We thank Ursula Lammersen, Angelika Hallenberger, Hanna Bellert and Ralf Fassbender for excellent technical support.

Conflicts of Interest: The authors have no conflict of interest.

Supplementary materials

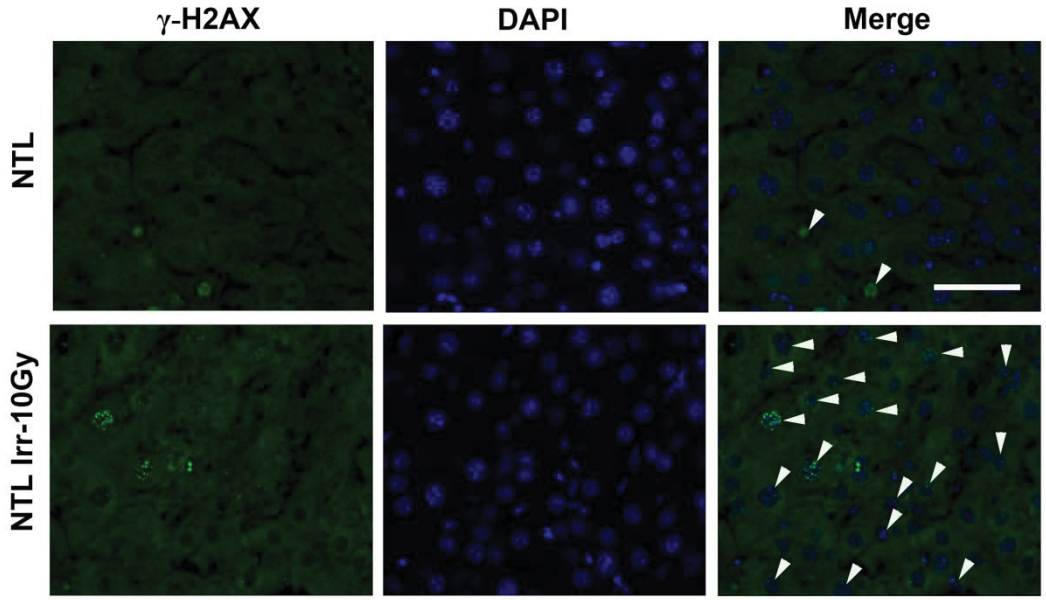

Fig. S1 Representative high magnification photomicrographs of γ-H2AX immunoreactive (+) (green) in DAPI stained nuclei (blue) in non-tumoral liver (NTL) without or with irradiation (Irr-10Gy) at ZT02. γ-H2AX + cells were defined by co-localization of γ-H2AX foci (arrows) and DAPI. Scale bar, 50 μm.

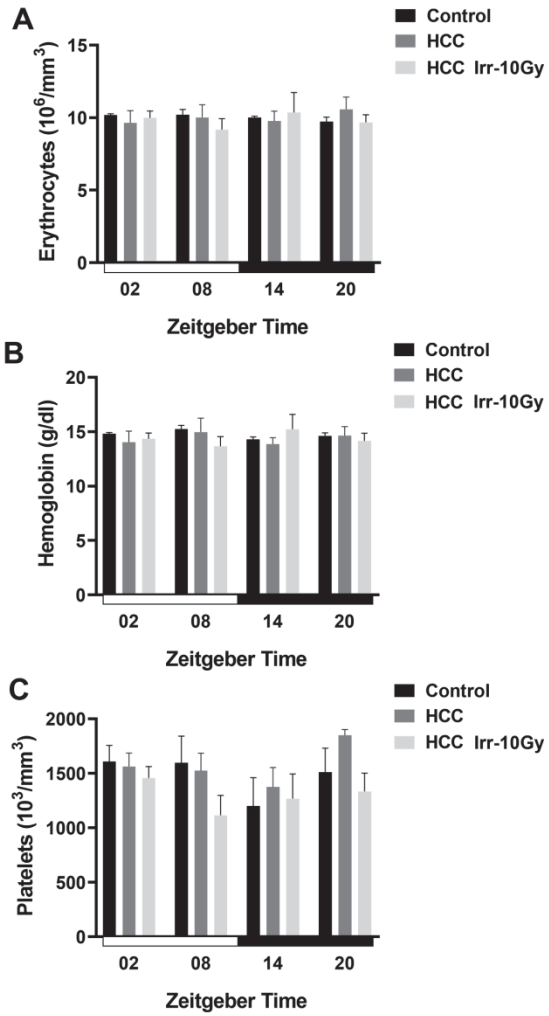

Fig. S2 Blood cell analysis in control and hepatocellular carcinoma (HCC) bearing mice without and with irradiation. At different *Zeitgeber* times (ZT00= the onset of the light phase), mice were irradiated (Irr) with a dose of 10 Gy (n= 3-6/time point) or handled similarly but not irradiated. 48 hours later, mice were sacrificed and the blood was collected at the same ZTs. Erythrocyte numbers (**A**). Hemoglobin concentration (**B**). Platelet numbers (**C**). Plotted are the mean numbers ± SEM. White and black bars indicate the light and dark phases, respectively.

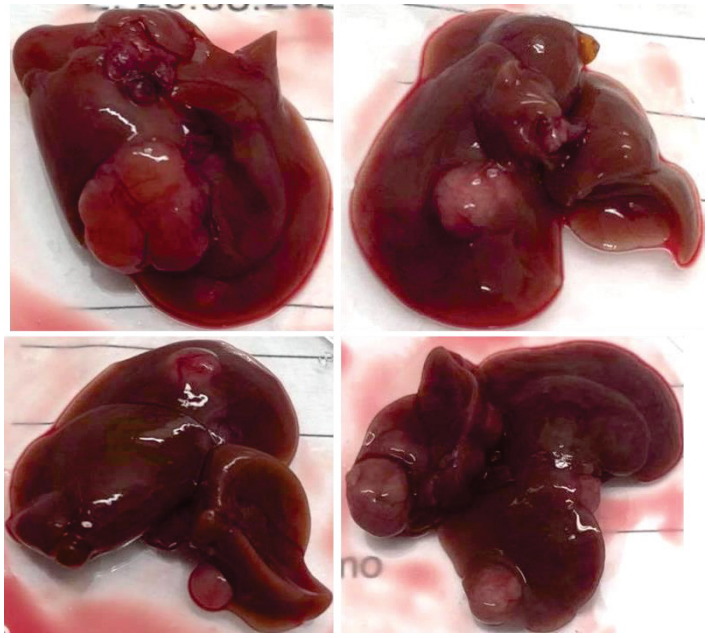

Fig. S3 Representative photographs of single and multiple hepatocellular carcinomas (HCC) at the age of 7-10 months. The mice received a single injection of diethylnitrosamine (DEN) at the age of two weeks and chronic treatment of phenobarbital (PB) in the drinking water to accelerate the HCC induction.

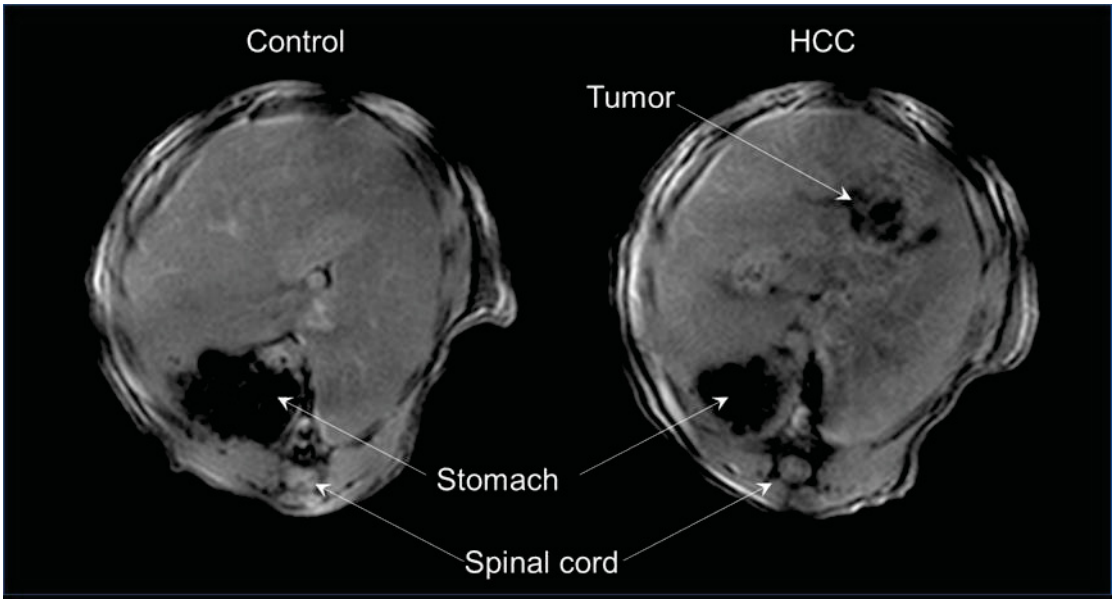

Fig. S4 Representative axial MRI images from healthy and HCC bearing mice demonstrating the unequivocal identification of tumor tissue within the liver.

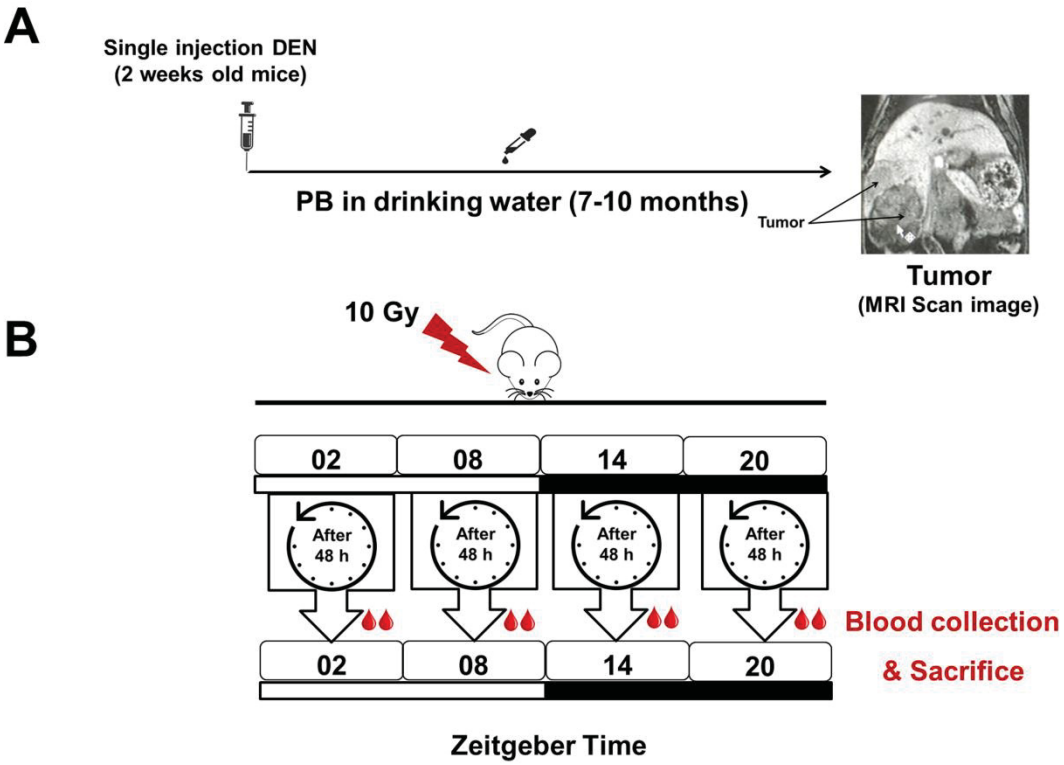

Fig. S5 Diagram for the experimental design of tumor induction, animals' irradiation and *ex vivo* analyses. **A,** Transgenic *Per2::luc* mice (n=48 mice) received a single injection of diethylnitrosamine (DEN) at the age of two weeks and chronic treatment of phenobarbital (PB) in the drinking water to accelerate the hepatocellular carcinoma (HCC) induction. HCC developed in animals in either single or multiple tumors at the age of 7-10 months. Tumor development was screened via magnetic resonance imaging (MRI) and validated by post mortem inspection. **B,** 24 animals of the HCC bearing mice were selected for irradiation with a dose of 10 Gy at four different *Zeitgeber* time (ZT) points (ZT02, ZT08, ZT14 and ZT20) (6 animals per time point). 48 hours later, blood was collected and animals were sacrificed at the same ZTs used for irradiation. 12 animals (n=3/ZT) were perfused for immunohistochemistry and 12 animals (n=3/ZT) were used for real-time PCR by collecting and snap freezing the native tissue. White and black bars indicate the light and dark phases, respectively.

References

1. Globocan. Liver cancer fact sheet **2019**.
2. IARC. Latest global cancer data: Cancer burden rises to 18.1 million new cases and 9.6 million cancer deaths in 2018. *PRESS RELEASE* **2018**, *N° 263*.
3. Sanchez, D.I.; Gonzalez-Fernandez, B.; Crespo, I.; San-Miguel, B.; Alvarez, M.; Gonzalez-Gallego, J.; Tunon, M.J. Melatonin modulates dysregulated circadian clocks in mice with diethylnitrosamine-induced hepatocellular carcinoma. *Journal of Pineal Research* **2018**, *65*, doi:ARTN e1250610.1111/jpi.12506.
4. Wild, A.T.; Gandhi, N.; Chettiar, S.T.; Aziz, K.; Gajula, R.P.; Williams, R.D.; Kumar, R.; Taparra, K.; Zeng, J.; Cades, J.A., et al. Concurrent versus sequential sorafenib therapy in combination with radiation for hepatocellular carcinoma. *Plos One* **2013**, *8*, e65726, doi:10.1371/journal.pone.0065726.
5. Rebouissou, S.; La Bella, T.; Rekik, S.; Imbeaud, S.; Calatayud, A.L.; Rohr-Udilova, N.; Martin, Y.; Couchy, G.; Bioulac-Sage, P.; Grasl-Kraupp, B., et al. Proliferation Markers Are Associated with MET Expression in Hepatocellular Carcinoma and Predict Tivantinib Sensitivity In Vitro. *Clin Cancer Res* **2017**, *23*, 4364-4375, doi:10.1158/1078-0432.CCR-16-3118.
6. Eriguchi, M.; Levi, F.; Hisa, T.; Yanagie, H.; Nonaka, Y.; Takeda, Y. Chronotherapy for cancer. *Biomedicine & Pharmacotherapy* **2003**, *57*, 92-95, doi:10.1016/j.biopha.2003.08.012.
7. Innominato, P.F.; Levi, F.A.; Bjarnason, G.A. Chronotherapy and the molecular clock: Clinical implications in oncology. *Adv Drug Deliv Rev* **2010**, *62*, 979-1001, doi:10.1016/j.addr.2010.06.002.
8. Mandal, A.S.; Biswas, N.; Karim, K.M.; Guha, A.; Chatterjee, S.; Behera, M.; Kuotsu, K. Drug delivery system based on chronobiology--A review. *J Control Release* **2010**, *147*, 314-325, doi:10.1016/j.jconrel.2010.07.122.
9. Li, H.X. The role of circadian clock genes in tumors. *Onco Targets Ther* **2019**, *12*, 3645-3660, doi:10.2147/OTT.S203144.
10. Ohri, N.; Dawson, L.A.; Krishnan, S.; Seong, J.; Cheng, J.C.; Sarin, S.K.; Kinkhabwala, M.; Ahmed, M.M.; Vikram, B.; Coleman, C.N., et al. Radiotherapy for Hepatocellular Carcinoma: New Indications and Directions for Future Study. *J Natl Cancer Inst* **2016**, *108*, doi:10.1093/jnci/djw133.
11. Chen, C.P. Role of Radiotherapy in the Treatment of Hepatocellular Carcinoma. *J Clin Transl Hepatol* **2019**, *7*, 183-190, doi:10.14218/JCTH.2018.00060.
12. Hassan, S.A.; Schmithals, C.; von Harten, M.; Piiper, A.; Korf, H.-W.; von Gall, C. Time-dependent changes in proliferation, DNA damage and clock gene expression in hepatocellular carcinoma and healthy liver of a transgenic mouse model. *International Journal of Cancer* **2021**, *148*, 226-237, doi:https://doi.org/10.1002/ijc.33228.
13. Harper, E.; Talbot, C.J. Is it Time to Change Radiotherapy: The Dawning of Chronoradiotherapy? *Clin Oncol (R Coll Radiol)* **2019**, *31*, 326-335, doi:10.1016/j.clon.2019.02.010.
14. Muller, M.H.; Rodel, F.; Rub, U.; Korf, H.W. Irradiation with X-rays phase-advances the molecular clockwork in liver, adrenal gland and pancreas. *Chronobiol Int* **2015**, *32*, 27-36, doi:10.3109/07420528.2014.949735.

15. Shih, H.C.; Shiozawa, T.; Kato, K.; Imai, T.; Miyamoto, T.; Uchikawa, J.; Nikaido, T.; Konishi, I. Immunohistochemical expression of cyclins, cyclin-dependent kinases, tumor-suppressor gene products, Ki-67, and sex steroid receptors in endometrial carcinoma: positive staining for cyclin A as a poor prognostic indicator. *Hum Pathol* **2003**, *34*, 471-478.
16. Johnson, K.; Chang-Claude, J.; Critchley, A.M.; Kyriacou, C.; Lavers, S.; Rattay, T.; Seibold, P.; Webb, A.; West, C.; Symonds, R.P., et al. Genetic Variants Predict Optimal Timing of Radiotherapy to Reduce Side-effects in Breast Cancer Patients. *Clin Oncol (R Coll Radiol)* **2019**, *31*, 9-16, doi:10.1016/j.clon.2018.10.001.
17. Shukla, P.; Gupta, D.; Bisht, S.S.; Pant, M.C.; Bhatt, M.L.; Gupta, R.; Srivastava, K.; Gupta, S.; Dhawan, A.; Mishra, D., et al. Circadian variation in radiation-induced intestinal mucositis in patients with cervical carcinoma. *Cancer* **2010**, *116*, 2031-2035, doi:10.1002/cncr.24867.
18. Rahn, D.A., 3rd; Ray, D.K.; Schlesinger, D.J.; Steiner, L.; Sheehan, J.P.; O'Quigley, J.M.; Rich, T. Gamma knife radiosurgery for brain metastasis of nonsmall cell lung cancer: is there a difference in outcome between morning and afternoon treatment? *Cancer* **2011**, *117*, 414-420, doi:10.1002/cncr.25423.
19. Kuo, L.J.; Yang, L. γ-H2AX – A Novel Biomarker for DNA Double-strand Breaks. *in vivo* **2008**, *22*, 305-310.
20. Sedelnikova, O.A.; Bonner, W.M. GammaH2AX in cancer cells: a potential biomarker for cancer diagnostics, prediction and recurrence. *Cell Cycle* **2006**, *5*, 2909-2913, doi:10.4161/cc.5.24.3569.
21. Liu, C.Y.; Hsieh, C.H.; Kim, S.H.; Wang, J.P.; Ni, Y.L.; Su, C.L.; Yao, C.F.; Fang, K. An indolylquinoline derivative activates DNA damage response and apoptosis in human hepatocellular carcinoma cells. *Int J Oncol* **2016**, *49*, 2431-2441, doi:10.3892/ijo.2016.3717.
22. Liu, S.L.; Han, Y.; Zhang, Y.; Xie, C.Y.; Wang, E.H.; Miao, Y.; Li, H.Y.; Xu, H.T.; Dai, S.D. Expression of metastasis-associated protein 2 (MTA2) might predict proliferation in non-small cell lung cancer. *Target Oncol* **2012**, *7*, 135-143, doi:10.1007/s11523-012-0215-z.
23. Ye, H.; Yang, K.; Tan, X.M.; Fu, X.J.; Li, H.X. Daily rhythm variations of the clock gene PER1 and cancer-related genes during various stages of carcinogenesis in a golden hamster model of buccal mucosa carcinoma. *Oncotargets and Therapy* **2015**, *8*, doi:10.2147/Ott.S83710.
24. Wood, P.A.; Du-Quiton, J.; You, S.; Hrushesky, W.J. Circadian clock coordinates cancer cell cycle progression, thymidylate synthase, and 5-fluorouracil therapeutic index. *Mol Cancer Ther* **2006**, *5*, 2023-2033, doi:10.1158/1535-7163.MCT-06-0177.
25. Zhou, D.; Wang, Y.; Chen, L.; Jia, L.; Yuan, J.; Sun, M.; Zhang, W.; Wang, P.; Zuo, J.; Xu, Z., et al. Evolving roles of circadian rhythms in liver homeostasis and pathology. *Oncotarget* **2016**, *7*, 8625-8639, doi:10.18632/oncotarget.7065.
26. Schibler, U.; Ripperger, J.; Brown, S.A. Peripheral circadian oscillators in mammals: time and food. *J Biol Rhythms* **2003**, *18*, 250-260, doi:10.1177/0748730403018003007.
27. Korf, H.-W.; von Gall, C. Circadian Physiology. In *Neuroscience in the 21st Century: From Basic to Clinical*, Pfaff, D.W., Ed. Springer New York: New York, NY, 2013; 10.1007/978-1-4614-1997-6_65pp. 1813-1845.

28. Huisman, S.A.; Oklejewicz, M.; Ahmadi, A.R.; Tamanini, F.; Ijzermans, J.N.; van der Horst, G.T.; de Bruin, R.W. Colorectal liver metastases with a disrupted circadian rhythm phase shift the peripheral clock in liver and kidney. *Int J Cancer* **2015**, *136*, 1024-1032, doi:10.1002/ijc.29089.
29. Yang, F.E.; Vaida, F.; Ignacio, L.; Houghton, A.; Nauityal, J.; Halpern, H.; Sutton, H.; Vijayakumar, S. Analysis of weekly complete blood counts in patients receiving standard fractionated partial body radiation therapy. *Int J Radiat Oncol Biol Phys* **1995**, *33*, 617-617.
30. Wersal, C.; Keller, A.; Weiss, C.; Giordano, F.; Abo-Madyan, Y.; Tuschy, B.; Suetterlin, M.; Wenz, F.; Sperk, E. Long-term changes in blood counts after intraoperative radiotherapy for breast cancer—single center experience and review of the literature. *Translational Cancer Research* **2019**, *8*, 1882-1903, doi:10.21037/tcr.2019.09.05.
31. Vucic, V.; Isenovic, E.R.; Adzic, M.; Ruzdijic, S.; Radojcic, M.B. Effects of gamma-radiation on cell growth, cycle arrest, death, and superoxide dismutase expression by DU 145 human prostate cancer cells. *Braz J Med Biol Res* **2006**, *39*, 227-236, doi:10.1590/s0100-879x2006000200009.
32. Schwarz-Finsterle, J.; Scherthan, H.; Huna, A.; González, P.; Mueller, P.; Schmitt, E.; Erenpreisa, J.; Hausmann, M. Volume increase and spatial shifts of chromosome territories in nuclei of radiation-induced polyploidizing tumour cells. *Mutation Research/Genetic Toxicology and Environmental Mutagenesis* **2013**, *756*, 56-65, doi:https://doi.org/10.1016/j.mrgentox.2013.05.004.
33. You, S.; Wood, P.A.; Xiong, Y.; Kobayashi, M.; Du-Quiton, J.; Hrushesky, W.J. Daily coordination of cancer growth and circadian clock gene expression. *Breast Cancer Res Treat* **2005**, *91*, 47-60, doi:10.1007/s10549-004-6603-z.
34. Echave Llanos, J.M.; Nash, R.E. Mitotic circadian rhythm in a fast-growing and a slow-growing hepatoma: mitotic rhythm in hepatomas. *J Natl Cancer Inst* **1970**, *44*, 581-585.
35. Klevecz, R.R.; Braly, P.S. Circadian and ultradian rhythms of proliferation in human ovarian cancer. *Chronobiol Int* **1987**, *4*, 513-523.
36. Fu, L.; Pelicano, H.; Liu, J.; Huang, P.; Lee, C. The circadian gene Period2 plays an important role in tumor suppression and DNA damage response in vivo. *Cell* **2002**, *111*, 41-50, doi:10.1016/s0092-8674(02)00961-3.
37. Yang, X.; Wood, P.A.; Ansell, C.M.; Quiton, D.F.; Oh, E.Y.; Du-Quiton, J.; Hrushesky, W.J. The circadian clock gene Per1 suppresses cancer cell proliferation and tumor growth at specific times of day. *Chronobiol Int* **2009**, *26*, 1323-1339, doi:10.3109/07420520903431301.
38. Haus, E. Chronobiology of the mammalian response to ionizing radiation. Potential applications in oncology. *Chronobiol Int* **2002**, *19*, 77-100, doi:10.1081/cbi-120002592.
39. Goyal, M.; Shukla, P.; Gupta, D.; Bisht, S.S.; Dhawan, A.; Gupta, S.; Pant, M.C.; Verma, N.S. Oral mucositis in morning vs. evening irradiated patients: a randomised prospective study. *Int J Radiat Biol* **2009**, *85*, 504-509, doi:10.1080/09553000902883802.
40. Wang, J.S.; Wang, H.J.; Qian, H.L. Biological effects of radiation on cancer cells. *Mil Med Res* **2018**, *5*, 20, doi:10.1186/s40779-018-0167-4.
41. Buhr, E.D.; Yoo, S.H.; Takahashi, J.S. Temperature as a universal resetting cue for mammalian circadian oscillators. *Science* **2010**, *330*, 379-385, doi:10.1126/science.1195262.

42. Bur, I.M.; Zouaoui, S.; Fontanaud, P.; Coutry, N.; Molino, F.; Martin, A.O.; Mollard, P.; Bonnefont, X. The comparison between circadian oscillators in mouse liver and pituitary gland reveals different integration of feeding and light schedules. *PLoS One* **2010**, *5*, e15316, doi:10.1371/journal.pone.0015316.
43. Mohawk, J.A.; Green, C.B.; Takahashi, J.S. Central and peripheral circadian clocks in mammals. *Annu Rev Neurosci* **2012**, *35*, 445-462, doi:10.1146/annurev-neuro-060909-153128.
44. Matsuo, T.; Yamaguchi, S.; Mitsui, S.; Emi, A.; Shimoda, F.; Okamura, H. Control mechanism of the circadian clock for timing of cell division in vivo. *Science* **2003**, *302*, 255-259, doi:10.1126/science.1086271.
45. Huisman, S.A.; Ahmadi, A.R.; JN, I.J.; Verhoef, C.; van der Horst, G.T.; de Bruin, R.W. Disruption of clock gene expression in human colorectal liver metastases. *Tumour Biol* **2016**, *37*, 13973-13981, doi:10.1007/s13277-016-5231-7.
46. Mteyrek, A.; Filipski, E.; Guettier, C.; Okyar, A.; Levi, F. Clock gene Per2 as a controller of liver carcinogenesis. *Oncotarget* **2016**, *7*, 85832-85847, doi:10.18632/oncotarget.11037.
47. Deng, F.; Yang, K. Current Status of Research on the Period Family of Clock Genes in the Occurrence and Development of Cancer. *J Cancer* **2019**, *10*, 1117-1123, doi:10.7150/jca.29212.
48. Oshima, T.; Takenoshita, S.; Akaike, M.; Kunisaki, C.; Fujii, S.; Nozaki, A.; Numata, K.; Shiozawa, M.; Rino, Y.; Tanaka, K., et al. Expression of circadian genes correlates with liver metastasis and outcomes in colorectal cancer. *Oncol Rep* **2011**, *25*, 1439-1446, doi:10.3892/or.2011.1207.
49. Lin, Y.M.; Chang, J.H.; Yeh, K.T.; Yang, M.Y.; Li, T.C.; Lin, S.F.; Su, W.W.; Chang, J.G. Disturbance of Circadian Gene Expression in Hepatocellular Carcinoma. *Molecular Carcinogenesis* **2008**, *47*, 925-933, doi:10.1002/mc.20446.
50. Sotak, M.; Polidarova, L.; Ergang, P.; Sumova, A.; Pacha, J. An association between clock genes and clock-controlled cell cycle genes in murine colorectal tumors. *International Journal of Cancer* **2013**, *132*, 1032-1041, doi:10.1002/ijc.27760.
51. Morgan, M.; Dvuchbabny, S.; Martinez, C.-A.; Kerr, B.; Cistulli, P.A.; Cook, K.M. The Cancer Clock Is (Not) Ticking: Links between Circadian Rhythms and Cancer. *Clocks & Sleep* **2019**, *1* 435–458, doi:doi:10.3390/clockssleep1040034.
52. Hunyor, I.; Cook, K.M. Models of intermittent hypoxia and obstructive sleep apnea: molecular pathways and their contribution to cancer. *Am J Physiol-Reg I* **2018**, *315*, R669-R687, doi:10.1152/ajpregu.00036.2018.
53. Yu, C.; Yang, S.L.; Fang, X.; Jiang, J.X.; Sun, C.Y.; Huang, T. Hypoxia disrupts the expression levels of circadian rhythm genes in hepatocellular carcinoma. *Mol Med Rep* **2015**, *11*, 4002-4008, doi:10.3892/mmr.2015.3199.
54. Mormont, M.C.; Levi, F. Cancer chronotherapy: Principles, applications, and perspectives. *Cancer* **2003**, *97*, 155-169, doi:10.1002/cncr.11040.
55. Lu, H.; Chu, Q.; Xie, G.; Han, H.; Chen, Z.; Xu, B.; Yue, Z. Circadian gene expression predicts patient response to neoadjuvant chemoradiation therapy for rectal cancer. *Int J Clin Exp Pathol* **2015**, *8*, 10985-10994.

56. Shuboni-Mulligan, D.D.; Breton, G.; Smart, D.; Gilbert, M.; Armstrong, T.S. Radiation chronotherapy-clinical impact of treatment time-of-day: a systematic review. *J Neurooncol* **2019**, *145*, 415-427, doi:10.1007/s11060-019-03332-7.
57. Antoch, M.P.; Kondratov, R.V.; Takahashi, J.S. Circadian clock genes as modulators of sensitivity to genotoxic stress. *Cell Cycle* **2005**, *4*, 901-907, doi:10.4161/cc.4.7.1792.
58. Dakup, P.P.; Porter, K.I.; Gajula, R.P.; Goel, P.N.; Cheng, Z.; Gaddameedhi, S. The circadian clock protects against ionizing radiation-induced cardiotoxicity. *Faseb J* **2020**, *34*, 3347-3358, doi:10.1096/fj.201901850RR.
59. Ohkura, N.; Oishi, K.; Sekine, Y.; Atsumi, G.-i.; Ishida, N.; Matsuda, J.; Horie, S. Comparative Study of Circadian Variation in Numbers of Peripheral Blood Cells among Mouse Strains: Unique Feature of C3H/HeN Mice. *Biological and Pharmaceutical Bulletin* **2007**, *30*, 1177-1180, doi:10.1248/bpb.30.1177.
60. Hassan, S.A.; Ali, A.A.H.; Yassine, M.; Sohn, D.; Pfeffer, M.; Jänicke, R.U.; Korf, H.-W.; von Gall, C. Relationship between locomotor activity rhythm and corticosterone levels during HCC development, progression and treatment in a mouse model. *J. Pineal Res. under review*
61. Nakagawa, M.; Terashima, T.; D'Yachkova, Y.; Bondy, G.P.; Hogg, J.C.; van Eeden, S.F. Glucocorticoid-induced granulocytosis: contribution of marrow release and demargination of intravascular granulocytes. *Circulation* **1998**, *98*, 2307-2313, doi:10.1161/01.cir.98.21.2307.
62. Stone, H.B.; Coleman, C.N.; Anscher, M.S.; McBride, W.H. Effects of radiation on normal tissue: consequences and mechanisms. *Lancet Oncol* **2003**, *4*, 529-536, doi:10.1016/s1470-2045(03)01191-4.
63. Terrones, C.; Specht, L.; Maraldo, M.V.; Lundgren, J.; Helleberg, M. Lymphopenia after Radiotherapy and Risk of Infection. *Open Forum Infectious Diseases* **2017**, *4*, S702-S702, doi:10.1093/ofid/ofx163.1882.
64. Moreno-Smith, M.; Lutgendorf, S.K.; Sood, A.K. Impact of stress on cancer metastasis. *Future oncology (London, England)* **2010**, *6*, 1863-1881, doi:10.2217/fon.10.142.
65. Distelhorst, C.W. Recent insights into the mechanism of glucocorticosteroid-induced apoptosis. *Cell Death & Differentiation* **2002**, *9*, 6-19, doi:10.1038/sj.cdd.4400969.
66. Bray, F.N.; Simmons, B.J.; Wolfson, A.H.; Nouri, K. Acute and Chronic Cutaneous Reactions to Ionizing Radiation Therapy. *Dermatol Ther (Heidelb)* **2016**, *6*, 185-206, doi:10.1007/s13555-016-0120-y.
67. Uribe-Querol, E.; Rosales, C. Neutrophils in Cancer: Two Sides of the Same Coin. *Journal of Immunology Research* **2015**, *2015*, 983698, doi:10.1155/2015/983698.
68. Verrill, C.; Davies, J.; Millward-Sadler, H.; Sundstrom, L.; Sheron, N. Organotypic liver culture in a fluid-air interface using slices of neonatal rat and adult human tissue--a model of fibrosis in vitro. *J Pharmacol Toxicol Methods* **2002**, *48*, 103-110, doi:10.1016/S1056-8719(03)00042-X.
69. Beaule, C.; Granados-Fuentes, D.; Marpegan, L.; Herzog, E.D. In vitro circadian rhythms: imaging and electrophysiology. *Essays Biochem* **2011**, *49*, 103-117, doi:10.1042/BSE0490103.

70. Pfaffl, M.W. Quantification strategies in real-time PCR. In: Bustin SA, e.A.-Z.o.q.P., Ed. La Jolla: International University Line (IUL): 2004; pp. 87-112.

Relationship between locomotor activity rhythm and corticosterone levels during HCC development, progression and treatment in a mouse model

Soha A. Hassan, Amira A. H. Ali, Mona Yassine, Dennis Sohn, Martina Pfeffer, Reiner U. Jänicke, Horst-Werner Korf*, Charlotte von Gall

* Corresponding author

Status of publication: The manuscript has been accepted and published as online open-access in *Journal of Pineal Research* (doi: 10.1111/jpi.12724).

Impact factor: 15.2

Contribution to the publication: Concept/design, performance most of the main experiments, acquisition, analysis and interpretation of most data and writing of the manuscript.

Title:

Relationship between locomotor activity rhythm and corticosterone levels during HCC development, progression and treatment in a mouse model

Running title:

Relation between HCC and circadian outputs

Authors:

Soha A. Hassan[1,2], Amira A. H. Ali[1], Mona Yassine[1], Dennis Sohn[3], Martina Pfeffer[1], Reiner U. Jänicke[3], Horst-Werner Korf[4], Charlotte von Gall[1]

1 Institute of Anatomy II, Medical Faculty, Heinrich-Heine-University, Universitätstrasse 1, 40225 Düsseldorf, Germany.
2 Zoology Department, Faculty of Science, Suez University, Suez 43111, Egypt.
3 Laboratory of Molecular Radiooncology, Clinic and Policlinic for Radiation Therapy and Radiooncology, Medical Faculty of Heinrich-Heine-University, Düsseldorf, Germany.
4 Institute of Anatomy I, Medical Faculty, Heinrich-Heine-University, Universitätsstr. 1, 40225 Düsseldorf, Germany.

Correspondence: Prof. Horst-Werner Korf, korf@uni-duesseldorf.de

Abstract

Cancer related fatigue (CRF) and stress are common symptoms in cancer patients and represent early side effects of cancer treatment which affect the life quality of the patients. CRF may partly depend on disruption of the circadian rhythm. Locomotor activity and corticosterone rhythms are two important circadian outputs which can be used to analyze possible effects on the circadian function during cancer development and treatment. The present study analyzes the relationship between locomotor activity rhythm, corticosterone levels, hepatocellular carcinoma (HCC) development and radiotherapy treatment in a mouse model. HCC was induced in mice by single injection of diethylnitrosamine (DEN) and chronic treatment of phenobarbital in drinking water. Another group received chronic phenobarbital treatment only. Tumor bearing animals were divided randomly into four groups irradiated at four different *Zeitgeber* time points. Spontaneous locomotor activity was recorded continuously; serum corticosterone levels as well as p-ERK immunoreaction in the suprachiasmatic nucleus (SCN) were investigated. Phenobarbital treated mice showed damped corticosterone levels and a less stable 24 h activity rhythm as well as

an increase in activity during the light phase, reminiscent of sleep disruption. The tumor mice showed an increase in corticosterone level during the inactive phase and decreased activity during the dark phase, reminiscent of CRF. After irradiation, corticosterone levels were further increased and locomotor activity rhythms were disrupted. Lowest corticosterone levels were observed after irradiation during the early light phase, thus this time might be the best to apply radiotherapy in order to minimize side effects.

Keywords: cancer related fatigue, hepatocellular carcinoma, locomotor activity, corticosterone, p-ERK, radiotherapy, mouse model

Introduction

Cancer-related fatigue (CRF) is one of the most pronounced symptoms in cancer patients and one of the early chronic side effects of cancer treatment. Many cancer patients suffer from severe sleep problems, disrupted locomotor activity rhythm and cortisol levels and a decrease in life quality which accompany CRF, particularly after radiotherapy treatment [1-5].

Sleep regulation involves two intertwined processes: the homeostatic regulation and the output from the circadian system [6]. Thus, CRF may partly depend on disruption of the circadian rhythm. In humans and all mammalian species, the circadian rhythm is generated by the suprachiasmatic nucleus (SCN) of the hypothalamus and synchronized to the environmental rhythms by external cues called "*Zeitgebers*". The most prominent "*Zeitgeber*" is the external light-dark (LD) cycle, the photoperiod. Photoperiod stimuli are perceived by the retina and are transmitted to the SCN via the retinohypothalamic tract (RHT), which utilizes glutamate and the neuropeptide pituitary adenylate cyclase-activating peptide (PACAP) as neurotransmitters. Signal transduction of these neurotransmitters activates the extracellular signal-regulated kinase 1/2 (ERK1/2) pathway which plays an important role in conveying photic information to the SCN. In addition, phosphorylated ERK (p-ERK) interacts directly with some clock proteins (e.g. BMAL1) and activates other transcription factors such as CREB which in turn modulates the expression of other clock genes (e.g. *Per1*) [7-11]. Via multiple output pathways, the circadian system controls a variety of overt body functions including the sleep-wake cycle, locomotor activity and hormone secretion (e.g. glucocorticoids) [7,12,13].

The locomotor activity rhythm is considered a reliable marker of the circadian output and the main index that reflects the sleep-wake cycle and the general behavior in mammals [14-16]. Recording the locomotor activity patterns has been used to analyze possible dysfunctions of the circadian system in patients with cancer and after applying the cancer treatment protocols [17,18].

Rhythmic secretion of glucocorticoids is another important marker for circadian output. Under chronic stress, the hypothalamus-pituitary-adrenal (HPA) axis is stimulated and induces glucocorticoid secretion [19,20] which used as a stress biomarker. Thus, there is a strong relation between the circadian system and stress [21]. Stress is observed in many patients suffering from cancer [3]. Recently, there is growing evidence that the sleep disruption in cancer patients may be closely related to dysfunction of circadian rhythms including glucocorticoid secretion [2].

The primary aim of the present study is to analyze how tumor development and irradiation treatment affect spontaneous locomotor activity rhythms. As experimental animal model, *Per2::luc* mice were selected based on previous studies [22]. Hepatocellular carcinomas (HCC) were induced by diethylnitrosamine (DEN) injection and phenobarbital in drinking water to accelerate tumor development. Spontaneous locomotor activity rhythms were recorded before and after therapeutic irradiation. In addition, serum corticosterone levels and p-ERK immunoreaction, a marker for rhythmic SCN neuronal activity, were analyzed. To explore the effect of chronic phenobarbital treatment without tumor induction, the analyses were also performed with mice which received phenobarbital in the drinking water only and compared with mice that received neither the DEN injection nor the chronic phenobarbital treatment.

Material and method

Experimental animals and tumor induction

The experiments were conducted using transgenic *Per2::luc* mice on a C57BL6/J background according to federal guidelines and Directive 2010/63/EU of the European Union of animal care. The experiments were approved by the Regierungspräsidium Darmstadt and LANUV (Reference number: AZ 81-02.04.2018-A146). The appropriate measures were taken to reduce the pain or

discomfort of experimental animals. Male offspring were selected at the age of 14 days and received a single intraperitoneal injection with DEN (10 mg/kg, Sigma Aldrich, St. Louis, USA) to induce HCC. To promote HCC induction, the animals were chronically treated with phenobarbital (PB) (Luminal, Desitin, Hamburg, Germany) added to the drinking water at a concentration of 0.05% according to [23,24]. Tumor development was confirmed by post mortem inspection (Fig. S1). These animals constituted the tumor group. A second group comprised animals which received chronic PB treatment but were not injected with DEN (phenobarbital group). A third group comprised animals which received neither DEN injection nor PB treatment (control group). HCC developed in animals of the tumor group at the age of 7 - 10 months. Food and drinking water (either with or without PB) were supplied *ad libitum*. All animals were kept under normal light-dark (LD) cycle (12:12).

Experimental design

Recordings of the locomotor activity were started in 7 month old animals and lasted for 30 consecutive days. Recordings were performed for 5 animals in the control and phenobarbital groups and for 20 animals in the tumor group under normal LD cycle (12:12). ZT00 (at 05.00 am) defines the light on and ZT12 (at 05.00 pm) defines the light off. The 20 animals of the tumor group were randomly selected for treatment with irradiation at four different *Zeitgeber* time (ZT) points (ZT02, ZT08, ZT14 and ZT20) (5 animals/time point). One day after irradiation, the locomotor activity was recorded for five consecutive days (Fig. S2).

Irradiation

Animals of the tumor group were irradiated at ZT02 (2 hours after light on), ZT08, ZT14 (2 hours after light off) and ZT20. Before irradiation, the animals were deeply anesthetized by intraperitoneal injection of a mixture of ketamine (100 mg/kg, Inresa, Freiburg, Germany) and xylazine (10 mg/kg, Rompun 2%, Bayer Leverkusen, Germany). The animals were then fixed on a styropore plate with their ventral side facing the irradiation source and irradiated with 10 Gy (at 175 kV and 15 mA for about 10 minutes) using a Gulmay RS225 X-ray system (X-Strahl, Camberley, UK). 10 Gy dose was used because this dose has been applied in palliative radiotherapy [25]. The night experiments were performed under dim red light.

Locomotor activity

All recording experiments were performed in light and sound proof cabinets with automatic control of the photoperiod (lights on/off) (Scanbur, Germany). The light conditions were kept constant during the whole experiment with light intensity during the light phase was 300 lx. Animals were adapted to the experimental conditions at least two weeks before the experiments. Mice were housed individually in cages equipped with infrared movement detectors linked to an automated recording system (Mouse-E-Motion, Hamburg, Germany). Spontaneous locomotor activity was continuously recorded during the entire experiment in 10-min intervals. The actograms, chi-squared periodograms, activity profiles as well as the relative power of phase (fast Fourier transformation; FFT) were analyzed by Clocklab software (Actimetrics, Wilmette, USA). In addition, median of activity (MOA) which is defined as time-point at which the mouse has achieved 50% of its daily activity was used to determine the chronotype. The variance of MOA is a measure for instability of the chronotype [16,26].

Blood collection and corticosterone measurement

In parallel groups, blood was collected from 8 month old animals of the tumor (20 animals, n=5/time point), phenobarbital (12 animals, n=3/time point) and control (20 animals, n=5/time point) groups at four different ZTs (ZT02, ZT08, ZT14 and ZT20). In the tumor + irradiation group, 20 HCCs bearing mice were randomly divided into 4 subgroups (n=5/time point) for irradiation with a dose of 10 Gy at the four different ZTs, i.e., ZT02, ZT08, ZT14 and ZT20. 48 hours later, the animals were sacrificed at the same ZTs used for irradiation, quickly dissected and the blood was withdrawn from the right atrium in serum separator tubes, allowed to clot for 20 minutes and then centrifuged at 1000 x g at 4° C for 10 minutes to separate the serum. Serum was aliquoted, snap frozen in liquid nitrogen and stored at -80° C until being assayed. Sampling during the night was performed under dim red light. Serum corticosterone levels were measured using an enzyme-linked immunosorbent assay (Corticosterone ELISA Kit #ab108821, Abcam, UK) following the manufacturer's instructions and using the microplate photometer Multiskan FC (Thermo-scientific, Shanghai, China).

Control for effects of short-term anesthesia

To control the effects of short-term anaesthesia, locomotor activity was recorded in HCC bearing mice for 7 days and then the animals were deeply anesthetized by intraperitoneal injection of a mixture of ketamine (100 mg/kg, Inresa, Freiburg, Germany) and xylazine (10 mg/kg, Rompun 2%, Bayer Leverkusen, Germany) at ZT20. Thereafter, the locomotor activity was recorded for 5 consecutive days and all locomotor activity parameters were evaluated as mentioned above.

To control the effects of short-term anaesthesia on corticosterone levels, the animals were deeply anesthetized as mentioned above at ZT20. Another group of animals were left without injection (control group). 48 hours after ketamine injection, the control and the injected animals were sacrificed at the same ZT, quickly dissected and the blood was withdrawn and processed as mentioned above and the corticosterone levels were evaluated.

Animal perfusion and immunohistochemistry

Immunohistochemistry was performed with 12 animals of the tumor, tumor + irradiation, phenobarbital and control groups. The animals were sacrificed at four different ZTs: ZT02, ZT08, ZT14 and ZT20 (n= 3/time point). All animals of the tumor and tumor + irradiation groups had either single or multiple tumors. The animals were anesthetized by intraperitoneal injection of a mixture of ketamine and xylazine as mentioned above and then perfused transcardially with 0.9% NaCl followed by 4% paraformaldehyde (PFA) in 0.1 M phosphate buffered saline (PBS, pH 7.4). Perfusion during the night was performed under dim red light. Brains were removed from the skull, post-fixed in 4% PFA for 24 h, and then cryoprotected in 30% sucrose for another 24 h. Coronal brain sections (30 µm thick) were prepared on a cryostat (Leica CM, Germany). Sections were washed with PBS containing 0.2% Triton-X 100 (PBST) and treated with 0.6% H_2O_2 for 30 min to block endogenous peroxidase. To reduce non-specific staining, sections were blocked for 1 h with 5% normal goat serum in PBST, then incubated overnight at 4° C with p-ERK (1:1000, monoclonal rabbit anti p-ERK, Cell Signaling Technology, Frankfurt am Main, Germany). On the next day, sections were incubated with biotinylated goat anti-rabbit IgG (1:500, Thermo Scientific, USA) diluted in blocking buffer and then incubated with VECTASTAIN® Elite® ABC solution (1:200, Vector Laboratories, USA) in

PBST for 1 h. This was followed by incubation with 0.05% 3, 3′-diaminobenzidine (DAB) (1:100, Sigma Aldrich, USA) for 5 min. Slides were cover-slipped using DePeX (SERVA Electrophoresis, Germany).

Data acquisition

Images were acquired using BZ-X800 series microscope (Keyence, Japan) with a 20x objective in bright field mode. All images were processed using constant settings. p-ERK immunoreactive cells in the SCN were quantitatively analyzed using Image J software (http://rsbweb.nih.gov/ij) as previously described [27].

Statistical analysis

Statistical analysis was performed by using Graph Pad Prism 8 software. Data are expressed as mean ± standard error of the mean (SEM). Paired t-test was used to estimate the significant differences between two groups. Comparison between more than 2 groups was performed using Ordinary one-way analysis of variance (ANOVA) followed by *Tukey's* test for multiple comparisons. Two-way analysis of variance (ANOVA) was used to examine differences according to time and groups followed by *Sidak's* test for multiple comparisons between groups. The results were regarded as significant at $p < 0.05$.

Results

Effects of phenobarbital and tumor on spontaneous locomotor activity rhythms

Animals of control, phenobarbital, and tumor (before irradiation) groups showed a higher activity during the dark phase as compared with the light phase (Fig. 1 and Fig. 2). However, in the phenobarbital group, the activity during the light phase was significantly increased as compared with the control group (Fig. 2). In the tumor group, the total activity especially the activity during the dark phase was significantly reduced as compared with the phenobarbital group (Fig. 2).

Periodograms (Fig. 3A) and FFT (Fig. 3B) revealed that the relative power of phase was significantly decreased in the phenobarbital group as compared with the control group ($p < 0.05$). There was no difference in the relative power of phase between the tumor and phenobarbital groups ($p > 0.05$, Fig. 3B).

Neither the chronotype (MOA) (Control: n=5, 20.08 ± 0.6; Phenobarbital: n=5, 19.9 ± 0.6; Tumor: n=20, 20.5 ± 0.3) nor the variance of MOA was different among the three groups ($p > 0.05$, Fig. 3B).

Effects of irradiation on spontaneous locomotor activity rhythms

Locomotor activity profiles of mice with HCC (tumor group) were compared before and after irradiation at different ZTs. Before irradiation, all mice showed a higher activity during the dark phase as compared with the light phase (Fig. 1 and Fig. 4). However, after irradiation, the difference in activity during the light and the dark phase disappeared (Fig. 4), except for the mice which were irradiated at ZT20 (Fig. 4D). Moreover, the total activity especially the activity during the dark phase was significantly decreased after irradiation (Fig. 4).

The irradiation did not affect the chronotype (Table 1). However, periodograms and FFT revealed that the relative power of phase was significantly reduced in mice which received irradiation at ZT20 (Fig. 5). Moreover, in this subgroup, the variance of MOA was also significantly increased (Fig. 5B).

Short-term anesthesia on its own does not elicit any effect on the spontaneous locomotor activity rhythms (Fig. S3A).

Effects of phenobarbital, tumor and irradiation on serum corticosterone levels and SCN activity

The control group showed daily changes in serum corticosterone levels with a peak at ZT14 (2 hours after light off). In the phenobarbital group, this peak was blunted. The tumor group before irradiation showed an additional peak in serum corticosterone at ZT08. In mice irradiated at ZT08 and ZT20, the corticosterone levels were significantly increased as compared with the tumor group (Fig. 6). Short-term anesthesia on its own does not elicit any effect on the corticosterone levels (Fig. S3B).

In the control group, the number of p-ERK immunoreactive cells was higher at ZT02 and ZT08 as compared with ZT14 and ZT20. In the phenobarbital group, the number of p-ERK immunoreactive cells was also higher at ZT02 and ZT08 as compared with the time points during the dark phase and significantly higher as compared with the respective time points in the control group. In the tumor group before irradiation, the number of p-ERK immunoreactive cells showed a peak at ZT02, but at ZT08, the

number of p-ERK immunoreactive cells was significantly reduced as compared with the phenobarbital group.

Irradiation of the animals did not affect the number of p-ERK immunoreactive cells at all irradiated ZTs except at ZT20 at which the number of p-ERK immunoreactivity was significantly higher ($p < 0.001$) as compared with the HCC bearing mice before irradiation (Fig. 7).

Discussion

The primary aim of our study was to analyze how tumor development and radiotherapy at different times of the day affect the circadian system. As readouts for a functional circadian system, rhythms in spontaneous locomotor activity and serum corticosterone levels were determined before and after therapeutic irradiation. In addition, p-ERK immunohistochemistry was used as a marker for rhythmic SCN neuronal activity under light/dark conditions [28-30].

Impact of chronic phenobarbital treatment

The mice treated with phenobarbital showed a higher spontaneous locomotor activity during the dark phase as compared with the light phase and a period length close to 24 h. This indicates that phenobarbital does not affect the response of the circadian system to light *per se*. However, the activity counts during the light phase were significantly increased as compared with the control mice, reminiscent of sleep disruption. In nocturnal rodents, light suppresses locomotor activity [31]. Thus, an increased locomotor activity during the light phase suggests a reduced effect of light or an increased agitation during the sleep phase, which overrides the suppressive effect of light. Our findings are in agreement with studies by Forcelli *et al.* [32] and Quinlan *et al.* [33] who reported that administration of phenobarbital in the sensitive postnatal period can cause impairments in the behavior of rodents including abnormalities in locomotor activity and social behavior which become obvious in later life. In addition, patients treated with anticonvulsant drugs including phenobarbital suffer from sleep disruption [34]. One side effect of chronic phenobarbital treatment is the reduction in GABA receptor expression [35]. GABA is known as a potent inhibitory neurotransmitter which plays an important role in the sleep-wake cycle [36]. Presynaptic GABA receptors, which modulate transfer of light information to

retinal ganglion cells [37], could also be affected by chronic phenobarbital treatment. However, as p-ERK immunoreaction was highly rhythmic in the phenobarbital group, a severe corruption of the light input pathway is unlikely.

The relative power of phase was significantly decreased in the phenobarbital group as compared with the control group. This parameter reflects how much of the activity rhythm is due to the 24 h component and thus reflects rhythm stability. Consistently, the daily variation of serum corticosterone was damped in the phenobarbital group. Phenobarbital affects the amplitude of time-of-day dependent rhythms of locomotor activity and corticosterone levels presumably distal to the SCN as p-ERK-immunoreaction was highly rhythmic. The levels of corticosterone during the light/inactive phase were not increased upon phenobarbital treatment. This conforms to a study in humans which reported that acute and chronic phenobarbital treatment does not alter the cortisol levels during the night/inactive phase [38].

Impact of HCC development

The mice which developed HCC showed a higher spontaneous locomotor activity during the dark phase as compared with the light phase and a period length close to 24 h. This indicates that tumor development does not affect the response of the circadian system to light *per se*. In comparison with the phenobarbital treated mice, the total activity especially the activity during the dark phase was significantly reduced, reminiscent of fatigue. This is consistent with the results of Verma *et al.* [39] who reported that mice with HCC showed alterations of the locomotor activity rhythm. Curiously, in contrast to a disruption of rhythmic locomotor activity in mice with chemically induced HCC [39], rhythmic locomotor activity was not affected in mice injected with a human HCC cell line [40]. However, it is unknown how the different methods of tumor induction could impose different effects on the circadian system. In the tumor group, the relative power of phase was as low as in the phenobarbital group, thus tumor development had no additional effect on rhythm stability.

In contrast to the phenobarbital group, the corticosterone levels in the tumor group were significantly increased during the early activity phase as in the control group (ZT14) but also abnormally increased during the light/inactive phase (ZT08). This increase in corticosterone levels during the inactive phase might reflect an increase in

chronic stress and/or neuroinflammation (see below). Interestingly, the immunoreaction for p-ERK in the SCN at ZT08 is significantly reduced in the tumor group as compared with the phenobarbital group. Although glucocorticoid receptor signaling acts by altering the activity of various kinases including p-ERK and impinges on circadian regulation [21], little is known on the direct effects of stress on p-ERK expression in the SCN.

Severe sleep problems, disrupted and decreased locomotor activity rhythm and decreased life quality, which are associated with CRF, were reported in HCC, breast and metastatic colorectal cancer patients [1-3]. Moreover, alterations of the glucocorticoid rhythm and its increase at sleep time were observed in HCC and ovarian cancer patients and this was closely related to poor sleep quality and fatigue [2,41]. In a cross-sectional study, the elevation in the cortisol level at the rest phase was shown to be related to short sleep duration and high sleep disturbance suggesting a direct relation between both rhythms [42]. Patients with liver metastasis of colorectal cancer had increased levels of the proinflammatory cytokines IL-6 and transforming growth factor-alpha (TGF-α) which coincided with increased fatigue and disturbances in the cortisol and rest/activity rhythms [3].

Impact of radiotherapy

Over 50% of cancer patients who undergo chemo- or radiotherapy suffer from CRF as well as sleep problems [4,5]. Breast cancer patients subjected to radiotherapy tended to have more sleep disturbance and longer sleep latency than breast cancer patients who did not receive treatment [1]. Administration of cancer therapies at the right time-of-day can minimize the circadian alterations and improve the life quality [43]. However, little is known about the effect of radiotherapy on rest/activity and glucocorticoid rhythms if administered at different time points during the day. In our study, mice bearing HCC were irradiated at four different ZTs (ZT02, ZT08, ZT14 and ZT20) to investigate the short-term effect of radiotherapy on the locomotor activity rhythm and corticosterone levels.

Total locomotor activity especially activity during the dark phase was significantly decreased after irradiation with 10 Gy, irrespective of the time of irradiation. Moreover, the difference between activity counts during the light and the dark phase was abolished after irradiation, except after irradiation at ZT20. However, specifically

after irradiation at ZT20, the relative power of phase was significantly decreased and the variance of MOA was significantly increased, both indicating rhythm instability. York *et al.* [44] also reported a decrease in the spontaneous locomotor activity in mice 6 hours after irradiation with two different doses of gamma radiation. This decrease in the locomotor activity after irradiation was related with the rapid activation of the neuroimmune system leading to an increased expression of proinflammatory tumor necrosis factor (TNF) in the hippocampus followed by an increase in interleukin-1 receptor antagonist (IL-1RA) in the cortex and hippocampus and a reduction in activity-regulated cytoskeleton-associated protein (Arc) in the cortex. Activation of the immune system with increased release of cytokines from the central and peripheral tissues induces the sleep disruption and the fatigue symptoms in mice [44,45].

Radiotherapy is the common cause of the HPA axis dysfunctions in cancer patients [46,47]. The additional stress induced by radiotherapy further heats up the pro-inflammatory response leading to a vicious circle [48,49]. Rats exposed to 1-10 Gy irradiation showed a significant increase in the plasma corticosterone levels as compared with non-irradiated rats [49,50]. Consistently, in this study the serum corticosterone levels were significantly increased in tumor + irradiated group as compared with the tumor group, especially after irradiation at ZT08 and ZT20 reflecting increased chronic stress and/or neuroinflammation. The number of p-ERK immunoreactive cells in the SCN was significantly increased in mice which received radiotherapy at ZT20. This increase at ZT20 is unexpected as p-ERK in the SCN is induced by light [29,51,52], but supports our hypothesis that stress related glucocorticoid receptor signaling affects p-ERK expression in the SCN and subsequent locomotor activity rhythm stability.

In conclusion, irradiation strongly affects locomotor activity rhythm and corticosterone levels but the timing of administration makes small but significant differences. The corticosterone levels were lowest after irradiation at ZT02 which reflects less stress. Moreover, at this time point no effects were observed on the rhythm stability and the number of p-ERK immunoreactive cells. In contrast, the effect on rhythm instability was highest at ZT20 consistent with a significant increase in the corticosterone levels which reflects more stress. Thus, in order to minimize stress and disruption of the circadian system, it appears that radiotherapy should be applied at the beginning of the rest phase, but not at the end of the active phase, at

least in the HCC mouse model investigated here. Translational studies are now required to clarify whether these findings in night-active animals can be confirmed in day-active humans and to test whether also for patients suffering from HCC irradiation at the beginning of the rest phase minimizes stress and disruption of the circadian system.

Acknowledgements

S. A. H. is supported by German Egyptian Research Long-term Scholarship (GERLS) Program of the DAAD. We acknowledge support by the Heinrich-Heine-University Düsseldorf for open access funding. We thank Ralf Fassbender, Hanna Bellert, Angelika Hallenberger and Ursula Lammersen for excellent technical support.

Conflict of interest

The authors have no conflict of interest.

Author contributions:

Soha A. Hassan: concept/design, acquisition, analysis and interpretation of data and drafting of the manuscript. **Amira A. H. Ali:** acquisition, analysis and interpretation of data. **Mona Yassine:** acquisition and analysis of data. **Dennis Sohn:** acquisition of data. **Martina Pfeffer:** data analysis/interpretation. **Reiner U. Jänicke:** critical revision of the manuscript. **Horst-Werner Korf:** concept/design, acquisition and interpretation of data, supervision and drafting of the manuscript. **Charlotte von Gall:** data interpretation and drafting of the manuscript. All authors have read and approved the manuscript.

Data Availability Statement: The data that support the findings of this study are available from the corresponding author upon reasonable request.

References

1. Fortner BV, Stepanski EJ, Wang SC, Kasprowicz S, Durrence HH. Sleep and quality of life in breast cancer patients. *J Pain Symptom Manage.* 2002;24(5):471-480.
2. Huang T-W, Cheung DST, Xu X, et al. Relationship between diurnal cortisol profile and sleep quality in patients with Hepatocellular Carcinoma. *Biological Research for Nursing* 2019;22(1):139-147.
3. Rich T, Innominato PF, Boerner J, et al. Elevated serum cytokines correlated with altered behavior, serum cortisol rhythm, and dampened 24-hour rest-activity patterns in patients with metastatic colorectal cancer. *Clin Cancer Res.* 2005;11(5):1757-1764.
4. Hofman M, Ryan JL, Figueroa-Moseley CD, Jean-Pierre P, Morrow GR. Cancer-related fatigue: the scale of the problem. *Oncologist.* 2007;12 Suppl 1:4-1.0
5. Bower JE, Ganz PA, Desmond KA, et al. Fatigue in long-term breast carcinoma survivors: a longitudinal investigation. *Cancer.* 2006;106(4):751-758.
6. Borbely AA. A two process model of sleep regulation. *Hum Neurobiol.* 1982;1(3):195-204.
7. Korf H-W ,von Gall C. Circadian Physiology. In: Pfaff DW, ed. *Neuroscience in the 21st Century: From Basic to Clinical.* New York, NY: Springer New York; 2013:1813-1845.
8. Partch CL, Green CB, Takahashi JS. Molecular architecture of the mammalian circadian clock. *Trends Cell Biol.* 2014;24(2):90-99.
9. Mohawk JA, Green CB, Takahashi JS. Central and peripheral circadian clocks in mammals. *Annu Rev Neurosci.* 2012;35:445-462.
10. Coogan AN, Piggins HD. Circadian and photic regulation of phosphorylation of ERK1/2 and Elk-1 in the suprachiasmatic nuclei of the Syrian hamster. *J Neurosci.* 2003;23(7):3085-3093.
11. Gau D, Lemberger T, von Gall C, et al. Phosphorylation of CREB Ser142 regulates light-induced phase shifts of the circadian clock. *Neuron.* 2002;34(2):245-253.
12. Yamaguchi S, Isejima H, Matsuo T, et al. Synchronization of cellular clocks in the suprachiasmatic nucleus. . *Science.* 2003;302:1408–1412.
13. Ye H, Yang K, Tan XM, Fu XJ, Li HX. Daily rhythm variations of the clock gene PER1 and cancer-related genes during various stages of carcinogenesis in a golden hamster model of buccal mucosa carcinoma. *Oncotargets Ther.* 2015;8.
14. Galani R, Duconseille E, Bildstein O, Cassel JC. Effects of room and cage familiarity on locomotor activity measures in rats. *Physiol Behav.* 2001;74(1-2):1-4.
15. Sallam AE-D, Hassan SA, Hassaneen E, Ali EM. Environmental stress of mobile phone EM radiation on locomotor activity and melatonin circadian rhythms of rats. *Biological Rhythm Research.* 2016;47(4):597-607.
16. Pfeffer M, Wicht H, von Gall C, Korf HW. Owls and larks in mice. *Front Neurol.* 2015;6:101.
17. Mormont MC, Levi F. Circadian-system alterations during cancer processes: a review. *Int J Cancer.* 1997;70(2):241-247.

18. Innominato PF, Giacchetti S, Bjarnason GA, et al. Prediction of overall survival through circadian rest-activity monitoring during chemotherapy for metastatic colorectal cancer. *Int J Cancer.* 2012;131(11):2684-2692.
19. Gong S, Miao YL, Jiao GZ, et al. Dynamics and correlation of serum cortisol and corticosterone under different physiological or stressful conditions in mice. *PLoS One.* 2015;10(2):e0117503.
20. De la Roca-Chiapas JM, Barbosa-Sabanero G, Martinez-Garcia JA, et al. Impact of stress and levels of corticosterone on the development of breast cancer in rats. *Psychol Res Behav Manag.* 2016;9:1-6.
21. Koch CE, Leinweber B, Drengberg BC, Blaum C, Oster H. Interaction between circadian rhythms and stress. *Neurobiol Stress.* 2017;6:57-67.
22. Muller MH, Rodel F, Rub U, Korf HW. Irradiation with X-rays phase-advances the molecular clockwork in liver, adrenal gland and pancreas. *Chronobiol Int.* 2015;32(1):27-36.
23. Tolba R, Kraus T, Liedtke C, Schwarz M, Weiskirchen R. Diethylnitrosamine (DEN)-induced carcinogenic liver injury in mice. *Lab Anim.* 2015;49(1 Suppl):59-69.
24. Bakiri L, Wagner EF. Mouse models for liver cancer. *Mol Oncol.* 2013;7(2):206-223.
25. Vucic V, Isenovic ER, Adzic M, Ruzdijic S, Radojcic MB. Effects of gamma-radiation on cell growth, cycle arrest, death, and superoxide dismutase expression by DU 145 human prostate cancer cells. *Braz J Med Biol Res.* 2006;39(2):227-236.
26. Wicht H, Korf HW, Ackermann H, Ekhart D, Fischer C, Pfeffer M. Chronotypes and rhythm stability in mice. *Chronobiol Int.* 2014;31(1):27-36.
27. Trainor BC, Pride MC ,Villalon Landeros R, et al. Sex differences in social interaction behavior following social defeat stress in the monogamous California mouse (Peromyscus californicus). *PLoS One.* 2011;6(2):e17405.
28. Arima H, House SB, Gainer H, Aguilera G. Neuronal Activity Is Required for the Circadian Rhythm of Vasopressin Gene Transcription in the Suprachiasmatic Nucleus in Vitro. *Endocrinology.* 2002;143(11):4165-4171.
29. Smith VM, Jeffers RT, Wu C, Vijaya Shankara J, Antle MC. Temporal changes of light-induced proteins in the SCN following treatment with the serotonin mixed agonist/antagonist BMY7378. *Exp Brain Res.* 2015;233(9):2723-2731.
30. Sanada K, Okano T, Fukada Y. Mitogen-activated protein kinase phosphorylates and negatively regulates basic helix-loop-helix-PAS transcription factor BMAL1. *J Biol Chem.* 2002;277(1):267-271.
31. Mrosovsky N. In Praise of Masking: Behavioural Responses of Retinally Degenerate Mice to Dim Light. *Chronobiology International.* 1994;11(6):343-348.
32. Forcelli PA, Kozlowski R, Snyder C, Kondratyev A, Gale K. Effects of neonatal antiepileptic drug exposure on cognitive, emotional, and motor function in adult rats. *J Pharmacol Exp Ther.* 2012;340(3):558-566.
33. Quinlan SMM, Rodriguez-Alvarez N, Molloy EJ, et al. Complex spectrum of phenobarbital effects in a mouse model of neonatal hypoxia-induced seizures. *Sci Rep.* 2018;8(1):9986.
34. Bazil CW. Epilepsy and sleep disturbance. *Epilepsy Behav.* 2003;4 Suppl 2:S39-45.

35. Ruiz G, Hamon M, Verge D. Chronic phenytoin treatment decreases GABAA but not beta-adrenoceptors in the cerebellum of young rats. *Eur J Pharmacol.* 1989;168(2):251-255.
36. Gottesmann C. The involvement of noradrenaline in rapid eye movement sleep mentation. *Front Neurol.* 2011;2:81.
37. Pan F, Toychiev A, Zhang Y, et al .Inhibitory masking controls the threshold sensitivity of retinal ganglion cells. *J Physiol.* 2016;594(22):6679-6699.
38. Prinz PN, Vitiello MV, Roehrs TA, Linnoila M, Weitzman ED. Effect of phenobarbital on sleep and nighttime plasma growth hormone and cortisol levels. *Can J Physiol Pharmacol.* 1981;59(11):1139-1145.
39. Verma D, Hashim OH, Jayapalan JJ, Subramanian P. Effect of melatonin on antioxidant status and circadian activity rhythm during hepatocarcinogenesis in mice. *J Cancer Res Ther.* 2014;10(4):1.1044-040
40. Huang A, Bao B, Gaskins HR, et al. Circadian clock gene expression regulates cancer cell growth through glutaminase. *Acta Biochim Biophys Sin (Shanghai).* 2014;46(5):409-414.
41. Weinrib AZ, Sephton SE, Degeest K, et al. Diurnal cortisol dysregulation, functional disability, and depression in women with ovarian cancer. *Cancer.* 2010;116(18):4410-4419.
42. Kumari M, Badrick E, Ferrie J, Perski A, Marmot M, Chandola T. Self-reported sleep duration and sleep disturbance are independently associated with cortisol secretion in the Whitehall II study. *J Clin Endocrinol Metab.* 2009;94(12):4801-4809.
43. Ortiz-Tudela E, Iurisci I, Beau J, et al. The circadian rest-activity rhythm, a potential safety pharmacology endpoint of cancer chemotherapy. *Int J Cancer.* 2014;134(11):2717-2725.
44. York JM, Blevins NA, Meling DD, et al. The biobehavioral and neuroimmune impact of low-dose ionizing radiation. *Brain Behav Immun.* 2012;26(2):218-227.
45. Lira FS, Esteves AM, Pimentel GD, et al. Sleep pattern and locomotor activity are impaired by doxorubicin in non-tumor-bearing rats. *Sleep Sci.* 2016;9(3):232-235.
46. Firoozi M, Besharat MA. Cortisol-a Key Factor to the Understanding of the Adjustment to Childhood Cancer. *Iran J Cancer Prev.* 2013;6(1):1-7.
47. Schmiegelow M, Feldt-Rasmussen U, Rasmussen AK, Lange M, Poulsen HS, Muller J. Assessment of the hypothalamo-pituitary-adrenal axis in patients treated with radiotherapy and chemotherapy for childhood brain tumor. *J Clin Endocrinol Metab.* 2003;88(7):3149-3154.
48. Crews FT, Sarkar DK, Qin L, Zou J, Boyadjieva N, Vetreno RP. Neuroimmune Function and the Consequences of Alcohol Exposure. *Alcohol Res.* 2015;37(2):331-341, 344-351.
49. Kandasamy SB, Thiagarajan AB, Harris AH. Possible involvement of prostaglandins in increases in rat plasma adrenocorticotropic hormone and corticosterone levels induced by radiation and interleukin-1 alpha alone or combined. *Fundam Appl Toxicol.* 1995;25(2):196-200.
50. Cohen EP, Bruder ED, Cullinan WE, Ziegler D, Raff H. Effect of high-dose total body irradiation on ACTH, corticosterone, and catecholamines in the rat. *Transl Res.* 2011;157(1):38-47.

51. Coogan AN, Piggins HD. Circadian and Photic Regulation of Phosphorylation of ERK1/2 and Elk-1 in the Suprachiasmatic Nuclei of the Syrian Hamster. *The Journal of Neuroscience.* 2003;23(7):3085-3093.
52. Obrietan K, Impey S, Storm DR. Light and circadian rhythmicity regulate MAP kinase activation in the suprachiasmatic nuclei. *Nat Neurosci.* 1998;1(8):693-700.

Figure 1

Representative double-plotted actograms of spontaneous locomotor activity from mice of the control group (A), the phenobarbital group (B), and the tumor group before and after irradiation at ZT02 (C), at ZT08 (D), at ZT14 (E) and at ZT20 (F). Animals were kept in LD cycle 12:12 and the locomotor activity was recorded for 30 consecutive days. Animals were irradiated with a dose of 10 Gy at different *Zeitgeber* time (ZT) points (ZT02, ZT08, ZT14 and ZT20) (5 animals per time point) and the locomotor activity was recorded for five additional consecutive days after irradiation. Red lighting indicates time of irradiation.

Figure 2

Analyses of day, night and total spontaneous locomotor activity counts in mice of the control (n=5), the phenobarbital (n=5) and the tumor (n=20, before irradiation) groups. Plotted are the mean counts ± SEM. §§: $p < 0.01$; §§§: $p < 0.001$ differences between day and night activity counts. ***: $p < 0.001$ differences between control and phenobarbital groups. #: $p < 0.05$ differences between phenobarbital and tumor groups.

Figure 3

Periodograms, relative power of phase and variance of median of activity (MOA) in mice of the control (n=5), the phenobarbital (n=5) and the tumor (n=20, before irradiation) groups. Periodograms of the different groups (A) and relative power of phase and variance of MOA of the different groups (B). Plotted are the mean ± SEM. *: $p < 0.05$ differences between control and phenobarbital groups.

Figure 4

Analyses of day, night and total spontaneous locomotor activity counts in mice of the tumor group before and after irradiation. Animals were irradiated with a dose of 10 Gy at different *Zeitgeber* time (ZT) points (ZT02, ZT08, ZT14, and ZT20) (5 animals per time point). Spontaneous locomotor activity counts of animals irradiated at ZT02 (A), at ZT08 (B), at ZT14 (C) and at ZT20 (D). Plotted are the mean numbers ± SEM. §: $p < 0.05$; §§: $p < 0.01$ differences between day and night activity counts. *: $p < 0.05$; **: $p < 0.01$; ***: $p < 0.001$; ****: $p < 0.0001$ differences between before and after irradiation. n.s: not significantly different.

Figure 5

Periodograms, relative power of phase and variance of median of activity (MOA) in mice of tumor group before and after irradiation. Animals were irradiated with a dose of 10 Gy at different *Zeitgeber* time (ZT) points (ZT02, ZT08, ZT14 and ZT20) (5 animals per time point). Periodograms before and after irradiation at different ZTs (A), and relative power of phase and variance of MOA before and after irradiation at different ZTs (B). Plotted are the mean numbers ± SEM. *: $p < 0.05$ differences between before and after irradiation.

Figure 6

Serum corticosterone levels in 8 month old mice of the control (20 animals, n=5/time point) and the phenobarbital (12 animals, n=3/time point) groups as well as the tumor group before irradiation (20 animals, n=5/time point). Animals in tumor + irradiation group (20 animals, n=5/time point) were irradiated with a dose of 10 Gy at different *Zeitgeber* time (ZT) points (ZT02, ZT08, ZT14 and ZT20). 48 h later, mice were sacrificed at the same time points used for irradiation and blood was collected. Plotted are the mean ± SEM. White and black bars indicate day and night, respectively. ##: $p<0.01$ differences between this ZT and ZT02. £: $p<0.05$ differences between this ZT and ZT20. *: $p<0.05$ differences between before and after irradiation.

Figure 7

p-ERK immunoreactivity in the SCN of 8 month old mice of the control (3 animals/time point), the phenobarbital (3 animals/time point) and the tumor groups before and after irradiation (3 animals/time point). Animals were irradiated with a dose of 10 Gy at different *Zeitgeber* time (ZT) points (ZT02, ZT08, ZT14 and ZT20) and sacrificed 48 h later at the same time points. Representative photomicrographs of p-ERK immunoreactive cells in the SCN (A) and quantification (B). Plotted are the mean ± SEM. White and black bars indicate day and night, respectively. £: $p<0.05$; ££: $p<0.01$; ££££: $p<0.0001$ differences between this ZT and ZT20. $: $p<0.05$ differences between control and phenobarbital groups. ####: $p<0.0001$ differences between phenobarbital and tumor groups. ***: $p<0.001$ differences between before and after irradiation.

Table 1. The chronotype (Median of activity, MOA) in mice of tumor group before and after irradiation with a dose of 10 Gy at four different *Zeitgeber* time (ZT) points. Values are the mean numbers ± SEM.

ZT	Before	After	*p* value
02	20.44 ± 0.33	20.65 ± 1.37	> 0.99
08	20.51 ± 0.67	19.5 ± 0.8	0.09
14	21.56 ± 1.11	21.25 ± 1.22	0.9
20	19.84 ± 0.38	18.33 ± 0.78	0.13

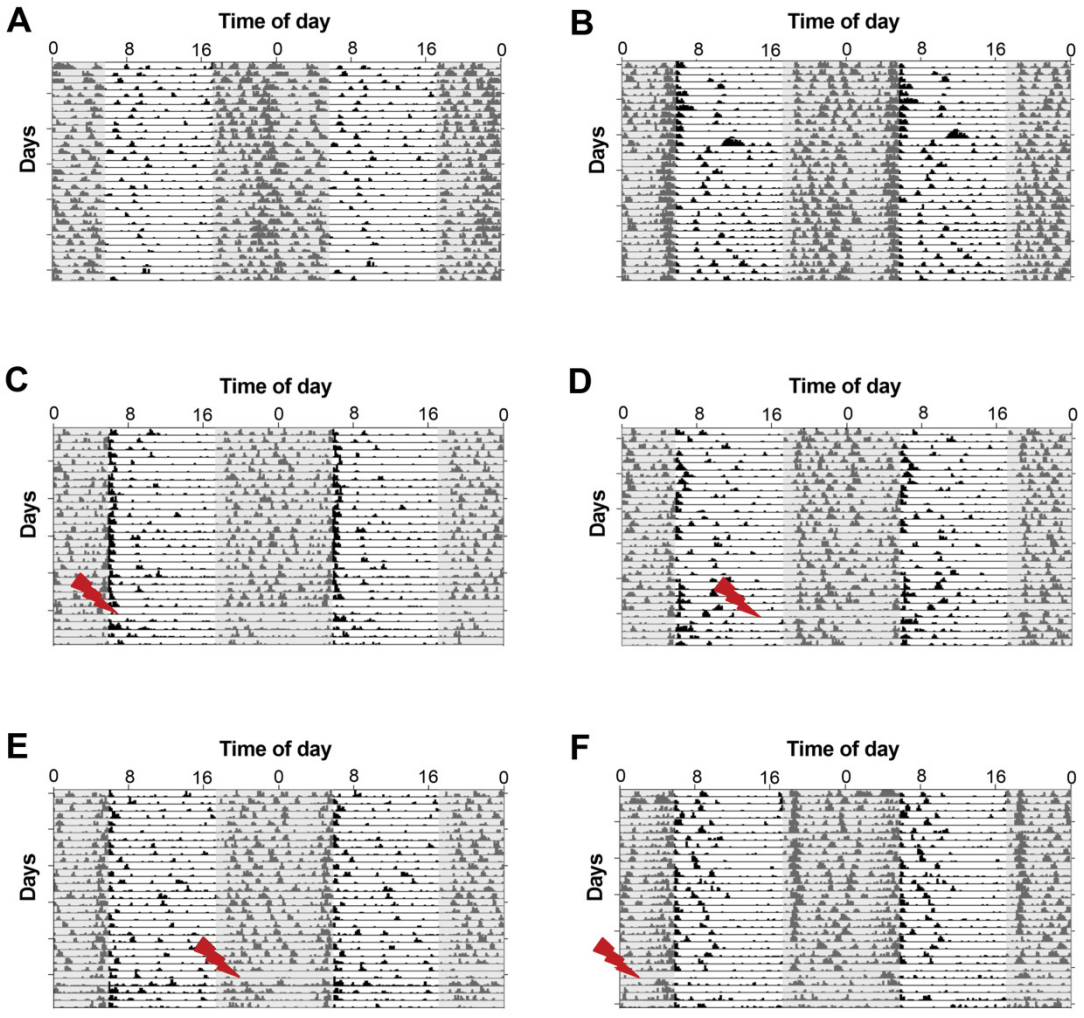

jpi_12724_f1.tiff

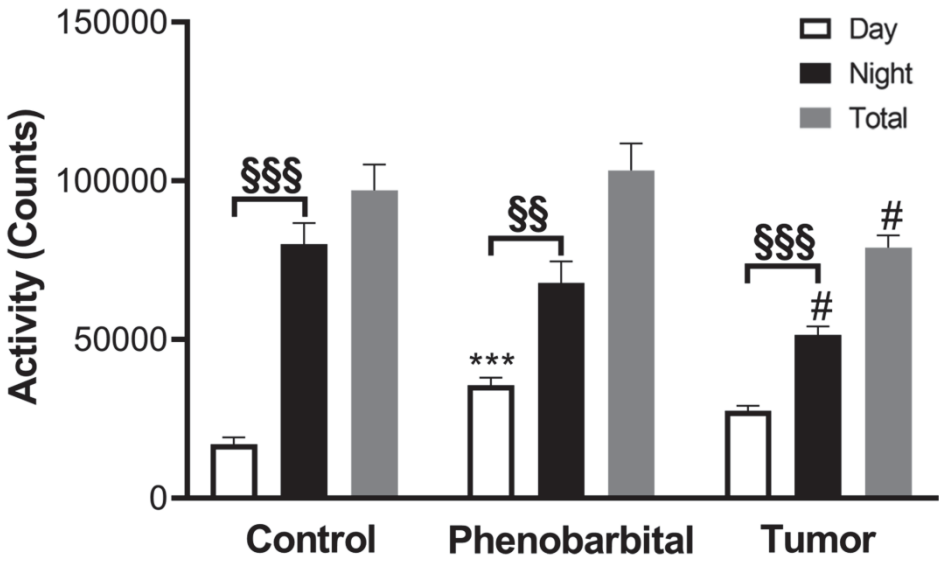

jpi_12724_f2.tiff

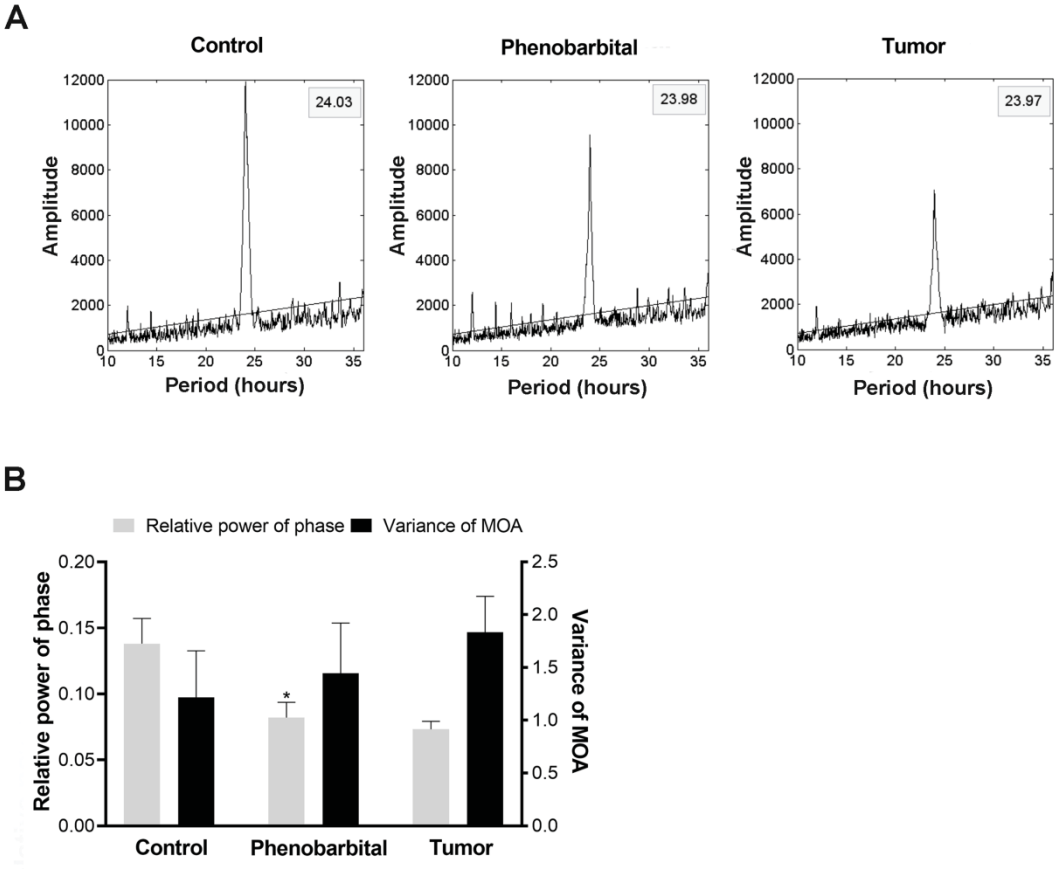

jpi_12724_f3.tiff

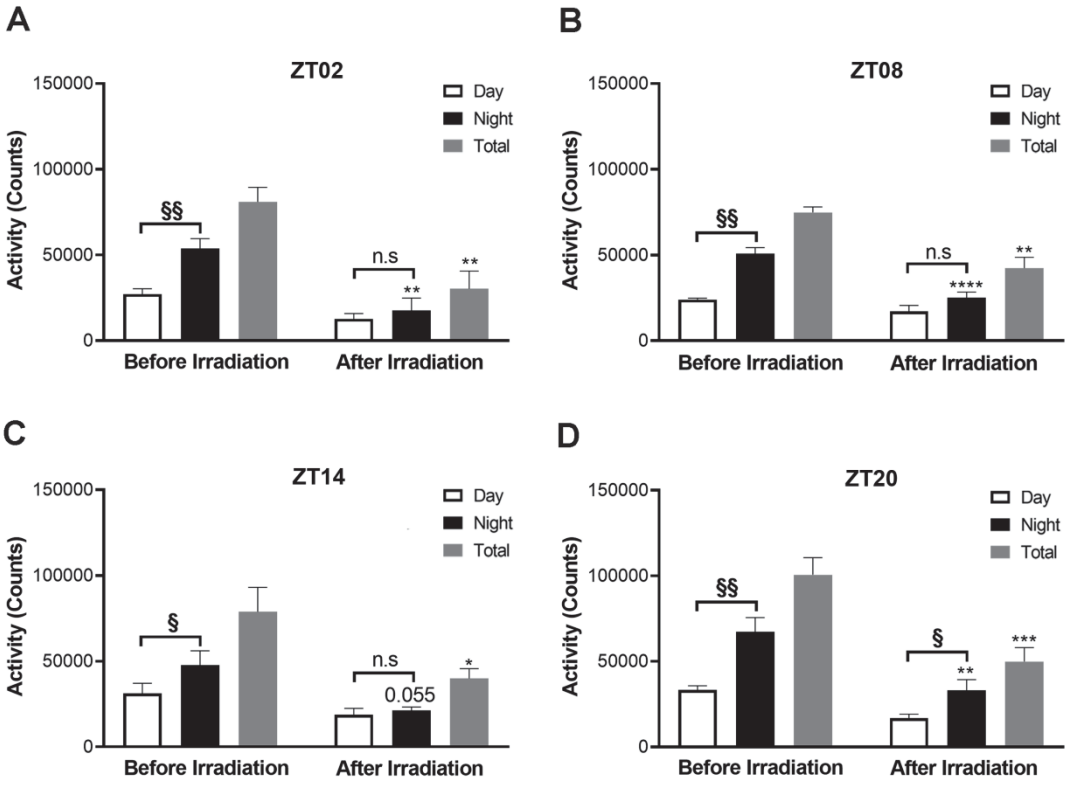

jpi_12724_f4.tiff

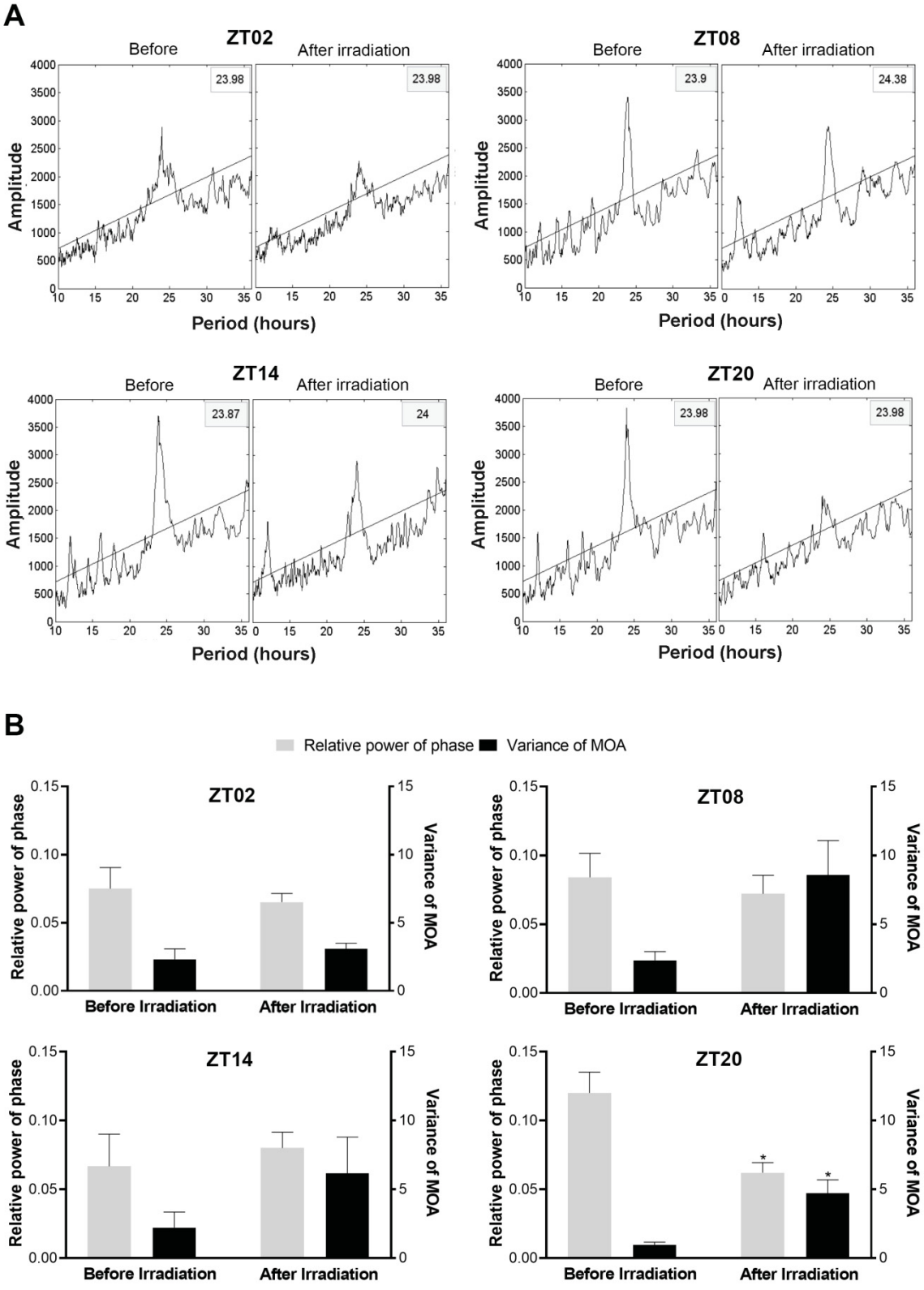

jpi_12724_f5.tiff

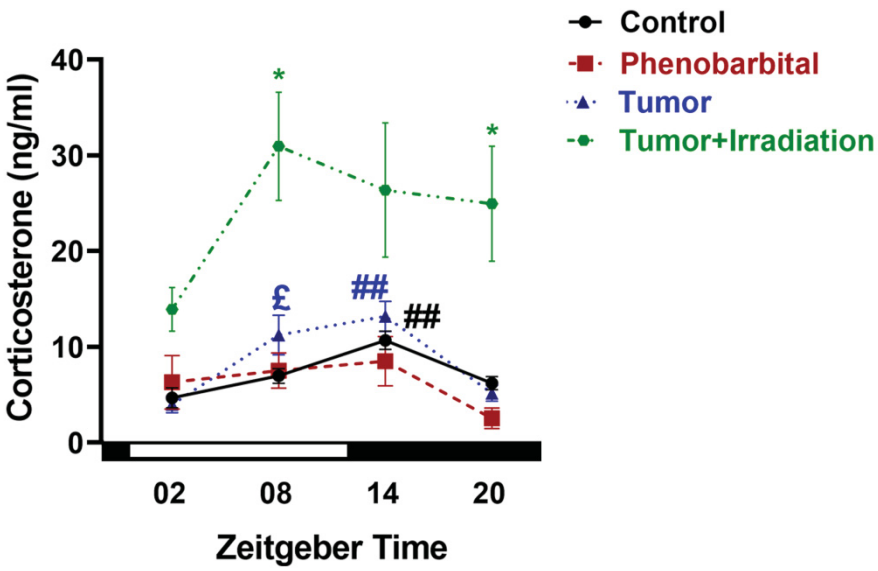

jpi_12724_f6.tiff

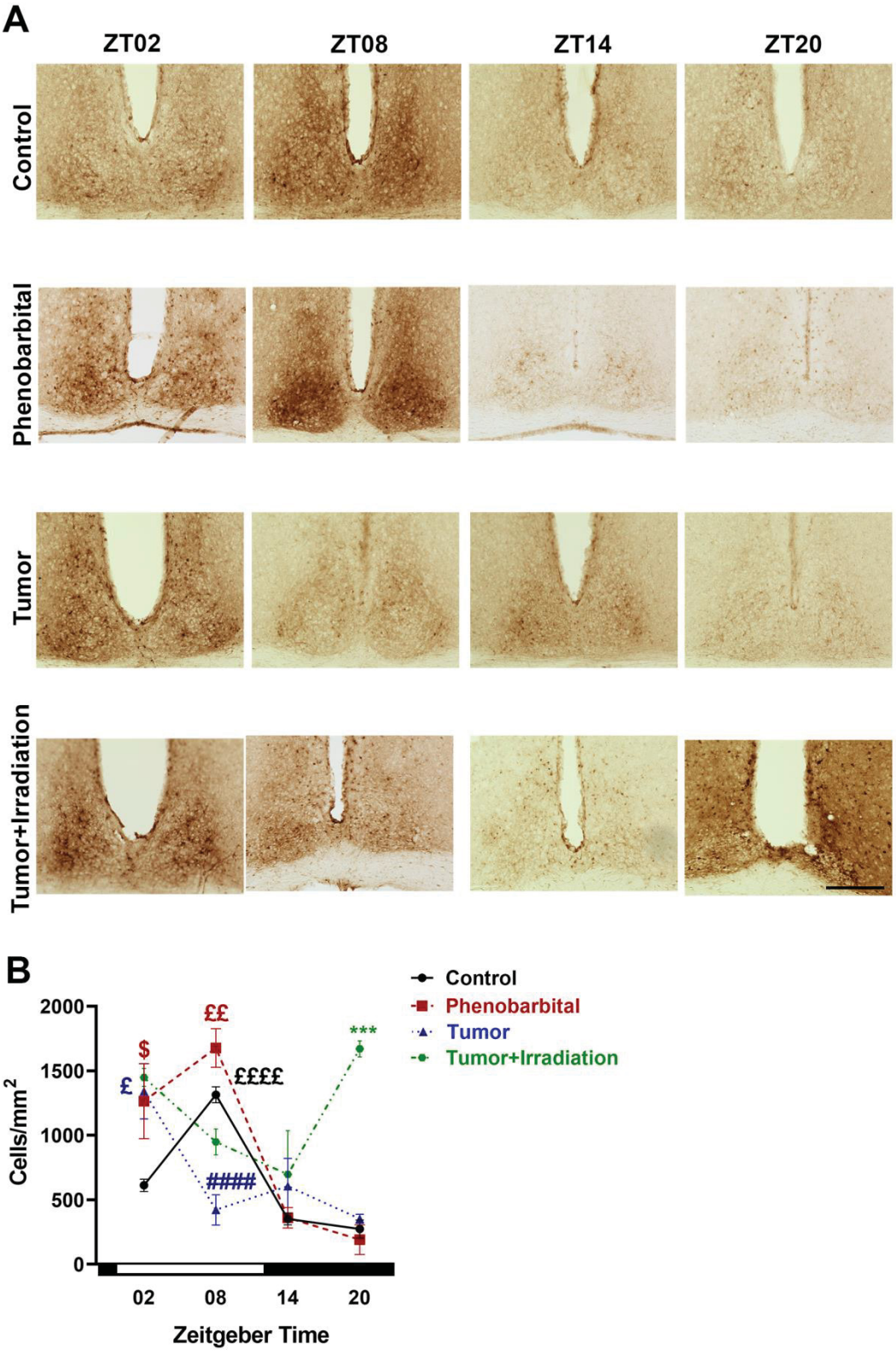

jpi_12724_f7.tiff

Supplementary materials:

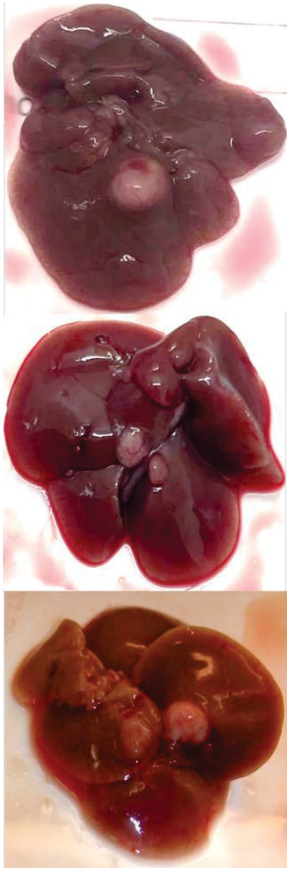

Figure S1

Representative photographs of single and multiple hepatocellular carcinomas (HCC) at the age of 8 months. The mice injected with a single dose of diethylnitrosamine (DEN) at the age of two weeks and then chronically treated with phenobarbital (PB) in the drinking water to accelerate the HCC development.

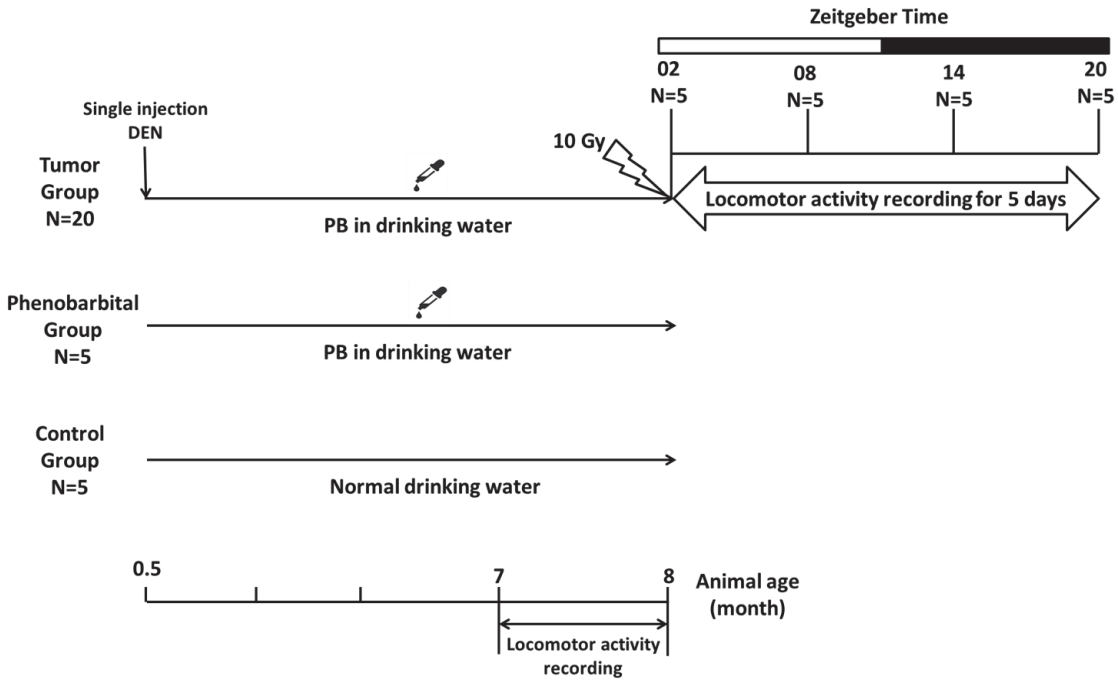

Figure S2

Diagram for the experimental design of locomotor activity recording. Recordings of the spontaneous locomotor activity were started in 7 month old animals of control, phenobarbital and tumor groups and lasted for 30 consecutive days. Control group comprises animals (n=5 animals) which received neither the diethylnitrosamine (DEN) injection nor the chronic phenobarbital treatment. Phenobarbital group comprises animals (n=5 animals) that were chronically treated with phenobarbital in the drinking water, but did not receive the DEN injection and tumor group comprises animals (n=20 animals) that received a single injection of DEN at the age of two weeks and chronic treatment of phenobarbital in the drinking water. The 20 animals of the tumor group were randomly selected for treatment with irradiation (dose of 10 Gy) at four different *Zeitgeber* time (ZT) points (ZT02, ZT08, ZT14 and ZT20) (5 animals per time point) and the spontaneous locomotor activity was recorded for five additional consecutive days after irradiation.

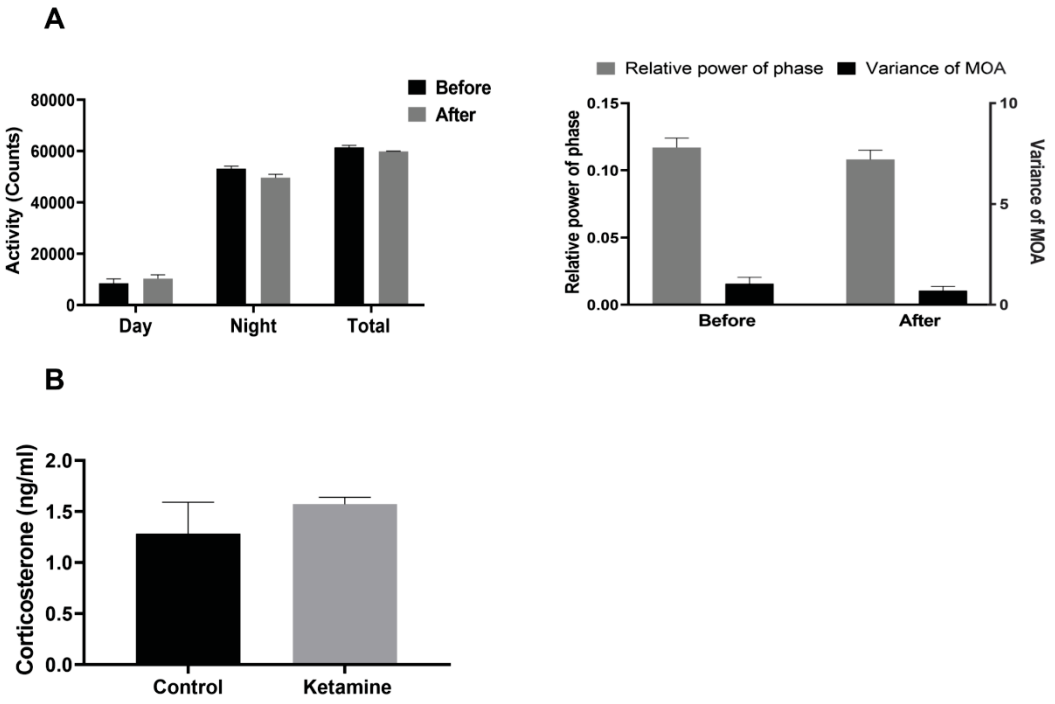

Figure S3

Effects of short-term of anesthesia on spontaneous locomotor activity rhythm and serum corticosterone levels in mice. Locomotor activity was recorded for 7 days. Mice were injected with a mixture of ketamine and xylazine at ZT20. Thereafter, the locomotor activity was recorded for 5 consecutive days. For corticosterone, mice were injected with a mixture of ketamine and xylazine at ZT20 and another group was left without injection (control). Mice were sacrificed 48 h later at the same time points used for injection and blood was collected. Spontaneous locomotor activity counts, relative power of phase and variance of median of activity (MOA) (A) and serum corticosterone levels (B). Plotted are the mean numbers ± SEM.

Summary

Hepatocellular carcinoma (HCC) is highly resistant to anticancer therapy and novel therapeutic strategies are needed. Chronotherapy may become a promising approach because it may improve the efficacy of antimitotic radiotherapy and ameliorate its side effects by considering timing of treatment. Ki67 and γ-H2AX are two important cell cycle components whose expression changes during the day and are regulated by the circadian clock. These two biomarkers can be used to predict the response of HCC to the radiotherapy. The main aim of this thesis is to introduce the concept of chronotherapy to radiobiological cancer research by identifying an optimal time point at which HCC is increasingly susceptible, whilst the surrounding healthy liver (HL) tissue becomes increasingly resistant to the damaging effects of cancer therapy.

In our first publication, we investigated whether cell proliferation and DNA repair mechanisms in HCC tissue follow a daily pattern and whether this pattern differs from that in the surrounding HL. Also, we analyzed whether the circadian molecular clockwork is altered in HCC as compared with the surrounding HL. These questions were addressed by immunohistochemical demonstration of Ki67 (as a marker for proliferation rate) and γ-H2AX (as a marker for DNA damage/repair) in the HCC and the surrounding HL using mouse model for hepatocellular carcinoma, double transgenic c-myc/TGFα mice. In addition, core clock genes (*Per1*, *Per2*, *Cry1*, *Cry2, Bmal1, Rev-erbα* and *Clock*) were examined by qPCR. Data were obtained from samples collected *ex vivo* at 4 different time points and from organotypic slice cultures (OSC). The results showed that significant differences in proliferation rate as well as DNA damage and repair mechanisms between the HCC and the surrounding HL which depend on the time of day. In addition, expressions of *Per2* and *Cry1* were significantly lower and had different daily variation patterns in the HCC and the surrounding HL. The results revealed also that OSC from HCC and the surrounding HL may be a helpful model to establish the therapeutic strategies. The data from the first publication support the concept of chronotherapy of HCC.

As it is well known that the efficacy and side effects of any antimitotic therapy depend on proper timing and that determination of the optimal time point for application of antimitotic therapies may help to improve the efficacy of HCC treatment. In our second publication, we tested this hypothesis by investigating the effect of irradiation at four different time points of the day in transgenic *Per2::luc* mice bearing HCCs. To this end, Ki67 and γ-H2AX in HCC and HL were analyzed before and after the irradiation in OSC and *ex vivo* samples. OSC was used to investigate whether the model is suitable to determine the optimal time points of radiotherapy. In addition, we investigated whether the radiotherapy altered the circadian molecular clockwork (*Per1*, *Per2*, *Cry1*, *Cry2, Bmal1, Rev-erbα* and *Clock*) in HCC and the surrounding HL if the treatment was performed at different *Zeitgeber* time (ZT) points. Finally, we analyzed the number of blood cells in transgenic *Per2::luc* HCC bearing mice before and after irradiation at different ZTs to monitor the possible acute side effects of the radiotherapy at each time point. The results revealed time-dependent changes in the effect of radiotherapy on the proliferation rate and DNA damage and repair mechanisms in the HCC and the surrounding HL. Importantly, irradiation dramatically decreased the proliferation rate in both tissues and was most effective when applied at the peaks of the proliferation which were different between the HL (ZT02) and the HCC (ZT02 and ZT20). In addition, γ-H2AX expression was significantly increased at all irradiated ZTs in both tissues but the radiosensitivity of the HL was lowest when the animals were irradiated at late activity phase (ZT20). All investigated clock genes except *Per1* showed disruption in the daily variations and/or down-regulation in their expressions in the non-irradiated HCC as compared with HL. Dysregulation of clock gene expression was observed in HL and HCC at all irradiated ZTs except ZT20 and this might be closely linked with the higher radiosensitivity of the irradiated HL at these ZTs. The percentages of leukocyte types were altered after irradiation regardless of the irradiation time point. Notably, irradiation at ZT20 had no significant effect on the total leukocyte number. Unfortunately, OSC is not an ideal model to test the chronotherapeutic approach which needs studies with whole animals but can be useful to determine dose-dependent effects. The data allow to define ZT20 (late activity phase) as the optimal time point at which the HCC was more sensitive to radiotherapy (94.3% decrease in the proliferation rate), whilst the surrounding HL was more resistant to the side effects (less effect on the proliferation rate (32.6%) and DNA damage and repair mechanism

(32.2%) as well as no effect on the core clock genes and total leukocyte number) in the investigated model. In addition, the results indicate the value of a chronotherapeutic approach for treatment of HCC mouse models.

HCC radiotherapy can also affect other biological systems in the body. Cancer-related fatigue (CRF) and stress are common symptoms in cancer patients and also observed as early chronic side effects of cancer treatment. CRF may partly depend on dysfunction/disruption of the circadian rhythm. In our third publication, we investigated spontaneous locomotor activity rhythm and serum corticosterone levels in transgenic *Per2::luc* HCC bearing mice as two important circadian outputs which can be used to analyze possible effects on the circadian system during HCC development and radiotherapy at 4 different ZTs. In addition, p-ERK immunoreaction in the SCN, a marker for rhythmic neuronal activity, was analyzed. The tumor mice showed an increase in corticosterone level during the late inactivity phase (ZT08) and decreased activity during the dark phase, reminiscent of CRF. After irradiation, corticosterone levels were further increased and locomotor activity rhythms were disrupted. When the animals were irradiated at ZT02, the effect on corticosterone levels was lowest which indicates less stress on the animals. In addition, no effects were observed on the rhythm stability and the number of p-ERK immunoreactive cells. In contrast, radiotherapy applied at ZT20 revealed more stress on the animals which is reflected by a significant increase in the corticosterone levels, more rhythm instability and a significant increase in the number of p-ERK immunoreactive cells. Thus, in order to minimize stress and disruption of the circadian system, it appears that radiotherapy should be applied at the early inactivity phase (ZT02) but not at the late activity phase (ZT20) in the investigated HCC mouse model.

Although we defined ZT02 as the best time point to apply radiotherapy with less stress and disruption on the circadian system, it is very important to mention that at ZT02, the HL tissue was more sensitive to damage by radiotherapy which is reflected by 89.8% decrease in the proliferation rate, 90.7% increase in the DNA-DSBs damage and down-regulation in the expression of clock genes; *Clock, Bmal1* and *Cry2*. On the other hand, irradiation at ZT20 revealed more rhythm instability in the spontaneous locomotor activity and more stress on the animals than the other irradiated ZTs. However, at this time point, the HCC was more sensitive to

radiotherapy, whilst the surrounding HL was more resistant, as well as no significant effects on the total leukocyte number, was observed.

It is known that some side effects after irradiation might be accepted especially if there is a reasonable probability of the tumor control. After weighing all effects and side effects, we can define ZT20 (late activity phase) as the optimal time point for the radiotherapy of HCC in the nocturnal mice.

Zusammenfassung

Das hepatozelluläre Karzinom (HCC) ist sehr resistent gegen eine Krebstherapie, und es werden daher neue therapeutische Strategien benötigt. Die Chronotherapie könnte sich zu einem vielversprechenden Ansatz entwickeln, da sie die Wirksamkeit der antimitotischen Strahlentherapie durch Berücksichtigung des Behandlungszeitpunkts verbessern könnte. Ki67 und γ-H2AX sind zwei wichtige Komponenten des Zellzyklus, deren Expression sich im Laufe des Tages ändert und die durch die zirkadiane Uhr reguliert werden. Diese beiden Biomarker können zur Vorhersage des Ansprechens des HCC auf die Strahlentherapie verwendet werden. Das Hauptziel dieser Arbeit ist es, das Konzept der Chronotherapie in die strahlenbiologische Krebsforschung einzuführen, indem ein optimaler Zeitpunkt identifiziert wird, zu dem das HCC zunehmend anfällig wird, während das umgebende gesunde Leber-(HL-)Gewebe zunehmend resistent gegen die Krebstherapie wird.

In unserer ersten Publikation untersuchten wir, ob Zellproliferation und DNA-Reparaturmechanismen im HCC-Gewebe ein tageszeitliches Muster aufweisen und ob sich dieses Muster von dem im umgebenden HL unterscheidet. Außerdem analysierten wir, ob das zirkadiane molekulare Uhrwerk im HCC im Vergleich zum umgebenden HL verändert ist. Diese Fragen wurden durch den immunhistochemischen Nachweis von Ki67 (als Marker für die Proliferationsrate) und γ-H2AX (als Marker für DNA-DSBs) im HCC und dem umgebenden HL in einem Mausmodell für das hepatozelluläre Karzinom, (doppelt transgene c-myc/TGFα Mäuse) untersucht. Zusätzlich wurde die Expression zentraler Uhrengene (*Per1*, *Per2*, *Cry1*, *Cry2*, *Bmal1*, *Rev-erbα* und *Clock*) mittels qPCR untersucht. Die Daten wurden an Proben erhoben, die *ex vivo* aus Tieren und *in vitro* aus organotypischen Schichtkulturen (OSC) zu 4 verschiedenen Zeitpunkten gewonnen wurden. Die Ergebnisse zeigten signifikante Unterschiede in der Proliferationsrate sowie in den DNA-Schäden und Reparaturmechanismen zwischen dem HCC und dem umgebenden HL, die von der Tageszeit abhängen. Darüber hinaus waren die Expressionen von *Per2* und *Cry1* signifikant niedriger und wiesen unterschiedliche tägliche Variationsmuster im HCC und dem umgebenden HL auf. Die Ergebnisse zeigten auch, dass Untersuchungen von OSC aus HCC und HL hilfreich sein könnten,

um neue therapeutischen Strategien zu entwickeln. Die Ergebnisse der ersten Publikation unterstützen das Konzept der Chronotherapie des HCC.

Es ist bekannt, dass Wirksamkeit und Nebenwirkungen jeder antimitotischen Therapie vom richtigen Zeitpunkt abhängen und dass die Bestimmung des optimalen Zeitpunkts bei der Anwendung antimitotischer Therapien dazu beitragen kann, die Wirksamkeit der HCC-Behandlung zu verbessern. In unserer zweiten Publikation prüften wir diese Hypothese, indem wir die Wirkung einer Bestrahlung zu vier verschiedenen Tageszeitpunkten *an* transgenen *Per2::luc* Mäusen mit HCC untersuchten. Zu diesem Zweck wurden Ki67 und γ-H2AX in HCC und HL vor und nach der Bestrahlung in OSC- und *ex vivo*-Proben analysiert. Die OSC wurden untersucht um zu prüfen, ob *in vitro* Modelle geeignet sind, die optimalen Zeitpunkte für eine Strahlentherapie zu bestimmen. Weiterhin untersuchten wir, ob die Strahlentherapie das zirkadiane molekulare Uhrwerk (*Per1*, *Per2*, *Cry1*, *Cry2*, *Bmal1*, *Rev-erbα* und *Clock*) im HCC und im umgebenden HL verändert, wenn die Behandlung zu verschiedenen *Zeitgeber*-Zeitpunkten (ZT) durchgeführt wurde. Schließlich bestimmten wir die Anzahl der Blutzellen von transgenen *Per2::luc* HCC-tragenden Mäusen vor und nach der Bestrahlung an verschiedenen ZTs, um die möglichen Nebenwirkungen der Strahlentherapie zu jedem Zeitpunkt nachzuweisen. Die Ergebnisse zeigten zeitabhängige Veränderungen in der Wirkung der Strahlentherapie auf die Proliferationsrate sowie DNA-Schäden und Reparaturmechanismen im HCC und dem umgebenden HL. Die Bestrahlung verringerte die Proliferationsrate in beiden Geweben dramatisch. Sie war am wirksamsten, wenn sie zu den Zeitpunkten der maximalen Proliferation angewendet wurde, die sich jedoch zwischen HL (ZT02) und HCC (ZT02 und ZT20) unterschieden. Die Expression von γ-H2AX war in beiden Geweben zu jedem untersuchten Zeitpunkt signifikant erhöht, aber in HL war sie besonders hoch, wenn die Tiere bei ZT02 bestrahlt wurden. Eine Dysregulation der Expression von Uhrengenen wurde bei HL und HCC zu allen bestrahlten ZTs mit Ausnahme von ZT20 beobachtet. Die Gesamtzahl der Leukozyten und die Prozentzahlen der Leukozyten-Typen waren nach der Bestrahlung unabhängig vom Bestrahlungszeitpunkt verändert. An ZT20 war das HCC deutlich empfindlicher gegenüber der Strahlentherapie, während das umgebende HL durch die Strahlentherapie am wenigsten beeinflusst wurde. Daher kann ZT20 als am besten

geeigneter Zeitpunkt für eine Strahlentherapie des HCC bei Mäusen angesehen werden. Künftige Studien müssen nun klären, ob sich diese an Mäusen erhobenen Befunde auf den Menschen übertragen lassen. Bei Mäusen ist ZT20 die späte Aktivitätsphase. Beim Menschen liegt diese bei ZT08. Leider erwiesen sich *in vitro* Untersuchungenn als ungeeignet, den optimalen Zeitpunkt einer Therapie zu bestimmen. Hierzu sind *ex vivo* Untersuchungen notwendig, dennoch erscheinen in vitro Untersuchungen hilfreich zur Bestimmung der effektiven Dosis.

Krebserkrankungen und Strahlentherapie können zur sog. krebsbedingten Müdigkeit (chronic fatigue syndrome, CRF) und Stress führen. CRF kann teilweise auf eine Dysfunktion des zirkadianen Rhythmus zurückzuführen sein. In der dritten Publikation untersuchten wir den Rhythmus der spontanen Bewegungsaktivität und die Serumkortikosteronspiegel in transgenen *Per2::luc* HCC-tragenden Mäusen. Beide gelten als wichtige Ausgangswege des zirkadianen Systems und wurden hier untersucht, um zu prüfen, in welchem Zusammenhang Nebenwirkungen, Tumorentwicklung und Zeitpunkt der Bestrahlung stehen. Darüber hinaus wurde ein Marker für die rhythmische neuronale Aktivität im SCN, die p-ERK-Immunreaktion, analysiert. Die Tumormäuse zeigten einen Anstieg des Kortikosteronspiegels während der inaktiven Phase (ZT08) und eine verminderte Konzentration während der Dunkelphase. Ähnliche Befunde wurden bei Patienten mit CRF erhoben. Nach der Bestrahlung kam es zu einer weiteren Erhöhung der Kortikosteronspiegel und zu einer Störung des Rhythmen in der Bewegungsaktivität. Die Kortikosteron-Werte waren nach Bestrahlung an ZT02 am wenigsten erhöht und eine Bestrahlung an ZT20 führte zur größten Rhythmusinstabilität. Um Stress und Störungen des zirkadianen Systems zu minimieren, sollte die Strahlentherapie daher zumindest im hier untersuchten HCC-Mausmodell zu Beginn der Ruhephase, nicht aber am Ende der aktiven Phase angewendet werden.

Wenn die Tiere bei ZT02 bestrahlt wurden, war der Effekt auf den Corticosteronspiegel am geringsten, was auf eine geringere Belastung der Tiere hinweist. Außerdem wurden keine Auswirkungen auf die Rhythmusstabilität und die Anzahl der p-ERK-immunreaktiven Zellen beobachtet. Im Gegensatz dazu zeigte eine bei ZT20 applizierte Strahlentherapie mehr Stress für die Tiere, was sich in einem signifikanten Anstieg der Corticosteronspiegel, mehr Rhythmusinstabilität und einem signifikanten Anstieg der Anzahl der p-ERK-immunreaktiven Zellen widerspiegelt.

Um den Stress und die Störung des zirkadianen Systems zu minimieren, scheint es für das untersuchte HCC-Mausmodell günstig, die Strahlentherapie in der frühen Inaktivitätsphase (ZT02), aber nicht in der späten Aktivitätsphase (ZT20) anzuwenden.

Es ist bekannt, dass einige Nebenwirkungen der Bestrahlung billigend in Kauf zu nehmen sind, wenn hierdurch eine bessere Tumorkontrolle erreicht werden kann. Bezüglich der Effektivität der Bestrahlung auf das Tumorwachstum ist ZT20 (die späte Aktivitätsphase) als der optimale Zeitpunkt für die Strahlentherapie des HCC in den nachtaktiven Mäusen zu definieren, obwohl die Tiere zu diesem Zeitpunkt eine höhere Rhythmusinstabilität und höhere Kortikosteronspiegel aufwiesen als zu den anderen Zeitpunkten der Bestrahlung.

Conclusion and future perspectives

Radiotherapy is used in cancer treatment because it induces cytotoxicity by increasing the lethal DNA-DSBs which lead subsequently to cancer cell death (Hein, Ouellette et al. 2014). Tumor radiotherapy affects the proliferation and other biological processes of the tumor but it can also damage healthy tissues surrounding the tumor (Wang, Wang et al. 2018) and thus cause severe side effects. Radiotherapy has a limited role in treating liver metastasis due to the increased risk of radiation-induced liver damage (RILD) which follows the hepatic radiotherapy (Ohri, Dawson et al. 2016, Chen 2019). Also, radiotherapy is rarely used in the management of the HCC due to lacking trail data which support the safety and efficacy of the radiotherapy and the absence of effective strategies which can reduce or either protect against RILD (Ohri, Dawson et al. 2016). Thus, low-dose radiotherapy can be used only to palliate symptoms from end-stage HCC or in a combination with chemotherapy (e.g. RT-SOR) (Wild, Gandhi et al. 2013, Ohri, Dawson et al. 2016). To date, it is unknown whether these side effects can be reduced if the therapy were applied at the right time. Such a chronotherapeutic approach has been taken in humans for other tumors such as breast, rectal, cervical and non-small cell lung cancers, bone and brain metastases, squamous cell carcinoma of oral cavity/pharynx/larynx, head and neck carcinoma and prostate adenocarcinoma but not for HCC (Harper and Talbot 2019).

In this thesis, we confirmed that there are significant differences in proliferation rate, DNA damage and repair mechanisms and core clock genes between the HCC and the surrounding HL using two different experimental mouse models for hepatocellular carcinoma. The results support the concept of chronotherapy of HCC and allow to define ZT20 as an optimal time point at which the HCC was more sensitive to radiotherapy, whilst the surrounding HL was more resistant to the side effects in the mouse model investigated here, although the animals revealed more rhythm instability and stress. The chronotherapeutic approach for treatment of HCC may be an effective strategy to reduce the RILD.

It is well known that different organs of the body are controlled by the two branches of autonomic nervous system (ANS): the sympathetic (SNS) and parasympathetic (PNS) nervous systems. The SNS prevails during the active phase to

control the physical activity by enhancing the heart rate, for instance, to provide the blood which is required for movement. In contrast, the PNS prevails during the rest/inactive phase and decreases the heart rate and blood pressure during sleeping. These different autonomic signals are time of day-dependent and determine the activity status of the organism (Kreier, Yilmaz et al. 2003, Zoccoli and Amici 2020).

On the other hand, all key factors of immune system (e.g. circulating blood cells and cytokines) which play a very important role in the immune response against the tumor cells, are under the control of the circadian system. Importantly, the release/retention of these parameters is regulated by sympathetic innervation which mediates the rhythmic regulation of their expression according to the rest-activity phase of the species regardless of whether the species is nocturnal (e.g. mice) or diurnal (e.g. human). Thus, there are mutual connections between the ANS, rest-activity cycle and immune system and these connections are phase-dependent. Therefore, any chronotherapeutic strategy of antimitotic therapies seems to have the same phase relation with the rest-activity cycle in mice and humans (Mormont and Levi 2003, Scheiermann, Kunisaki et al. 2013, Pritchett and Reddy 2015, Zoccoli and Amici 2020). Based on data about locomotor activity, activity of the autonomic nervous and the immune system, time points which are determined in nocturnal species (mouse) might be easily transferred to diurnal species (e.g. human). We defined the late activity phase (ZT20) as the optimal time point to apply the radiotherapy for HCC bearing mice. This means for human, ZT08, i.e. the late activity phase, might be the optimal time point to apply the radiotherapy for HCC patients. Translational studies are now required to clarify whether these findings can be confirmed for patients suffering from HCC.

Introducing the concept of chronotherapy to translational radiobiological research for other types of cancer (e.g. pancreas and lung cancers) is also required. This can improve the efficacy of the antimitotic therapies and reduce the severity of the side effects which subsequently improve the life quality of many cancer patients. We also concluded that the disruption of some clock gene expressions after irradiation of HL at some ZTs might be closely linked to the higher radiosensitivity of the tissue at these ZTs. Further investigations are required to elucidate the possible relation between disruption of the molecular clockwork and the sensitivity to the radiotherapy. In addition, we proved that OSC may be a useful model to determine dose-dependent

effects but unfortunately, it is unsuited to test the chronotherapeutic approach which needs studies with whole animals.

References

Chen, C. P. (2019). "Role of Radiotherapy in the Treatment of Hepatocellular Carcinoma." J Clin Transl Hepatol **7**(2): 183-190.

Harper, E. and C. J. Talbot (2019). "Is it Time to Change Radiotherapy: The Dawning of Chronoradiotherapy?" Clin Oncol (R Coll Radiol) **31**(5): 326-335.

Hein, A. L., M. M. Ouellette and Y. Yan (2014). "Radiation-induced signaling pathways that promote cancer cell survival (review)." Int J Oncol **45**(5): 1813-1819.

Kreier, F., A. Yilmaz, A. Kalsbeek, J. A. Romijn, H. P. Sauerwein, E. Fliers and R. M. Buijs (2003). "Hypothesis: shifting the equilibrium from activity to food leads to autonomic unbalance and the metabolic syndrome." Diabetes **52**(11): 2652-2656.

Mormont, M. C. and F. Levi (2003). "Cancer chronotherapy: principles, applications, and perspectives." Cancer **97**(1): 155-169.

Ohri, N., L. A. Dawson, S. Krishnan, J. Seong, J. C. Cheng, S. K. Sarin, M. Kinkhabwala, M. M. Ahmed, B. Vikram, C. N. Coleman and C. Guha (2016). "Radiotherapy for Hepatocellular Carcinoma: New Indications and Directions for Future Study." J Natl Cancer Inst **108**(9).

Pritchett, D. and A. B. Reddy (2015). "Circadian Clocks in the Hematologic System." Journal of Biological Rhythms **30**(5): 374-388.

Scheiermann, C., Y. Kunisaki and P. S. Frenette (2013). "Circadian control of the immune system." Nat Rev Immunol **13**(3): 190-198.

Wang, J. S., H. J. Wang and H. L. Qian (2018). "Biological effects of radiation on cancer cells." Mil Med Res **5**(1): 20.

Wild, A. T., N. Gandhi, S. T. Chettiar, K. Aziz, R. P. Gajula, R. D. Williams, R. Kumar, K. Taparra, J. Zeng, J. A. Cades, E. Velarde, S. Menon, J. F. Geschwind, D. Cosgrove, T. M. Pawlik, A. Maitra, J. Wong, R. K. Hales, M. S. Torbenson, J. M. Herman and P. T. Tran (2013). "Concurrent versus sequential sorafenib therapy in combination with radiation for hepatocellular carcinoma." PLoS One **8**(6): e65726.

Zoccoli, G. and R. Amici (2020). "Sleep and autonomic nervous system." Current Opinion in Physiology **15**: 128-133.

Abbreviations

ANOVA	Analysis of variance
ANS	Autonomic nervous system
Arc	Activity-regulated cytoskeleton-associated protein
BSA	Bovine serum albumin
CCGs	Clock-controlled genes
CRF	Cancer-related fatigue
CT	Circadian time
DEN	Diethylnitrosamine
DNA-DSBs	DNA-double strand breaks
ERK	Extracellular signal-regulated kinase
FFT	Fast Fourier transformation
Gy	Gray
HCC	Hepatocellular carcinoma
HIF-1	Hypoxia-inducible factors 1
HL	Healthy liver
HPA	Hypothalamus-pituitary-adrenal
IL	Interleukin
IL-1RA	Interleukin-1 receptor antagonist
IR-induced	Irradiation-induced
Irr-	Irradiation
LD	Light-dark
MOA	Median of activity
MRI	Magnetic resonance imaging

OSC	Organotypic slice culture
PACAP	Pituitary adenylate cyclase-activating peptide
PB	Phenobarbital
PBS	Phosphate buffered saline
PBST	Phosphate buffered saline with triton
p-ERK	Phosphorylated-ERK
PFA	Paraformaldehyde
PNS	Parasympathetic nervous system
RHT	Retinohypothalamic tract
RILD	Radiation-induced liver damage
RT	Room temperature
RT-SOR	Sorafenib therapy in combination with radiation
SCN	Suprachiasmatic nucleus
SEM	Standard error of the mean
SNS	Sympathetic nervous system
TGF-α	Transforming growth factor-alpha
TNF-α	Tumor necrosis factor-alpha
ZT	Zeitgeber time

Acknowledgement

First of all, my deep thanks to "ALLAH" for the ability, patience and perseverance that ALLAH has been bestowed upon me during my PhD study, and indeed, throughout my life. Thanks to all collaborators and co-authors in this work.

I want to thank the German Egyptian Research Long-term Scholarship (GERLS) Program of the DAAD for the personal funding and supporting my PhD study. Thanks for giving me the chance to travel abroad, learn better, make new collaborations with many researchers, acquire much knowledge and achieve one of my dreams.

I wish to express my deepest thanks, appreciation and gratitude to my supervisor "Doktorvater", Prof. Dr. Horst-Werner Korf for giving me a great opportunity to be a part of his scientific research and suggesting this interesting research point. It is my honor to be his PhD student. Thanks for his guidance, valuable advices during the course of this study, continuous encouragement, constructive criticism and insightful discussion regarding the manuscripts. Also, I am very grateful for his great support and efforts in the practical part of the research project especially at the night irradiation sessions, providing me with his field experience and without his constructive guidance, this work would not have been possible.

I wish also to express my appreciation and sincere thanks to Prof. Dr. Charlotte von Gall for the great opportunity to continue my practical part of the research in her laboratory, for her continuous support and valuable advices. Also, I am very grateful for her great support and useful discussions in writing and reviewing the manuscripts.

Furthermore, I would like to acknowledge with much appreciation Prof. Dr. Andreas Reichert for accepting to be my mentor and for his support.

Thanks to my research group, colleagues and technician at Institute of Anatomy II&III, Goethe University, Frankfurt am Main, Germany for being nice and cooperative. I am grateful to Prof. Dr. Frank Nürnberger, Prof. Dr. Amin Derouiche and Prof. Dr. Thomas Deller for their continuous support and advice and Dr. Qian Zhang for teaching me the confocal microscope imaging. Thanks to Prof. Dr. Jörg Stehle to give me the chance to learn and perform Western Blot experiments in his lab. Special thanks to my lab partner (lab mother) Elke Laedtke, who taught me a lot in the lab works and for being friendly with me all the time.

I am grateful for the collaboration with Prof. Albrecht Piiper and Dr. Christian Schmithals (Department of Medicine, University Hospital Frankfurt, Frankfurt, Germany). Thanks for providing us with the c-myc/TGFα mice and teaching me the MRI.

Thanks to my research group, colleagues and technician (Ralf, Hanna, Ulla and Angelika) at Institute of Anatomy II, Medical Faculty, Heinrich Heine University, Düsseldorf, Germany for their cooperation, support and teaching me a lot. Thanks for having really good and nice time with you. Special thanks and deepest appreciation to Dr. Amira Ali for helping in the animals' dissection and collecting the blood samples. Thanks for your continuous encouragement, fruitful discussion and your great support to me in the lab and generally in my life in Germany. Thanks for your friendship, being beside me all the time and sharing with me the sad moments before the happy ones.

I am grateful for the collaboration with Dr. Dennis Sohn (Laboratory of Molecular Radiooncology, Clinic and Policlinic for Radiation Therapy and Radiooncology, Medical Faculty of Heinrich-Heine-University, Düsseldorf, Germany) for organizing and participating in the irradiation sessions especially the night sessions.

I am grateful for the collaboration with Prof. Ulrich Flögel (Department of Molecular Cardiology, Heinrich Heine University, Düsseldorf, Germany) for organizing and performing the MRI sessions.

I greatly thank members of the animal facility, Zentrale Einrichtung für Tierforschung und Wissenschaftliche Tierschutzaufgaben (ZETT) for helping me with the animal breeding and organization of the experiments there.

I deeply thank the sacrificed mice which contribute their lives for science.

Last but not least, I would like to thank my parents for their continuous support, encouragement, patience and understanding throughout my life and hard time. I would also like to thank my family, sisters, brothers, friends and my DAAD colleagues for their support. Special thanks to my best friends from Egypt "Noha" and from DAAD "Sarah, Dina, Marwa, Asmaa and Mervat" for their support and for being always there for me all the time, "Thanks for making special moments, trips and giving a taste for Germany".

I am very grateful for all as without your encouragement and support, I would not have finished this thesis. Thanks for believing in me. So it is my honor to dedicate this work to you.

Declaration

Ich, Frau M.Sc. Soha Abdelaliem Hassan Hassan erkläre an Eides statt, dass die vorliegende Dissertation von mir selbständig und ohne unzulässige fremde Hilfe unter Beachtung der "Grundsätze zur Sicherung guter wissenschaftlicher Praxis an der Heinrich-Heine-Universität Düsseldorf" erstellt worden ist. Diese Dissertation hat in gleicher oder ähnlicher Form noch keiner anderen Prüfungsbehörde vorgelegen. Ich habe bisher keine erfolglosen Promotionsversuche unternommen.

Düsseldorf, den Unterschrift